1-1-1987

Studies of solvent vapor sorption and diffusion in phase segregated polyurethanes/

Ta-Min Feng
University of Massachusetts Amherst

STUDIES OF SOLVENT VAPOR SORPTION AND DIFFUSION IN PHASE SEGREGATED POLYURETHANES

A Dissertation Presented

By

Ta-Min Feng

Submitted to the Graduate School of the
University of Massachusetts in partial fulfillment
of the requirements for the degree of

DOCTOR OF PHILOSOPHY

September 1987

Department of Polymer Science and Engineering

STUDIES OF SOLVENT VAPOR SORPTION AND DIFFUSION IN PHASE SEGREGATED POLYURETHANES

A Dissertation Presented

By

Ta-Min Feng

Approved as to Style and Content by:

W. J. MacKnight, Chairman

R. W. Lenz, Member

E. L. Thomas, Member

E. L. Thomas
Department Head
Polymer Science and Engineering

ACKNOWLEDGEMENTS

I wish to thank Professor William J. MacKnight, my dissertation advisor, for his guidance, patience and encouragement during the course of this research. I also wish to acknowledge the help of the other members of my committee, Professor E. L. Thomas and R. W. Lenz. I would like to thank Dr. Kantor for his support in the final defence.

I am very grateful to Dr. N. S. Schneider for supplying the materials used in this dissertation and for many informative discussions. I would also like to thank Dr. H. Ling for his assistance and stimulating discussion.

Thanks also go to Mr. C. W. Chu for his help with NMR experiments, and J. M. Connolly for his editorial assistance with this manuscript.

Finally, I would like to thank my wife, Emily, for her love and support during the last four years.

ABSTRACT

STUDIES OF SOLVENT VAPOR SORPTION AND DIFFUSION IN PHASE SEGREGATED POLYURETHANES

September 1987

Ta-Min Feng

B.A., National Chen-Kung University

M.S., University of Delaware

Ph.D., University of Massachusetts

Directed by: Professor William J. MacKnight

Incremental vapor sorption and desorption experiments of 1,2-dichloroethane have been carried out in polyurethane samples with different 4,4'-methylenebis(phenyl isocyanate) (MDI) : butanediol (BD) : poly(tetramethylene oxide) (PTMO) ratios as well as different molecular weights of the PTMO. The sorption isotherm, diffusion behavior, and diffusivity as a function of concentration have been determined. Hysteresis behavior in the sorption isotherm curves was observed for samples with relatively high hard segment contents. The sigmoidal and two-stage sorption curves were found for high swelling (higher soft segment content) and relatively low swelling (lower soft segment content) samples at moderate and high solvent concentrations or activities, respectively. In order to determine the origin of these sorption anomalies, hysteresis studies,

thickness studies, and annealing studies have been carried out. The results of these studies indicate that the anomalous diffusion behavior is a result of the relaxation process in the glassy hard phase and/or interfacial phase induced by the presence of the solvent.

The anomalous diffusion behavior can be modeled very well by the Joshi-Astarita equation for Fickian diffusion coupled with a relaxation process. The diffusivity-concentration curves show a pronounced maximum for all samples. This observation can be attributed to the thermodynamic factor which is usually a decreasing function of the solvent concentration. The results of DSC and NMR experiments show an increase in the molecular motions of the hard segment in the glassy hard phase and/or interfacial phase for swollen sample, indicating that the interaction between the solvent and the glassy hard segment is indeed present.

TABLE OF CONTENTS

LIST OF TABLES

LIST OF FIGURES

CHAPTER I

GENERAL INTRODUCTION

1.1 Structure and Properties

Polyurethane block copolymers have received a great deal of attention during the last decade. This is primarily due to the two phase structure of these materials in the solid state and the commercial applications, including hard and soft forms, fibers, films and coating, and thermoplastic elastomers. The segmented polyurethanes are linear, heterophase copolymers which consist of alternating soft and hard segments. The soft phase of these materials is usually an amorphous, rubbery mixture at room temperature composed of soft segments which can be either polyether-, polyester-, or polyalkyl- glycols. The hard phase consists of glassy or semi-crystalline thermoplastic microdomains dispersed in this rubbery matrix. The hard phase also includes some soft segments and a more or less diffuse interphase is usually present between the hard and soft segments. The hard segment unit is usually an aromatic diisocyanate that has been chain entended with a low molecular weight diol such as 1,4-butanediol to form a urethane segment.

A substantial amount of work has shown that the physical properties and morphologies of these materials depend on the composition and chemical structure of hard and soft segments, and are a

direct consequence of the phase segregated structure. The hard segment domians act as both physical crosslinks and reinforcing fillers that are well bonded to the rubbery matrix. The extent of phase segregation is influenced by the chemical nature of the constituents, their stereochemistry, the length of hard and soft segments, and any interactions between hard and soft segments. Cooper and Tobolsky (1) compared the mechanical behavior of block copolymers to that of linear segmented polyurethanes and suggested the presence of microdomains in the latter on this basis. Techniques such as small angle x-ray scattering (SAXS), differential scanning calorimetry (DSC), dynamic mechanical analysis (DMA), and electron microscopy have been used to establish the existence and/or the extent of phase segregation (2-6). Aside from directly imaging the microdomains by microscopy these techniques infer phase separation from the presence of a low angle interlamellar peak (SAXS) or the existence of two separate Tg's, one for the soft segment and one for the hard segment (DSC, DMA), and an elevated plateau modulus (DMA).

Extensive studies concerning the effect of the chemical structure, the molecular weight, and molecular weight distribution of the soft and the hard segments on the extent of phase segregation, domain formation and thus polymer properties have been reported (7-15). The effect of hydrogen bonding on hard and soft segment mixing in polyurethane elastomers has also been studied (16-22). Because of the complex structure of polyurethane materials,

the structure-property relationships of these materials are still not completely understood.

1.2 Transport Properties

An understanding of the transport behavior in multiphase polymers is important in terms of applications: membranes for novel gas separations, transport of liquids as in the case of reverse osmosis, membrane reactors in biotechnology, selective gas permeabilities in the food packaging industry, enhancement of impurity removal, and various biomedical applications. Particularly, block copolymers have the ability to provide a wide range of structures and properties and hence, a large number of potential applications.

A substantial amount of work has involved modeling the diffusion and sorption behavior in a variety of penetrant-polymer systems at conditions below and above the glass transition temperature, and a number of experiments have been carried out to investigate the transport properties for homopolymers and heteropolymers. However, the small molecule transport behavior of polyurethane block copolymers has received little attention. In the past, studies of transport in polyurethanes have concentrated mainly on water vapor sorption (23,24) and gas diffusion (25-27). Recently, Goydan et al. (28) have studied the incremental vapor sorption and desorption for a commercial polyurethane, Estane, with ortho-dichlorobenzene as a solvent, and a two-stage sorption anomaly

was observed at intermediate and high vapor concentrations, but was generally absent in the desorption runs. It was postulated that the two-stage sorption curves are related to a relaxation process in the hard segment induced by the presence of the solvent. To define this non-Fickian two-stage sorption behavior further studies of the solvent vapor sorption and diffusion in segmented polyurethanes are clearly needed.

1.3 Objective

The principle objective of this work is to determine the extent of interaction of the chosen solvent, 1,2-dichloroethane, with the hard segment phase in a variety of polyurethanes which consist of different diphenylmethane-4,4'-diisocyanate (MDI) : 1,4-butanediol (BD) : polytetramethylene oxide (PTMO) ratios as well as different molecular weights of PTMO soft segments by conducting incremental vapor sorption and desorption experiments. The sorption isotherms, the behavior of the diffusion coefficient as a function of solvent concentration, and the extent of any relaxation effect are determined. The diffusion behavior for samples of various film thicknesses and for heat treated samples, as well as the hysteresis studies in terms of the transport behavior have also been investigated. The diffusion coefficient was calculated by the initial slope method for Fickian curves, while, for non-Fickian curves, the

diffusivity was determined by the Joshi and Astarita equation (29) This equation was also used to fit the experimental data.

In addition, to understand the results of the vapor sorption experiments, the structure and properties of polyurethane materials were determined by performing DSC, dynamic mechanical thermal analysis (DMTA), and tensile testing analysis. Moreover, the effect of swelling on the structure and properties of polyurethanes was studied by DSC and nuclear magnetic resonance (NMR), with particular emphasis on the response of the hard domains. Combining the incremental vapor sorption and desorption experiments with those complementary analytical techniques, the effect of solvent sorption on the structure and properties of polyurethanes can be defined.

1.4 Scope of the Dissertation

This dissertation investigates the diffusion and sorption behavior of the solvent vapor in the polytetramethylene oxide polyurethanes. The structure and properties of these materials were also studied in order to understand the transport properties of the polyurethanes. Chapter II briefly reviews the structure and properties of segmented polyurethanes. An overview of the transport of small molecules in rubbers, glasses, and into a particular class of multiphase block copolymers is described in chapter III in terms of experimental observations and theoretical background.

The experimental results of studies of structure and properties in a variety of polyurethanes are given in chapter IV. DSC, DMTA, and tensile tests were used to determine the extent of phase segregation, soft and hard segment Tg's, the crystallinity of the hard phase, the storage and loss moduli, and the stress-strain behavior.

Studies of incremental vapor sorption and desorption of solvent vapor in segmented polyurethanes are described in chapter V. The experimental apparatus and experimental results in terms of sorption isotherm, diffusion behavior, diffusivity as a function of solvent concentration and calculation of diffusion coefficient are presented in this chapter.

Chapter VI examines the interaction between the solvent and polymer, with particular emphasis on the response of the hard domains. DSC and NMR techniques were used to determine the effect of the swelling on the molecular motions in the hard phase. In addition, suggestions for future work are also given in this chapter.

1.5 References

1. S. L. Cooper and A. V. Tobolsky, J. Appl. Polym. Sci., 10, 1837 (1966).

2. S. B. Clough, N. S. Schneider, and A. King, J. Macromol. Sci.- Phys., B2, 641 (1968).

3. C. S. P. Sung, and N. S. Schneider, J. Mat. Sci., 13, 1689 (1978).

4. C. G. Seefried, Jr., J. V. Koleske, and F. E. Critchfield, J. Appl. Polym. Sci., 19, 2493 (1975).

5. T. R. Hesketh, J. W. C. Van Bogart, and S. L. Cooper, Polym. Eng. Sci., 20, 190 (1980).

6. N. S. Schneider, and C. S. P. Sung, Polym. Eng. Sci., 17, 73 (1977).

7. L. L. Harrell, Jr., Macromolecules., 2(6), 607 (1969).

8. N. H. Ng, A. E. Allegrezza, Jr., R. W. Seymour and S. L. Cooper, Polymer, 14, 255 (1973).

9. C. G. Seefried, J. V. Koleske and F. E. Critchfield, J. Appl. Polym. Sci., 19, 2493 (1975).

10. C. G. Seefried, J. V. Koleske and F. E. Critchfield, J. Appl. Polym. Sci., 19, 2503 (1975).

11. C. G. Seefried, J. V. Koleske, F. E. Critchfield, and J. L. Dodd, Polym. Eng. Sci., 15, 646 (1975).

12. C. S. P. Sung and N. S. Schneider, Macromolecules., 10, 452 (1977).

13. N. S. Schneider, C. S. P. Sung, R. W. Matton, and S. L. Illinger, Macromolecules., 8, 62 (1975).

14. C. S. P. Sung and N. S. Schneider, Macromolecules., 8, 68 (1975).

15. Z. Ophir and G. Wilkes, J. Polym. Sci.-Phys., 18, 1469 (1980).

16. Y. M. Boyarchuk, L. Y. Rappoport, V. N. Mikitin, and N. P. Apukhtine, Polym. Sci. USSR, 7, 859 (1965).

17. T. Tanaka, T. Yokeyama, and Y. Yamaguchi, J. Polym. Sci., 6(A1), 2137 (1968).

18. K. Nakayama, T. Ino, and I. Matsubura, J. Macromol. Sci. Chem., A3(5), 1005 (1969).

19. R. W. Seymour, G. M. Estes and S. L. Cooper, Macromolecules, 3, 579 (1970).

20. R. W. Seymour and S. L. Cooper, Macromolecules, 6, 48 (1973).

21. W. J. Macknight and M. Yang, J. Polym. Sci., Polym. Symp. Ser., 42, 817 (1973).

22. V. W. Srichatrapimuk and S. L. Cooper, J. Macromol. Sci.-Phys., B15(2), 267 (1978).

23. N. S. Schneider, L. V. Dusablon, E. W. Snell and R. A. Prosser, J. Macromol. Sci.-Phys., B3(4), 623 (1969).

24. J. A. Barrie and A. Nunn, Div. Org. Coat. Plast. Chem. Pap., 34, 489 (1974).

25. K. D. Ziegel, J. Macromol. Sci., B5, 11 (1971).

26. J. S. McBride, T. A. Massaro and S. L Cooper, J. Appl. Polym. Sci., 23, 201 (1979).

27. M. Serrano, Ph.D. Thesis, Univ. of Massachusetts, 1986.

28. R. Goydan, N. S. Schneider, and J. Meldon, Polym. Mater. Sci. Eng., 49, 249 (1983).

29. S. Joshi and G. Astarita, Polymer, 20, 455 (1979).

C H A P T E R II

REVIEW OF STRUCTURE AND PROPERTIES

Considerable attention has been devoted toward an understanding of the property-structure relationships in segmented polyurethanes in the last decade. The polyurethane synthesis, studies of hard segment length distributions, the characteristics of phase segregation, polyurethane morphology, and the mechanical properties of polyurethanes have been studied extensively. Literature concerning the studies of structure and properties is reviewed in this chapter in terms of phase separation, hydrogen bonding, morphology, and mechanical properties.

2.1 Phase Separation

The segmented polyurethanes are the reaction products of a macroglycol, a diisocyanate, and a diol or diamine. The soft segments are the hydroxy-terminated polyesters, polyethers, or polybutadienes with molecular weight ranges from 600 to 3000, and are composed of a rubbery polymer with its glass transition temperature well below the use temperature. The hard segments, which are generally formed from the extension of an aromatic diisocyanate with a low molecular weight diol provide physical crosslinking and reinforcement for the soft phase and are

responsible for the higher temperature performance. Much of the interest in these materials arises from their thermal reversibility which allows them to be processed conventionally as thermoplastics at high temperatures but behave like crosslinked elastomers upon cooling.

Most of the usable properties of polyurethanes are a result of phase segregation. The existence of phase segregation, caused by the clustering of hard and soft segments into separated domains, has been well documented (1-3). Clough et al. (1) studied polyurethanes with MDI/BD hard segments and polyester and polyether soft segments. The results indicate that in general phase segregation occurs to a higher degree in the polyether-based elastomers than in the equivalent polyester-based samples. The explanation given for the better phase separation in the polyether-based polyurethanes is that the carbonyl of the polyester soft segment is a much more effective hydrogen bond acceptor than is the polyether oxygen. Hence this greater specific interaction between hard and soft segments enhances phase mixing for polyester-based polyurethanes. The extent of phase segregation is determined by the type and composition of the formulation as well as the method and condition of polymerization. It is generally accepted that longer segmental lengths (molecular weights) improve the degree of phase segregation (4-10); higher hard segment content results in more hard segment mixing into the soft phase (8,9,10), and that polar soft segments which form strong interactions, such as hydrogen bonding, with the hard segment

exhibit a higher degree of phase mixing (4,11,12). Hesketh et al. (5) investigated polyurethanes with 1000 and 2000 molecular weight poly(tetramethylene oxide)(PTMO) soft segments and MDI+BD hard segments using differential scanning calorimetry (DSC) at various annealing temperatures. The Tg's of the soft segment of 1000 MW PTMO are in the range of -30 to -40°C, however, for 2000 MW PTMO sample, the Tg of the soft segment is about -70°C, indicating an improved phase segregation for samples with 2000 MW soft segment. Bogart et al. (9) studied the structure-property relationships of polycaprolactone-based segmented polyurethanes using DSC, small-angle x-ray scattering (SAXS), wide-angle x-ray diffraction (WAXD), dynamic mechanical analysis, and tensile testing. In general, increasing the soft-segment molecular weight from 830 to 2000 at a fixed hard-segment length gives (i) materials with lower tensile strength because the hard-segment content is lower, (ii) copolymers in which the amount of interfacial material relative to purer soft-segment material decreases dramatically, (iii) an increased tendency of the soft segments to crystallize, especially at low hard-segment content, and (iv) an increased tendency for the hard-segment domains to be isolated in the soft-segment matrix, indicating a better phase separation. The effects of increasing hard-segment content at constant soft-segment molecular weight are (i) increased crystallinity, (ii) increased hard-segment crystalline melting point due to the thicker lamellae possible with large hard segments, (iii) increased tendency of the materials to form a morphology with a

hard-segment matrix and isolated soft-segment domains, and increased interfacial area. At a soft-segment molecular weight of 830, increasing the hand-segment content leads to a large amount of phase-mixed material, resulting in a higher Tg of the soft segment, whereas for the 2000-MW soft segment materials, there is not as noticeable an effect on phase mixing because the ratio of phase-mixed or interfacial material to purer soft-segment material is much less. The above observations are general for segmented polyurethanes.

The influence of the soft segment type, i.e., polyester versus polyether, on the morphology of segmented polyurethanes was investigated by SAXS (11). The results suggest that in both materials the two-phase structure can be described somewhat as alternating regions of soft and hard segments. A wider transition zone in the polyester than in the polyether based urethane was observed, indicating the stronger interactions between the soft and hard segments in the case of polyester soft segments (more polar). Recently, Miller et al. (13) studied the effects of hard segment length distribution on the properties of polyether-based polyurethane block copolymers. Two sets of polyether-polyurethane block polymers, single-step and multistep polymerized samples, based on PTMO, MDI and BD were prepared to produce materials with equivalent stoichiometries but different hard segment length distributions. The results indicated that the multistep materials exhibit a greater degree of phase mixing, as the very short hard

segments are more likely to be dissolved in the soft phase than are longer hard segments. The hard phase volume fraction and crystallinity are greater in the single-step materials due to the lower degree of phase mixing in these polymers. The results of IR spectroscopy, DSC, DMA, stress-strain testing, and SAXS are all shown to be consistent with the differences in hard segment length distributions and the differences in phase mixing which accompany the distributional differences.

Crystallization in either hard or soft segments plays an important role in segmented polyurethanes, providing another driving force for phase segregation. The existence of crystallinity in both phases has been well documented. Electron microscopy reveals a characteristic structural organization consisting of poorly organized spherulites with an open fibrous texture in which the strands appear to be built up from microfibils for MDI-based polyurethanes (14). The crystalline melting peaks were observed by DSC measurement, and WAXD provides the degree of crystallinity. Briber and Thomas (15) investigated the MDI, BD and PPO-EO polyurethanes with optical and electron microscopy, electron diffraction, and WAXD. Two crystal forms of the hard segment have been observed, with their associated spherulites. Type I crystals are intrinsically disordered and exhibit only a few diffuse diffraction rings. Type II crystals form negative spherulites. Dark-field electron microscopy indicates that type II crystals are lath shaped and average about 12nm in width by about 50-70nm in

length. Type I crystals were not able to be resolved by dark-field on bright-field transmission electron microscopy, indicating that the crystals are very small, less than 10 nm.

Bogart et al. (9) have compared the phase segregation differences between crystalline MDI and non-crystalline H_{12}MDI based polyurethanes with the other constituents being identical. SAXS results indicate that the interfacial thickness of the amorphous hard segment material (H_{12}MDI) was significantly greater than that for the crystalline hard segments. Observed phase segregation in the materials of Harrell (16) most likely arises from the crystalline non-hydrogen bonded hard segments.

2.2 Hydrogen Bonding

The role of hydrogen bonding in phase segregation is not completely understood even though it is often used as a semi-quantitative measure of the extent of phase mixing (17). It is certain that the extent of hydrogen bonding is an important factor in phase mixing. Practically all polyurethanes are extensively hydrogen bonded. The hydrogen bond donor is the N-H group of the urethane linking and the acceptor could be either oxygen of the urethane or ester linkage or the ether oxygen of the soft segment.

Relative amounts of the hydrogen bonds are determined by the degree of microphase segregation, with increasing phase segregation favoring interurethane hydrogen bonding. The distribution of NH

bonding with respect to each type of acceptor depends on many factors, including the electron donating ability and relative proportions and spatial arrangement of the various proton acceptor groups in the polymer chain. Direct measurement of the extent and nature of H-bonding in polyurethanes and its influence on physical properties is still in an early stage of investigation.

The literature concerning the nature and extent of hydrogen bonding in polyurethane is extensive and has been reviewed by Seymour et al (18). The principal objective of these studies is to determine the distribution of H-bonds among the various possible acceptors. Infrared spectroscopy has proven to be a useful technique for polyether-, but not polyester-based polyurethanes by using the different vibration frequencies for free and H-bonded groups. It is generally found that in solid polyurethanes the majority of NH groups are involved in H-bonding, but only part of the urethane C=O are H-bonded (18,19). The extent of soft-hard phase mixing can be qualitatively estimated as the fraction between the difference of H-bonded N-H and H-bonded C=O stretching. However, this usually overestimates the extent of phase mixing since there are other parameters involved: (1) the possibility of urethane alkoxyl oxygen as a hydrogen acceptor, (2) the formation of H-bonding at the domain-matrix interface, (3) the restructuring of H-bonding, and (4) the dependence of H-bonding on morphology, hence the thermal and mechanical history.

Hydrogen bonding is likely to occur at the domain-matrix interface and should be treated differently from the actual phase mixing, i.e., the solubilization of hard segments into soft segments. Therefore, the fraction of actual phase mixing should be less than that calculated from the difference between H-bonded NH and CO. The interfacial H-bonding is expected to be related to the size and shape of the hard segment domains (18). If domain size is the only variable, the smaller domains should result in the higher concentration of interfacial H-bonding. However, there should be a critical domain size under which there is virtually no difference from actual phase mixing. Hydrogen bonding has been shown to influence morphological features such as crystalline chain ordering in semicrystalline polyurethanes (20). The relationship between H-bonding and thermal transitions in segmented polyurethanes is not clear. Sung and Schneider (21) studied the temperature dependence of H-bonding in PTMEG(1000Mn)/2.4-TDI/BD system where the free and bonded carbonyl absorptions showed little change from 0 to 150°C while 50% of the NH groups had dissociated by 150°C. They concluded that the thermal behavior of H-bonding is essentially independent of structure organization.

2.3 Morphology

Polyurethane morphologies are generally not well characterized. Briber (22) has compared a large number of morphological models that

have been proposed and concluded that none were sufficient to explain all the characteristics of polyurethanes. This is due to the variety of factors affecting polyurethane morphology: hard and soft segment polarity, presence of crystallinity, segment length and length distribution, volume fraction of each phase, method of sample preparation, and thermal and mechanical history of the sample.

Direct imaging of the domains by electron microscopy is difficult due to the lack of a significant degree of phase contrast, and the small size of the domains with respect to available speciman thickness. This method is also susceptible to artifacts and a critique of polyurethane morpholo-gical electron microscopy studies has been recently published (23). The morphology of polyurehtanes has been shown to be highly complicated (14,15,24,25), especially crystalline systems (22). Results of a study by Lunardon et al. (26) showed that three phases coexist in a crystalline polyurethane: a soft phase, a crystalline hard phase, and an interfacial phase.

2.4 Mechanical Properties

The commercial interest in polyurethanes derives from the variety and utility of the mechanical properties obtainable by use of different chemical systems. The mechanical properties of polyurethanes are greatly influenced by the size, shape and concentration of the hard segment domains, the deformational resistance of the hard domains, and the orientation of the segments

under strain (27,28). Generally, the polymer morphology has an overriding influence on mechanical properties. The hard domains in polyurethane thermoplastic elastomers increase both modulus and ultimate strength in roughly the same fashion as the particulate reinforcement of rubber (29). Plastic domains increase strength by preventing catastrophic crack propagation through the material. This is accomplished by the deflection or bifurcation of cracks, cavitation, and plastic deformation of the hard segment domains, which dissipate energy. Only two phase elastomers exhibit toughness over extended ranges of temperature and time or strain rate. Another reinforcing mechanism may also arise from the orientation of the chains, resulting in strain-induced crystallization of the soft segment.

The effect of hard segment content on polyurethane mechanical properties is quite pronounced. At low hard segment concentrations, the polyurethane is a thermoplastic elastomer with discrete reinforcing hard segment domains. For high hard segment content polyurethanes, the situation is reversed, with the soft segments serving as rubber modifiers for the continuous hard segment matrix. It is possible to tailor the mechanical properties for various end uses by changing the hard segment concentration.

The hard segment type also has been shown to affect the mechanical behavior of polyurethanes. Hard segments with crystallinity or higher cohesiveness usually increase the mechanical properties of the material. For example, crystalline hard segments

based on MDI are used in RIM processes for production of stiff structural materials, while polyurethanes with amorphous TDI based hard segments are generally only useful in soft form applications. Polyurethanes with urea hard segments usually have properties superior to those from urethane hard segments of similar composition (an oxygen is replaced by N-H). The more polar nature of the urea leads to more stable hard domains, resulting in enhancement of the properties.

2.5 References

1. S. B. Clough, N. S. Schneider and A. O. King, J. Macromol. Sci.- Phys., B2, 641 (1968).

2. G. M. Estes, S. L. Cooper and A. V. Tobolsky, J. Macromol. Sci., Rev. Macromol. Chem. C4(2), 313 (1970).

3. R. Bonart, L. Moribigzer and G. Hentze, J. Macromol. Sci., B3(2), 337 (1969).

4. C. S. Paik Sung and N. S. Schneider, J. Mat. Sci., 13, 1689 (1978).

5. T. R. Hesketh, J. W. C. Van Bogart, and S. L. Cooper, Polym. Eng. Sci., 20, 190 (1980).

6. N. S. Schneider and C. S. Paik Sung, Polym. Eng. Sci., 17, 73 (1977).

7. C. S. P. Sung, T. W. Smith, and N. H. Sung, Macromolecules, 13, 117 (1980).

8. J. W. C. Van Bogart, A. Lilaonitkul, L. E. Lerner, and S. L. Cooper, J. Macromol. Sci.-Phys., 17, 267 (1980).

9. J. W. C. Van Bogart, P. E. Gibson, and S. L. Cooper, J. Polym. Sci.-Phys., 21, 65 (1983).

10. C. B. Hu, R. S. Ward, Jr., and N. S. Schneider, J. Appl. Polym. Sci., 27 2167 (1982).

11. Z. Ophir and G. Wilkes, J. Polym. Sci.-Phys., 18, 1469 (1980).

12. R. W. Seymour and S. L. Cooper, J. Polym. Sci., B9, 689 (1971).

13. J. A. Miller, S. B. Lin, K. K. S. Hwang, K. S. Wu, P. E. Gibson, and S. L. Cooper, Macromolecules, 18, 32 (1985).

14. N. S. Schneider, C. R. Desper, J. L. Illinger, A. O. King and D. Barr, J. Macromolecular Sci.-Phys., B11(4), 527 (1975).

15. R. M. Briber and E. L. Thomas, J. Macromol. Sci.-Phys., B22(4), 509 (1983).

16. L. L. Harrell, Jr., Macromolecules, 2, 607 (1969).

17. C. M. Brunette, Ph. D. Thesis, University of Massachusetts (1982).

18. R. W. Seymour, G. M. Estes, and S. L. Cooper, Macromolecules, 3, 579 (1970).

19. T. Tanaka, T. Yokoyama, and Y. Yamaguchi, J. Polym. Sci., Part A-1, 6, 2153(1968).

20. R. Bonart, J. Macromol. Sci.-Phys., B2, 115 (1968).

21. C. S. P. Sung and N. S. Schneider, Macromolecules, 10, 452 (1977).

22. R. Briber, Ph. D. Thesis, University of Massachusetts (1984).

23. E. J. Roche and E. L. Thomas, Polymer, 22, 333 (1981).

24. A. L. Chang, R. M. Briber, E. L. Thomas, R. J. Zdrahaln, and F. E. Critchfield, Polymer, 23, 1060 (1982).

25. I. D. Fridman, E. L. Thomas, L. J. Lee, and C. W. Macosko, Polymer, 21, 393 (1980).

26. G. Lunardon, Y. Sumida, and O. Vogl, Angew Makromol. Chem., 87, 1 (1980).

27. L. E. Nielson, Rheol. Acta., 13, 86 (1974).

28. S. L. Aggarwal in "Block and Graft Copolymers", eds. J. Burke and V. Weiss, Syracuse University Press (1973), P. 157.

29. T. L. Smith, J. Polym. Sci.-Phys., 12, 1825 (1974).

C H A P T E R III

OVERVIEW OF TRANSPORT PHENOMENA

The earliest studies of the transport of fluids in polymers consisted of measuring permeation rates of various gases in natural rubber membranes and correlating the measured rates with the partial pressure difference across the membrane, the membrane thickness, and the temperature. The objective of later studies has been to define and model the sorption and transport processes that underlie permeation, to devise and implement experimental methods for determining model parameters, to seek correlations that allow the estimation of transport properties of unstudied penetrant-polymer pairs, or of studied pairs under previously unstudied conditions, to apply physical and thermodynamic theories of solution, diffusion, and stress relaxation in polymers to predict the dependence of transport and solubility coefficients on measurable system variables, to modify polymer compositions and structures in order to achieve or enhance desired permeability characteristics, and use measured transport rates and their dependences on experimental conditions to elucidate structure of polymers.

The objectives of this chapter are to, first of all, briefly describe the theoretical background in terms of the definition and determination of the diffusion coefficient and Fickian and non-Fickian features, and then, to review the experimental observations

and mathematical models of diffusion in rubbers, glasses, and multiphase polymers. The formidable amount of literature on this subject makes necessary the selection of a restricted number of references which comprise the relevant aspects of both experimental observations and theoretical models. More detailed expositions of the theory may be found in the comprehensive volume of Crank (1,2) and Park (1).

3.1 Fundamental Background

Fick, in 1855, first put diffusion on a quantitative basis by adopting the mathematical equation of heat conduction derived some years earlier by Fourier. The mathematical theory of diffusion in isotropic substances is therefore based on the hypothesis that the rate of transfer of a diffusing substance through unit area of a section is proportional to the concentration gradient measured normal to the section, i.e.

$$J = -D\left(\partial C/\partial X\right) \qquad (3.1)$$

where J is the rate of transfer per unit area of section, C the concentration of diffusing substance, X the space coordinate measured normal to the section, and D is called the diffusion coefficient. In some cases, e.g. diffusion in dilute solutions, D can reasonably be taken as constant, while in others, e.g. diffusion

in high polymers, it depends very markedly on concentration.

Wroblewski in 1879 postulated that the sorption of a gas at the surface of a rubber exposed to a gas obeys Henry's law

$$C = SP \qquad (3.2)$$

where C is the dissolved species concentration in equilibrium with a gas whose partial pressure is P, and that the absorbed gas diffuses through the membrane in accordance with Fick's law, equation 3.1. The solubility and diffusion coefficient S and D were assumed independent of concentration. Wroblewski showed that if these assumptions are valid, the steady-state permeation rate per unit area through a membrane of thickness h is

$$J = D\ S\ (\Delta P/h) = (P/h)\Delta P \qquad (3.3)$$

where ΔP is the partial pressure difference across the membrane. The product DS is the permeability of the membrane to the penetrant.

In 1944, Matthes observed a systematic deviation from Henry's law in the sorption of water by hydrated cellulose membranes. He postulated that two competitive phenomena were occurring: dissolution, which obeyed Henry's law, and adsorption, which followed a Langmuir isotherm, and he wrote the total isotherm as the sum of the isotherms corresponding to each phenomenon:

$$C = (abP/1+bP)+KP \qquad (3.4)$$

where the first term on the right is the Langmuir isotherm and the second one, KP, is Henry's law, and a and b are constants.
A similar hypothesis forms the basis of the modern theory of the transport of gases in glassy polymers (dual mode sorption), as discussed in a later section. Since then, a large number of investigators have found and, to a large degree, explained many systematic deviations from the ideal case of Henry's law sorption and Fickian diffusion with concentration-independent diffusion coefficients. The features of Fickian and non-Fickian diffusion are given in the following section.

3.2 Fickian and Non-Fickian Diffusion

Polymers above their glass transition temperature respond rapidly to changes in their condition (1,2). A rubbery polymer film exposed to a constant activity reservior of a smaller molecule capable of diffusing in the film (the penetrant) achieves very rapidly a constant penetrant concentration at the exposed film interface. This sorption equilibrium is achieved in times very much shorter than the characteristic times involved in the diffusion of the penetrant. In glassy polymers, there appear to be significant contributions to transport processes from longer relaxation time

parts of the characteristic spectrum of the polymer. In the presence of the penetrant motions of whole or portions of glassy polymer chains are not sufficiently rapid to completely homogenize the penetrant's environment. Penetrant can thus potentially sit in holes or irregular cavities with very different intrinsic diffusional mobilities. Assink (3) investigated the sorption of ammonia in polystyrene by NMR techniques, and proved the existence of these local heterogeneities. In addition, an examination of the validity of assuming that the molecules exchange rapidly between sites and that the absorbed species is relatively immobile found that both assumptions were substantially correct according to the relaxation data. However, Sefcik and Schaefer (4) found that the presence of small amounts of CO_2 in poly(vinyl chloride) (PVC) results in increased main-chain motions of the polymer as measured by the carbon rotating-frame relaxation rate from NMR techniques. These results cannot be reconciled with those of Assink, who claims that the gas molecules preferentially occupy preexisting sorption sites in a conditioned polymer with no perturbation of the polymer matrix. Further studies will be required to clarify these discrepancies.

The mathematical description (2) of the sorbed polymer transport in rubbery films (free of holes) is considerably simplified by the following: (i) Transport occurs by molecular diffusion satisfying Fick's first and second laws. (ii) The boundary conditions (BC) which usually apply at the film surface x=0, l are

constant values of the penetrant concentration, c, by virtue of the rapidly established sorption equilibrium. Fick's laws yield for one dimensional isothermal, isopiestic diffusion, in homogeneous films of sufficiently large area, the diffusion equation

$$\partial c/\partial t = \partial [D(c)\ (\partial c/\partial x)]/\partial x \qquad 0 < x < 1 \qquad (3.5)$$

The choice of frame of reference employed in equation 3.5 usually dictates the choice of the penetrant concentration unit employed to specify c and the nature of the mutual diffusion coefficient D(c). The latter is a product of a thermodynamic factor (the partial derivative of the chemical potential difference of the penetrant with respect to the logarithm of its concentration) and a mobility factor (sometimes called the self-diffusion coefficient). Both of these factors are only functions of the local thermodynamic variables, c, the absolute temperature and the total hydrostatic pressure difference; but not the time t.

The usual boundary conditions (BC) are:

$$C(0,t) = C_0\ , \qquad C(1,t) = C_1 \qquad (3.6)$$

with C_0 and C_1 constants. The boundary value problem requires also specification of an initial condition

$$C(x,0) = C_i \qquad (3.7)$$

where C_i is usually chosen experimentally to be a constant but could be a suitable function of x. Equations 3.5-7 describe: (a) desorption, when $C_0=C_1=0$, (b) sorption, when $C_0=C_1>C_i$ and (c) permeation, when $C_0>C_1$ and $C_0 \geqslant C_i$. In general, D(c) must be at least once continuously differentiable with respect to x and must satisfy the inequality

$$0 < D(c) \leqslant D_0 < \infty \qquad (3.8)$$

in $0 \leqslant x \leqslant 1$ in order that the boundary-value problem be well posed. The lower bound prevents "up-hill" diffusion and the upper bound prevents states of infinite dissipation. The complete boundary value problem, equations 3.5-7, together with equation 3.8 specifies mathematically what is called Fickian diffusion. It should be noted that a system will exhibit Fickian diffusion if Fick's first and second laws are obeyed with a history independent (no explicit time dependent) D and the time independent BC. The usual experimental arrangements for studying diffusion in rubbery polymers lead to systems which exhibit Fickian diffusion. Crank (2) and Fujita (5) have given excellent lists of the experimental characteristics of Fickian sorption and permeation curves, and the following is a summary of the features of particular importance in Fickian diffusion.

(a) Both sorption and desorption curves in $t^{1/2}$ coordinate are initially linear. For sorption with constant diffusivity the linear

region extends 60% of M_∞ , when the diffusion coefficient increases with concentration, the linear portion may be even greater.

(b) Both sorption and desorption curves are concave to the abscissa beyond the linear portion, irrespective of the form of D(c).

(c) A series of sorption curves for films of different thickness, with fixed initial and final concentrations, may be superimposed to form a single curve if each curve is plotted in reduced form, i.e. M_t vs. $t^{1/2}/l$. This also applies to the corresponding series of desorption curves.

(d) Reduced sorption curves always lie above the corresponding reduced desorption curves if D is an increasing function of c over the concentration interval. Both reduced curves coincide when D is constant. The divergence of the two curves becomes more marked as D varies more strongly with c.

Departures from Fickian diffusion can occur for many reasons. For instance, if sorption equilibrium cannot be achieved at a film surface (even if the film is rubbery) say because of an appreciable surface evaporation rate, sorption curves exhibit an inflection point and thus are sigmoidally non-Fickian (2). A useful classification scheme for non-Fickian diffusion and sorption associated with glassy polymers has been proposed by Alfrey et al. (6), also by Crank (2), and extended by Frisch (7). Three basic classes of diffusion behavior may be distinguished. (i) Case I or Fickian diffusion in which the rate of diffusion is much less than that of relaxation due to mechanical, structural, etc. modes of the

polymer-penetrant system. Sorption equilibrium is rapidly established leading to time independent BC exhibiting no dependence on swelling kinetics. (ii) Case II (6) or super Case II (8) transport, the other extreme in which diffusion is very rapid compared with other relaxation processes. Sorption processes may be complicated by strong dependence on swelling kinetics but there is no direct experimental data on the nature of the final equilibrium state of sorption. (iii) Non-Fickian or anomalous diffusion which occurs when the diffusion and relaxation rates are comparable. On the other hand, the diffusion coefficient is a function of both penetrant concentration and time. For simple gas and hydrocarbon vapor penetrants which have been studied, equilibrium sorption curves appear to contain additive contributions from a Henry's law solubility type term and a Langmuir adsorption contribution (dual mode sorption (9)). The latter contribution is envisioned to arise from penetrant molecules which are more or less partially immobilized at fixed sites in the medium.

Hopfenberg and Frisch (10) have summarized the observed transport phenomena in a graph, which is shown in Figure 3.1 as a plot of temperature vs. penetrant activity. For activities from 0 (infinitely dilute vapor) to 1 (pure liquid or saturated vapor) at temperatures well below Tg and for all temperatures at activities close to 0, concentration-independent Fickian diffusion is generally observed. At higher temperatures and activities, the diffusion coefficient exhibits a dependence on concentration. Still closer to

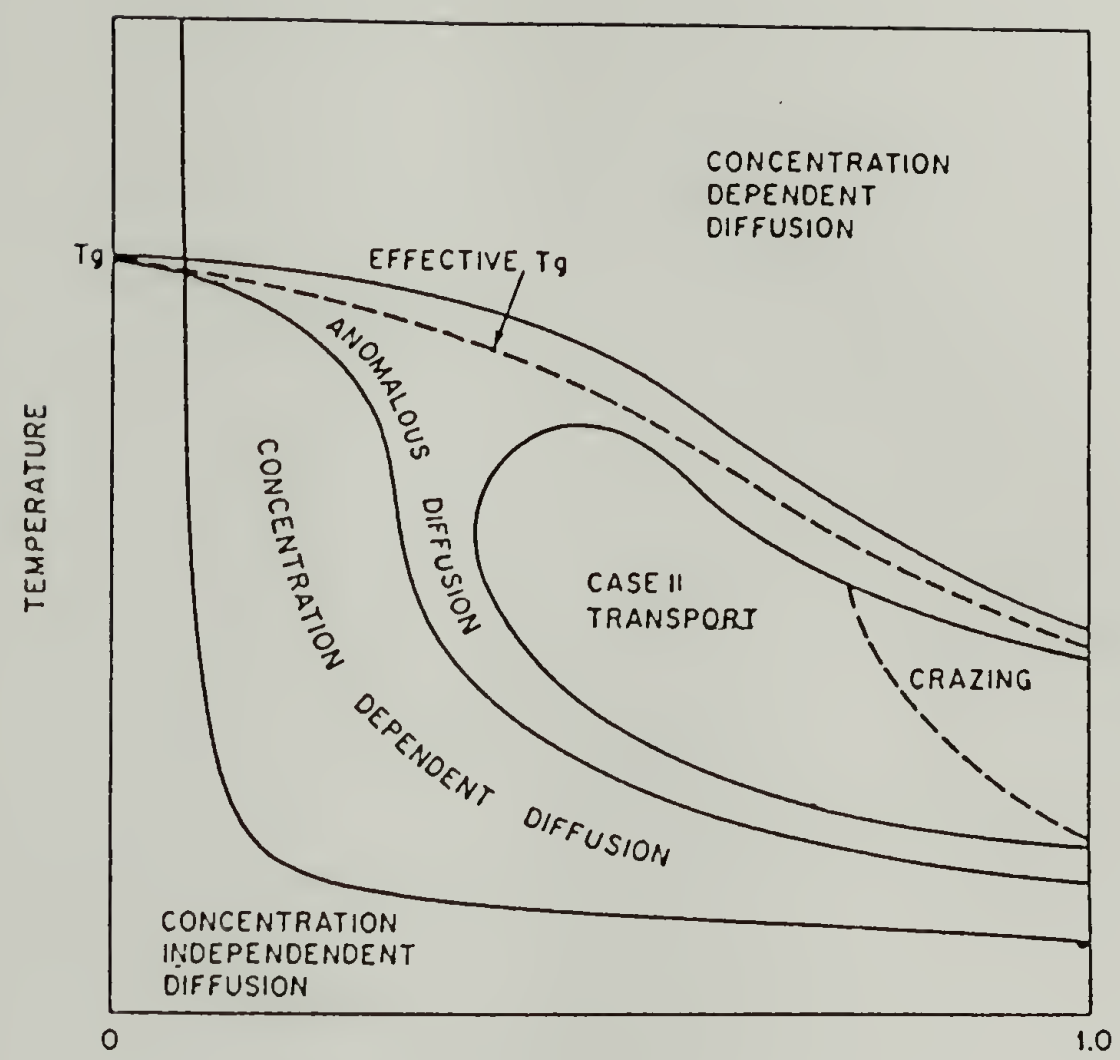

Figure 3.1 Hopfenberg-Frisch chart of anomalous transport phenomena.

Tg, D begins to depend on time explicitly as well as on concentration. The effective value of Tg itself decreases with increasing penetrant activity.

At moderate penetrant activities when swelling is appreciable and the temperature is less than but within about 10°C of Tg, the mechanism of penetration may change from Fickian diffusion to a stress relaxation-controlled process in which the penetrant advances in a sharply defined front at a nearly uniform velocity. This mechanism has been designated case II Transport. At sufficiently high penetrant activities, stress cracking and solvent crazing may occur. The term "anomalous diffusion" is used to designate transport under conditions where a combination of case I (Fickian) and case II diffusion takes place.

The two given modes of transport are easily distinguished using the results of sorption measurements. If M_t denotes the cumulative mass absorbed in the sorption run, then in both modes at small time t,

$$M_t = K \cdot t^n \qquad (3.9)$$

If case I transport occurs, n=1/2, while for case II transport n=1 (6). For super-case II transport which has been observed in the sorption of n-hexane vapor by a 1.5 mil polystyrene film (8), n>1. Its distinguishing characteristic is a sorption curve convex to the time axis at large times on a plot of penetrant uptake vs. time,

where a similar plot would be linear for case II transport and concave for case I transport. The phenomenon is attributed to the interaction of the Fickian tails that precede the case II fronts advancing toward the film midplane from both membrane boundaries.

A quantitative basis for the correlations of Hopfenberg and Frisch (10) has been derived by Vrentas et al. (11,12), who define a dimensionless group called a diffusional Deborah number:

$$(Deb)_D = \zeta_m/(x^2/D^*) \qquad (3.10)$$

where ζ_m is the characteristic stress relaxation time of the polymer-penetrant system at the condition of interest, D^* the molar average of the self-diffusion coefficients of the polymer and penetrant, and x a characteristic dimension of the polymer (e.g., the thickness of a membrane or the diameter of a sphere). For Fickian diffusion, $(Deb)_D << 1$ and $(Deb)_D >> 1$, while for anomalous behavior, $(Deb)_D$ is on the order of 1. A graphical representation of what is presumably a typical temperature-concentration diagram for an amorphous polymer-penetrant system is presented in Figure 3.2 (11). Three proposed regions of diffusional transport, separated by lines of constant $(Deb)_D$, are included in this figure as well as a curve representing the effective glass transition temperature Tg of the polymer-penetrant system as measured by experiments of conventional duration. T_E is the temperature below which pure polymer acts like an elastic solid, and T_V is the temperature above

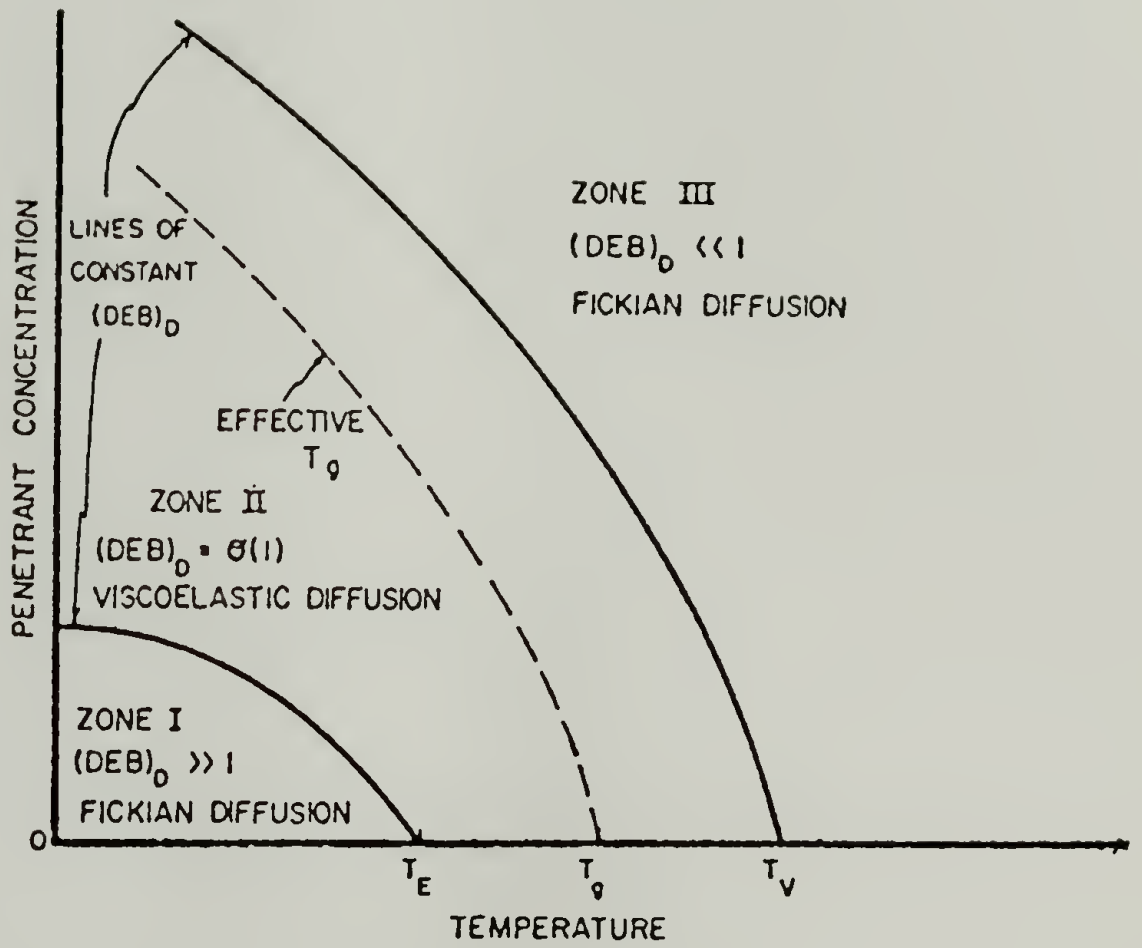

Figure 3.2 General temperature-penetrant concentration diagram.

which pure polymer acts like a viscous fluid. As can be seen from Figure 3.2, for $(Deb)_D$=O(1) (say from 0.1 to 10), we have diffusing molecules moving in a viscoelastic binary mixture. As the penetrant diffuses into the polymer, rearrangement of the polymer chains differs, in general, from the equilibrium structure of the polymer at the concentration of interest. Diffusion behavior in zone II is sometimes called anomalous transport because the influence of relaxation on the diffusive process leads to non-Fickian effects in permeation and sorption experiments.

Experiments in which swelling penetrants are sorbed by glassy polymers are frequently characterized by a rapid approach to an apparent equilibrium state, followed by a gradual shift to the true equilibrium state. This phenomenon has been attributed to a gradual relaxation of the elastic cohesive force in the polymer, and to a time-varying surface concentration of penetrant, and is called two-stage sorption behavior. Bagley and Long (13), Long and Richman (14), Fujita (15), Park (16), and Joshi and Astarita (17) have presented interpretations of the two-stage sorption process. It appears that the first stage of the sorption process reflects the rapid attainment of a quasi-equilibrium concentration at the surface of a polymer film followed by a diffusion process which attempts to establish this concentration level throughout the entire polymer film. The second stage can then be associated with an increase in surface concentration which results from relaxation processes in the polymer samples; this change in surface concentration occurs slowly

relative to the diffusion rate. Evidence in support of this interpretation has been provided by Long and Richman (14) who performed sorption experiments which showed that the surface concentration for a polymer-solvent system can approach the equilibrium value relatively slowly. Berens and Hopfenberg (18) have been partially successful in fitting two-stage sorption data by assuming Fickian diffusion with constant boundary conditon for the first stage, and a first-order relaxation process for the second stage.

Several different transport mechanisms for a sorption run followed by a desorption run to the original penetrant level are shown in Figure 3.3 (19). The sorption and desorption curves coincide for Fickian diffusion with D constant (Figure 3.3.a). If D increases with the penetrant concentration C, as it does for the diffusion of organic vapors in rubbers and at low activities in glasses, the sorption curve lies above the desorption curve, as in Figure 3.3.b. If D varies inversely with C, as, for instance, in the diffusion of water in hydrophobic polymers, the positions of the curves are reversed, as in Figure 3.3.c. If swelling is significant and stress relaxation controls the penetration rate, as in case II or anomalous transport, the sorption curve is sigmoidal, but desorption from the swollen polymer is Fickian and initially relatively rapid (Figure 3.3.d). If relaxation occurs slowly, two-stage sorption occurs, as in Figure 3.3.e. In the early stages of sorption, the amount of penetrant sorbed is linear with $t^{1/2}$. This

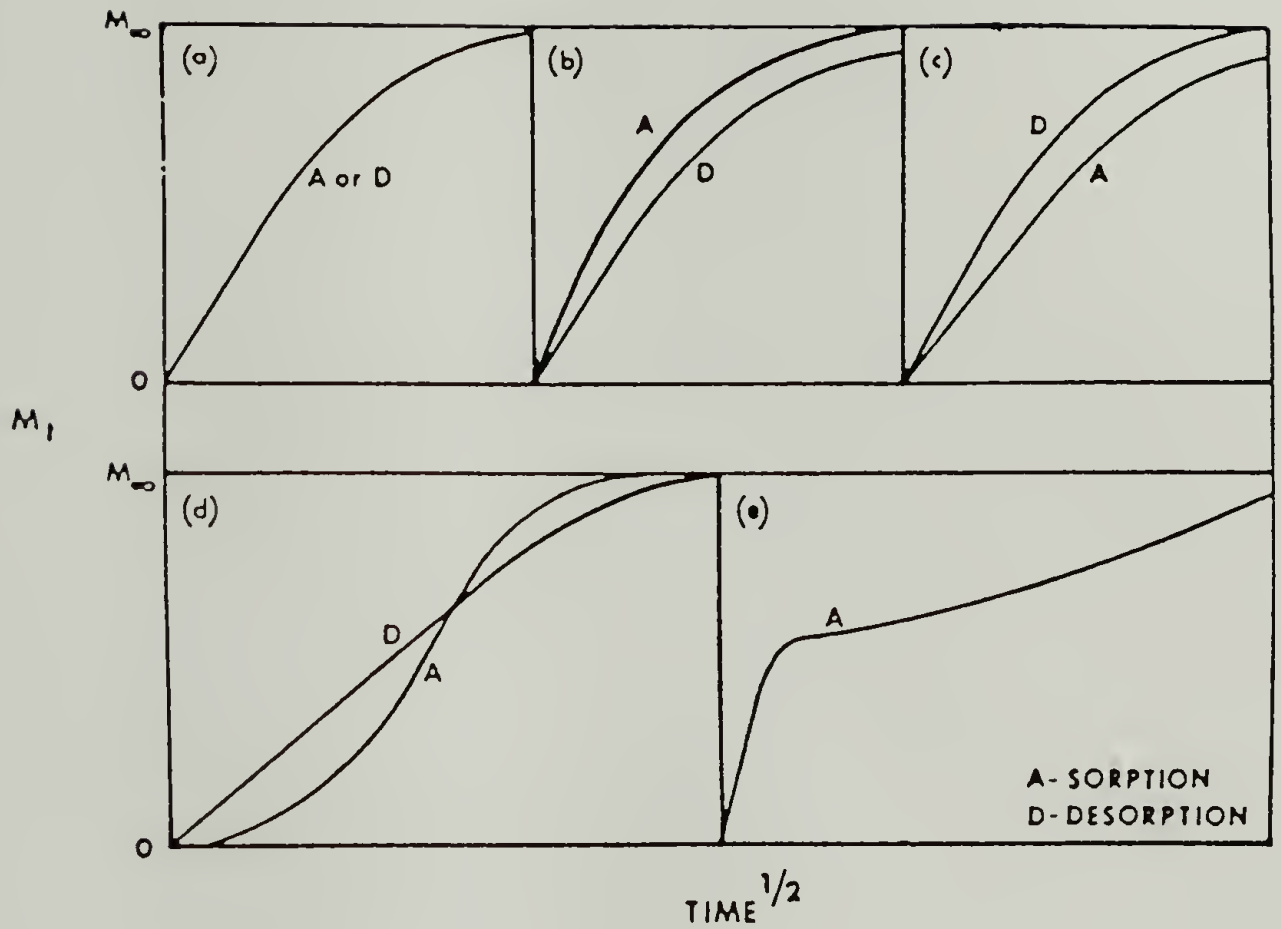

Figure 3.3 Sorption cycles for several transport mechanisms. (a) Fickian Diffusion, constant D; (b) Fickian diffusion, D increases with increasing C; (c) Fickian diffusion, D decreases with decreasing C; (d) anomalous or case II transport; (e) two-stage sorption.

initial rapid uptake leads to a quasi-equilibrium state followed by a slow approach to a final time equilibrium.

3.3 Determination of Diffusion Coefficient

(A) Constant Diffusion Coefficient

The appropriate solution of the diffusion equation for a plane sheet of thickness l can be derived from equations 3.5-7, assuming a constant diffusion coefficient D. The result may be written (2)

$$M_t/M_\infty = 1-(8/\pi^2)\{\sum_{m=0}^{\infty} [1/(2m+1)^2][\exp(-D(2m+1)^2\pi^2 t/l^2)]\} \quad (3.11)$$

Here, M_t is the total amount of vapor absorbed by the sheet at time t, and M_∞ the equilibrium sorption attained theoretically after infinite time. The application of above equation is based on the assumption that immediately the sheet is placed in the vapor the concentration at each surface attains a value corresponding to the equilibrium uptake for the vapor pressure existing, and remains constant afterwords. The sheet is considered to be initially free of vapor. The value of t/l^2 for which $M_t/M_\infty = 1/2$, conveniently written $(t/l^2)_{1/2}$, is given by

$$(t/l^2)_{1/2} = -(1/\pi^2 D)\{\ln[(\pi^2/16)-(1/9)(\pi^2/16)^9]\} \quad (3.12)$$

approximately, the error being about 0.001 per cent. Thus we have

$$D = 0.049/(t/l^2)_{1/2} , \qquad (3.13)$$

and so, if the half-time of a sorption process is observed experimentally for a system in which the diffusion coefficient is constant, the value of this constant can be determined from equation 3.13.

For small time and for a plane sheet, as $t \rightarrow 0$, the equation 3.11 reduces to

$$M_t/M_\infty = m \cdot t^{1/2} \qquad (3.14)$$

where

$$m = 4D^{1/2}/l\pi^{1/2} \qquad (3.15)$$

Here, m is the initial slope of a sorption or desorption curve as plotted M_t/M_∞ vs. $t^{1/2}$. Thus, the diffusion coefficient D can be determined by this initial slope method, and can be written

$$D = m^2 \cdot l^2 \cdot \pi/16 \qquad (3.16)$$

However, in deriving equation 3.11, the thickness l of the sheet is assumed to remain constant as diffusion proceeds. In practice it often happens that the sheet swells and the thickness increases as the vapor enters. In order to make a thickness correction due to swelling, we assume that there is no overall volume change on mixing, and that the swelling is an isotropic three-dimensional

increase in the size of the sheet. The diffusion coefficient D' after thickness correction is then derived and shown below

$$D' = D/\phi_2^{2/3} \qquad (3.17)$$

where ϕ_2 is the final volume fraction of the plane sheet or dry polymer.

(B) Concentration-Dependent Diffusion Coefficient

As the diffusion coefficient is concentration-dependent, application of the equation 3.13 yields some mean value $\overline{D}$, say, of the variable diffusion coefficient averaged over the range of concentration appropriate to each value. Crank and Park (1) assert that, with $C_i=0$, $\overline{D}$ is related approximately to D according to

$$\overline{D} = (1/C_0)\int_0^C D\, dc \qquad (3.18)$$

This leads to the integral method for determining D from a set of sorption experiments. Graphical differentiation of a plot of $\overline{D}C_0$ vs. C_0 gives an approximation to the relationship between D and C_0.

Duda and Vrentas (20) have developed a new technique, called the differential or step-change sorption method, for deducing the concentration dependence from a single sorption curve. They used the method of moments to solve the diffusion equation and assumed that, over a sufficiently small concentration interval, the diffusion coefficient is an exponential function of concentration.

They found that if D(c) increases exponentially with concentration, the average diffusion coefficient over the concentration interval, calculated by the initial slope method, is an excellent approximation to the value of D at $\bar{C}$= 0.7. Here, $\bar{C}=(C-C_i)/(C_f-C_i)$, where C_i and C_f are the initial and equilibrium concentrations of penetrant. Similarly, as D(c) decreases exponentially, the average diffusion coefficient $\bar{D}$ approximates the value of D at $\bar{C}$=0.56.

3.4 Experimental Observations

3.4.1 Transport in Rubbers

In general, the diffusion behavior of organic vapors in polymers is Fickian at temperatures well above the glass transition temperature Tg. It was mentioned in section 3.2 that the reduced sorption curves for films of different thickness are superimposed to form a single curve, indicating a Fickian diffusion. For most polymer and organic vapor systems, sorption curves do not concide with the corresponding desorption curves, suggesting that the diffusion coefficient is dependent on the concentration of organic vapor. For examples, for benzene in natural rubber (21) and low molecular weight hydrocarbons in polyisobutylene (22), the diffusion coefficient appeared to be an exponentially increasing function of the concentration. However, in most cases, especially for high swelling samples, the diffusion coefficient goes to a maximum (20,

23,24). This is because of the fact that the mutual diffusion coefficient is a product of a thermodynamic factor and a mobility factor (sometimes called the self-diffusion coefficient). As the solvent concentration increases, the thermodynamic factor dominates, and, therefore, the diffusion coefficient decreases. Duda and Vrentas (25,26) have developed a model of a combination of the free volume theory and the Flory-Huggins theory, in which the self-diffusion coefficient of a rubbery polymer can be determined.

3.4.2 Transport in Glasses

The anomalous or non-Fickian sorption behavior is frequently observed for the diffusion of organic vapors in glassy polymers up to approximately Tg+10°C (27). For example, in the case when the penetrant causes extensive swelling or any type of structure change the diffusion process cannot be described by a concentration dependent form of Fick's law with constant boundary condition. The deviations from Fickian behavior are considered to result from both the finite rate at which the polymer structure changes in response to be sorption or desorption of penetrant molecules as well as irreversible changes affected upon the transport. The anomalous or non-Fickian phenomena that have been observed in the study of diffusional transport in polymer-solvent systems have been described in detail by a number of investigators (2,5,7,15,16,28-31). The following examples of anomalous behavior have been observed for

differential (incremental) as well as integral sorption experiments which have been used to study penertrant diffusion in polymers.

(A) Thickness Anomalies

One of the more subtle deviations from the predictions of the classical theory is the thickness effect in a sortion experiment. Curves of M_t/M_∞ vs. $t^{1/2}/L$ do not coincide, as they should, when different thickness samples are used for fixed initial and final penetrant concentrations. For example, Kishimoto and Matsumoto (32) and Odani (33) collected sorption data which exhibited many of the features which characterize Fickian diffusion but which also showed pronounced thickness effects. Odani (33) investigated the integral absorption and desorption of methyl ethyl ketone in atactic polystyrene as functions of film thickness at 25 and 45°C with concentrations above the critical concentration of the system. In all cases studied, the reduced absorption and desorption curves for films of different thicknesses did not give a single curve, though the individual absorption and desorption curves appeared to have the shape expected from the Fickian diffusion mechanism. The initial slopes of the reduced curves increased with increasing film thickness for both absorption and desorption.

(B) Anomalous Sorption Curves

A more obvious example of non-Fickian behavior is a sorption experiment for which the shape of a sorption curve, a plot of M_t/M_∞ vs. $t^{1/2}$, does not conform to the characteristic features of a Fickian sorption curve (2,5,15). For classical diffusion, the

sorption curve is linear in the early stage of the diffusion process, and then the curve is concave to the $t^{1/2}$ axis as the final equilibrium concentration is approached. Odani and coworkers (34-37) performed both differential and integral sorption experiments involving the diffusion of organic vapors in glassy polymers, and they reported significant departures of the sorption curves from Fickian behavior. An illustration of this type of anomalous behavior is given by the successive differential sorption curves for the ethyl methyl ketone-polystyrene system at 25°C; sorption curves for these experiments are presented in Figure 3.4. The shape of the sorption curves changes with increasing initial penetrant concentration according to the following scheme depicted in Figure 3.4:

Sigmoid ⟶ Pseudo-Fickian ⟶ Two-stage ⟶ Pseudo-Fickian ⟶ Fickian

Pseudo-Fickian sorption curves resemble those for Fickian sorption but there is a limited linear initial region, a very slow approach to equilibrium, and a possible thickness anomaly. The two-stage sorption curve is characterized by a rapid initial sorption up to a quasi-equilibrium uptake followed by slow approach to a final true equilibrium state.

A thorough experimental study of diffusion of acetone and methyl iodide in cellulose acetate and polyvinyl acetate

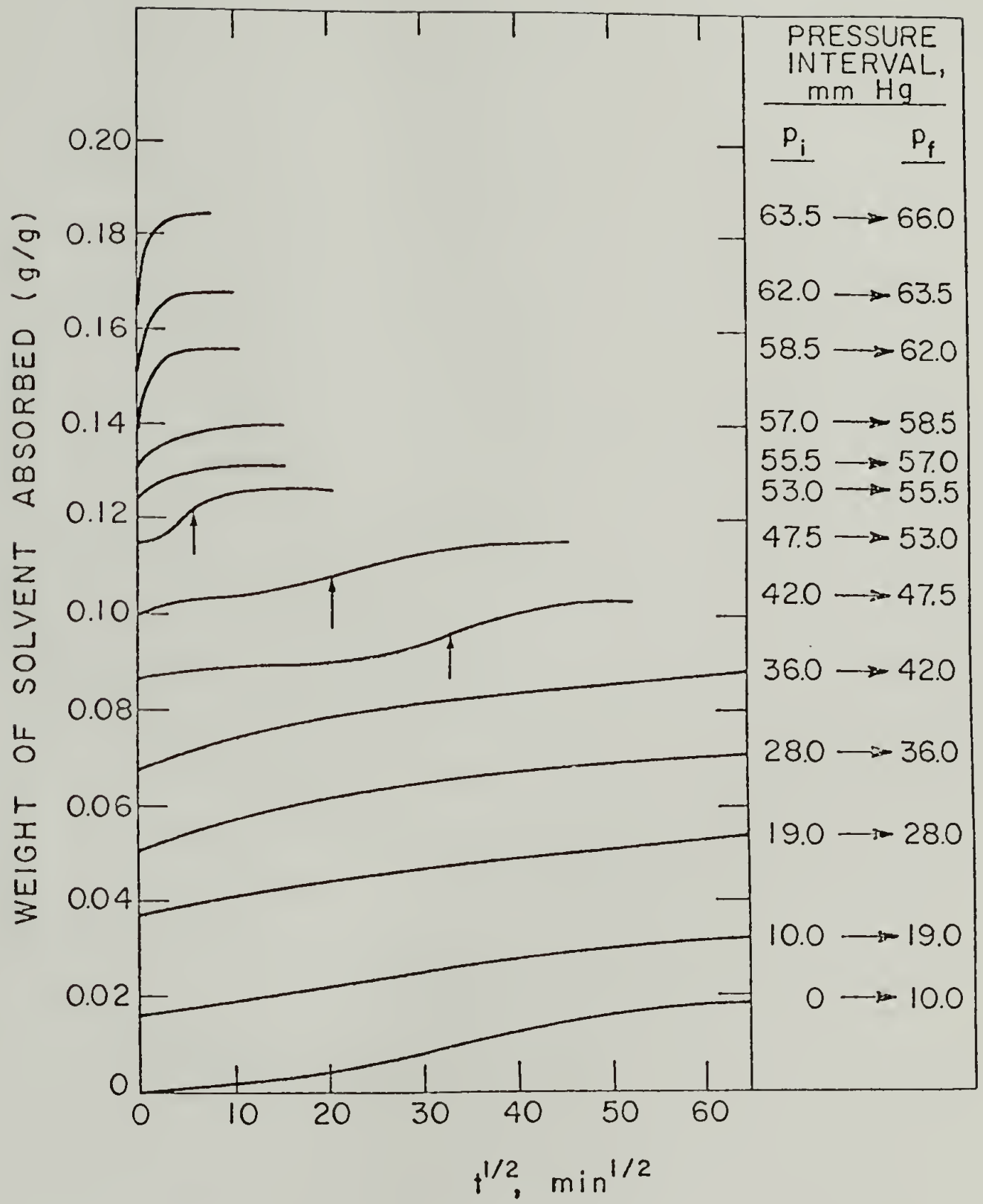

Figure 3.4 Successive differential absorption, initial and final pressures, P_i and P_f of each step are given in the right columns.

was executed by Bagley and Long (13) and Long and Richman (14). Long and Richman (14) have measured the concentration gradients resulting from the diffusion for the methyl iodide-cellulose acetate system using the microradiographic procedure. The observed gradients are very different from those found for diffusion into non-glassy polymers. In particular the surface concentrations, C_s, attain their equilibrium values only very slowly, varying with time according to the equation $C_s=C_0+(C_{eq}-C_0)[1-\exp(-kt)]$. The initial surface concentration C_0 is commonly only a small fraction of the final value C_{eq}. Here, k is a relaxation constant. With the above equation in terms of the boundary conditions for the penetrant-polymer system, the explicit solutions for Fick's law for diffusion both into an initially dry polymer and into a polymer pre-equilibrated with a given amount of the vapor were obtained (14). The resulting equations can explain the sigmoidal behavior found for the former case and the two-stage behavior found for the latter. The equation for the boundary conditions given by Long and Richman (14) directly resulted from experimental observation. Joshi and Astarita (17) have interpreted the boundary conditions using the concept of degree of swelling and the rate of evolution, and recast the equations into a closed form solution, which is similar to the solution given by Long and Richman (14). Recently, Berens, Hopfenberg and coworkers (18,38-42) have extensively studied the diffusion of organic vapors in glassy polymers, and developed a phenomenological model to fit the two-stage sorption curve by

assuming Fickian diffusion with a constant boundary condition for the first stage, and a first-order relaxation process for the second stage. One of their experiments showed that sample thermal and swelling history variation produce substantial changes in the sorption kinetics. These effects may be illustrated by the data in Figure 3.5 (41), showing M_t vs. $t^{1/2}$ curves for the sorption of n-hexane over the P_{rel}, P/P_o, interval from 0 to 0.75 in three samples of 0.53 um polystyrene powder. One sample was used in the "as-received" condition, one was annealed for 24 hours just below Tg, and the third was "preswollen" by exposure at 15°C to n-hexane vapor at P_{rel} =0.90 for 1 week, followed by removal of the n-hexane under vacuum. In sorption at P_{rel}=0.75, all three samples showed a similarly rapid Fickian initial sorption and reached similar ultimate levels of n-hexane absorbed, but the rate of the relaxation stage varied greatly. Since annealing presumably reduced the polystyrene free volume, and preswelling presumably left the sample in an expanded state of higher free volume than the "as-received" sample, these results indicate that the rate of the swelling relaxation is markedly elevated by an increase in the available free volume.

(C) Case II Sorption

One of the more dramatic manifestations of non-Fickian behavior involves the dependence of the total weight increase in a sorption experiment, W, on time, t, in the early stages of the sorption process. The relationship between W and t can generally be written as $W=kt^n$, and for case II sorption, n=1. Hopfenberg et al. (43)

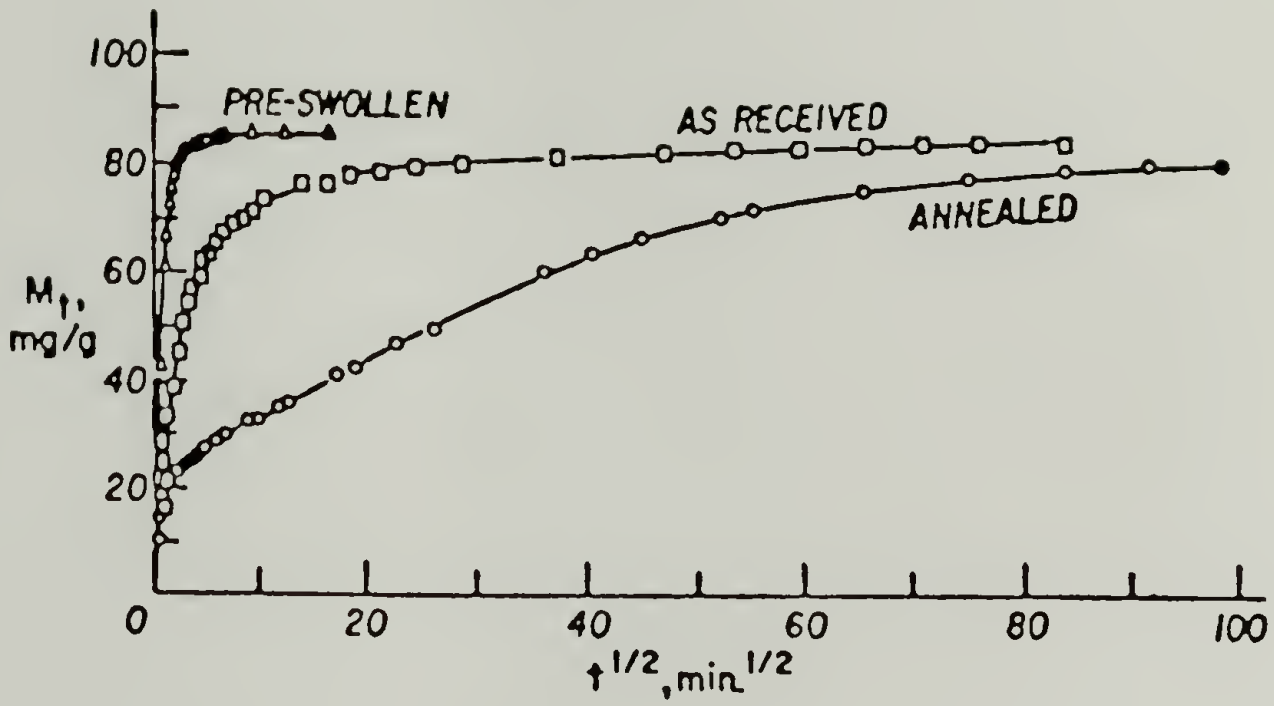

Figure 3.5 Sorption curves of n-hexane by 0.53 μm polystyrene powder samples of varied history, at $30^{o}C$, $P_{rel}=0 \rightarrow 0.75$.

used vapor and liquid sorption experiments to study alkane diffusion in glassy polystyrene. They observed case II transport at high penetrant activities, anomalous behavior ($0.5<n<1$) at moderate penetrant activities, and an approach to Fickian behavior ($n=0.5$) at low activities. The sorption behavior of penetrants in glassy polymers depends on the temperature, type of penetrant, penetrant activity, and sample dimensions. For example, Fickian diffusion occurs at low penetrant activities and case II transport is approached if the solvent activity is high enough so that swelling of polymer takes place. Also, Ensore et al. (39) and Hopfenberg (44) reported that the type of diffusion observed in a sorption experiment was dependent on the sample dimensions. This result can be anticipated from the Deborah number concept discussed in section 3.2. Case II transport appears to involve a boundary between a rubbery shell and a glassy core in the sample. This boundary advances at a constant velocity, and this leads to a weight gain which is proportional to time. In some cases, there is an acceleration of mass transfer near the end of a sorption experiment (8); this accelerted transport has been refered to as super case II transport. Interpretations and analysis of case II transport have been presented by a number of investigators (44-55).

(D) Solvent Crazing and Swelling Fracture

At very high penetrant activities in a sorption experiment, Hopfenberg et al. (43) observed solvent crazing. Solvent crazing can be viewed as an extreme limit of case II diffusion for which

the swelling stresses are sufficient to cause local polymer failure. The swelling stresses set up in the glassy polymer by the diffusion of solvent lead not only to the production of crazes but ultimately to fracture of the polymer specimen during a sorption experiment. For example, Alfrey et al. (6) showed that the dominant stress in long cylindrical samples was the axial tension on the glassy core. This stress led to transverse fracture of the glassy core when it exceeded the tensile strength of the glassy polymer.

(E) Dual Mode Sorption

In the sorption of simple gases in glassy polymers at low pressures, it would be expected (30) that the sorption isotherm is given by Henry's law (The concentration of penetrant in the polymer is directly proportional to the gas pressure) and that the diffusion process is described by the classical theory of diffusion with a constant diffusivity. At higher pressures, however, nonlinear sorption and transport behavior have been observed. For example, Koros et al. (56) studied the sorption and diffusion of CO_2 in glassy polycarbonate at pressures ranging from atmospheric to more than twenty times atmospheric pressure. These investigators reported a nonlinear sorption isotherm and a concentration dependent diffusion coefficient. One explanation of these observed data is that there exist distinct molecular populations of the penetrant in the polymer. One population is dissolved directly into the polymer matrix (Henry's law mode), and a second population is sorbed into microvoids or holes in the polymer (Langmuir mode).

Hence, the total concentration C of the penetrant in the polymer can be related to pressure P by the following equation

$$C = K_D P + [C'_H bP/(1+bP)] \qquad (3.19)$$

where K_D is a Henry's law solubility coefficient, C'_H is the Langmuir capacity constant, and b is the Langmuir affinity parameter. The above equation is similar to equation 3.4 obtained by Matthes in 1944. Equation 3.19 describes a non-linear sorption isotherm, and the basic concept of two melecular populations can be used to predict a concentration dependent diffusivity. A typical example of the dual-mode sorption curves is shown in Figure 3.6 (57), which shows the sorption of vinyl chloride monomer vapor (VCM) in poly-(vinyl chlorde) (PVC) resin powders with variations of temperature and vapor activity. Above the Tg of PVC (Tg= ~85°C), the Flory-Huggins equation describes the sorption isotherms over the full range of vapor activity. At low VCM activities below Tg, the isotherms show a pronounced downward curvature, which was interpreted in terms of the dual-mode sorption. The total sorption of VCM was ascribed to contributions of Flory-Huggins dissolution and Langmuirian "hole-filling", as shown in Figure 3.6. This typical example describes the sorption of organic solvent vapor in polymers but not gas sorption, which normally follows Henry's law dissolution and Langmuir adsorption.

A basic premise of the dual mode theory is that the penetrant

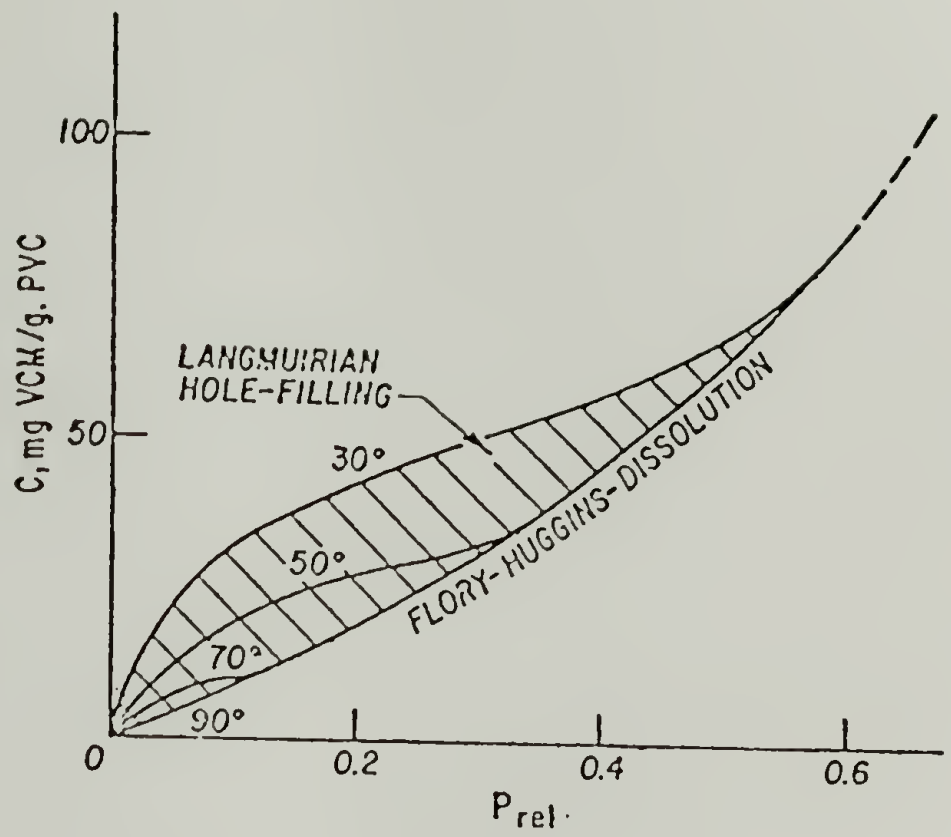

Figure 3.6 Sorption Isotherms for vinyl chloride in PVC.

does not interact with the polymer matrix and hence does not induce changes in the polymer characteristics. A number of investigators (7,56,58) have claimed that the nuclear magnetic resonance experiments of Assink (3) provide some direct evidence for the validity of the dual mode model. However, it should be noted that Sefcik and Schaefer (4) have correctly pointed out that the experiments of Assink (3) do not present conclusive evidence favoring the dual mode model. The above contradition results from a completely different explanation for the nonlinear sorption and transport behavior of penetrants in glassy polymers provided by the matrix model (4,59), which states that there is only one population of sorbed gas molecules in the polymer and that the properties of the polymer matrix are perturbed by the presence of the sorbed penetrant because of penetrant-polymer interactions. At the present time, it does not appear that any definitive evidence exists favoring either the dual mode or matrix models.

3.4.3 Transport Studies in Block Copolymers

Block copolymers are macromolecules whose most unique property is their two phase morphology. The structure and properties of the existing block copolymers have been extensively studied. However, only a few studies on the transport behavior of small molecules in block copolymers were reported. In this section a brief review of transport properties in block copolymers is presented.

Ziegel (60), in 1971, has investigated four types of commercial thermoplastic polyurethane elastomers using a gas flow method. The diffusive transport of several simple gases, i.e. H_2, O_2, Ar and N_2, in those polyurethanes was measured. Certain anomalies were observed with the larger-sized penetrants, namely Ar and N_2. It appears that these gaseous penetrants can distinguish between the rigid and flexible regions of certain block copolymers, the effect being more pronounced for the gas with the larger molecular diameter. The dependence of gas diffusion on temperature in a series of polyurethane block copolymers of differing aromatic urethane content and type of soft segment was examined by McBride et al (61). A discontinuity was observed in the Arrhenius plots for some materials, and this discontinunity was found to be related to the onset of the glass transition temperature in the hard domains. Serrano (62) studied the transport of small molecules in a series of well characterized random segmented polybutadiene polyurethanes to determine the diffusivity of these materials experimentally and to model the effective diffusion coefficient with effective medium theory (63). Goydan et al. (64) have recently studied the incremental vapor sorption and desorption of ortho-dichlorobenzene vapor in a commercial polyuethane, Estane. A two-stage sorption behavior was observed at intermediate and higher vapor concentrations, but was generally absent in the desorption runs. Two-stage sorption curves are related to the relaxation of hard segment induced by the presence of the solvent, and can be fitted by

a phenomenological model proposed by Berens and Hopfenberg (18) as the combination of Fickian diffusion and relaxation processes.

The most widely investigated copolymer system with respect to morphology is the copolymer of polybutadiene-polystyrene (SB). Part of the reason for the emphasis on this system is the existence of morphological predictions from thermodynamic theories and their agreement with the electron microscopy results. The transport properties of inert gases in SB copolymers was studied by Odani et al (65). The comparison between the transport properties of homopolybutadiene and the copolymer polybutadiene (PBD) showed that the segmental motions in the PBD phase are restricted compared to those in the homopolybutadiene. A more recent study from the same group (66) involved the use of n-hexane vapor in SB block copolymers. N-hexane is a good solvent for polybutadiene and a non-solvent for polystyrene. Two non-Fickian features were observed: (1) the thickness anomaly in the reduced sorption and desorption curves, and (2) the two-stage absorption curve at a certain concentration. These features suggest that the chain immobilization effect and geometric impedance effect due to the presence of impermeable polystyrene domains interfere with the transport of penetrant molecules in the copolymer solid. In addition, the equilibrium solubilities of n-hexane in the copolymers and polybutadiene homopolymer indicate that partial mixing of component block chains occurs at the interface between the polystyrene and polybutadiene domains, giving a rather diffuse boundary.

Chiang and Sefton (67) investigated the morphology of a styrene-butadiene-styrene (SBS) triblock copolymer. The sorption processes of different film thicknesses were found to deviate from the normal Fickian character because of the presence of an interfacial region for both polybutadiene and polystyrene. The time dependent diffusion was observed and was attributed to the inability of the polymer molecules to respond instantaneously to the change in concentration. The slow response appears to be due to sorption by the interfacial region at a temperature below its glass transition. Experimental studies, coupled with some theoretical calculations, allowed Caneba et al. (68) to observe the solvent effect on the interfacial volume fraction of the SB and SBS block copolymers. Experimental results indicated that minima occur at around 20-30% (by weight) styrene content in plots of the equilibrium sorption values of cyclohexane vs. styrene content in the rubbery SB samples. Also, relative maxima exist in plots of the mutual diffusion coefficient vs. concentration of cyclohexane in SB. For SBS samples, the relative portions of the sorption and desorption curves are generally dependent on their overall interphase volume fractions. As the overall interface volume fraction rises, the gap between these curves first increases and then decreases until the sorption and desorption cross. Kang et al. (69) investigated, experimentally and theoretically, the hexane vapor sorption in phase segregated polybutadiene/polystyrene blends. The experimental data, plus results derived from a model of

sorption in heterogeneous media containing a slowly permeable dispersed phase, indicate that the mere presence of two phases with different diffusion time constants is a sufficient condition for apparantly non-Fickian overall behavior.

3.5 Theories and Models

The transport of small molecules in rubbery polymers is accurately described by Fick's first and second laws. A number of theories and models have been reported and developed to describe the non-Fickian diffusion and sorption behavior below the glass transition temperature of the polymer. Although many mathematical models have attempted to explain the anomalous behavior, no rigorous model has yet been developed. In most analyses, a relaxation process, although not well understood physically, has been formulated mathematically in order to simulate non-Fickian sorption behavior (2,8,17,18,53). To explain non-linear sorption isotherms, the dual mode sorption (9) and recently the matrix model (59) have been developed. An extensive overview on the sorption and diffusion in glassy polymers has been given by Frisch (7), who has summarized all the existing theories and models in a table, and described the proposed explanations. In this section, only a brief description on the Joshi and Astarita model is given. This model was used to determine the diffusion coefficient and to fit the non-Fickian curves observed from the incremental vapor sorption and desorption

experiments in our solvent-penetrant system.

Joshi and Astarita (17) have developed a closed form solution to describe the non-Fickian anomalous behavior which is attributed to the coupling of diffusion and relaxation processes in polymer induced by the presence of the solvent. The closed form solution was originally given by Long and Richman (14), who deduced the boundary condition from direct experimental observations, and recast by Joshi and Astarita (17).

With the assumption of a constant diffusion coefficient D and of an exponential increase of the interface concentration and that the relaxation phenomenon is governed by simple linear kinetics, the relevant equation for a plane sheet is

$$\partial C/\partial t = D\,(\partial^2 C/\partial x^2) \qquad (3.20)$$

and the boundary conditions are

(1) $C(x,0) = C_0$ for $-L < x < L$

(2) $C(L,t) = C_1-(C_1-C_{10})\exp(-t/\Theta_R)$

(3) $\partial C(0,t)/\partial x = 0$ at $x=0$

Here, C is the concentration of penetrant in the sample; t is time; L is the half-thickness of the film; C_0 is the initial concentration; C_1 is the equilibrium concentration in the sample as time goes to infinity; C_{10} is the concentration established at the

interface at time zero, and Θ_R is the relaxation time. Based on the equation 3.20 and the boundary conditions, the closed form solution can be cast in the following instructive dimensionless form:

$$W = M_t/M_\infty = f_D(t) - m[f_{DR}(t) - (\tan \phi/\phi)(1-\exp -t\,\phi^2/\Theta_D)] \qquad (3.21)$$

where:

$$f_D(t) = 2 \sum_{n=1}^{\infty} [1-\exp(-a_N^2 t/\Theta_D)]/a_N^2$$

$$f_{DR}(t) = 2 \sum_{n=1}^{\infty} [1-\exp(-a_N^2 t/\Theta_D)]/(a_N^2-\phi^2)$$

$$a_N = \pi\,(n-0.5)$$

and

$$\Theta_D = L^2/D\ , \qquad \phi^2 = \Theta_D/\Theta_R = L^2/D\Theta_R$$

Θ_D is the diffusion time; parameter ϕ^2 is the ratio of characteristic times for the diffusion and relaxation precesses, and m is the ratio of the driving force corresponding to relaxation to that corresponding to ordinary diffusion as:

$$m = (C_1-C_{10})/(C_1-C_0) \qquad (3.22)$$

As $\phi >> \pi/2$,

$$W = f_D(t) \qquad (3.23)$$

$\phi << \pi/2$,

$$W = (1-m)f_D(t)+m[1-\exp(-\phi^2 t/\Theta_D)] \qquad (3.24)$$

Equation 3.23 reflects the fact that if relaxation is very fast one

would observe ordinary diffusion behavior: the final equilibrium structure is reached on a time scale negligible as compared to that of the diffusion phenomena. Conversely, equation 3.24 reflects the fact that, if relaxation is much slower than diffusion, the effect of the two phenomena is simply additive: one would observe a first stage governed by diffusion, followed by a second stage governed by relaxation. The equation 3.24 is thus similar to the equation developed by Berens and Hopfenberg (18). Should the value of ϕ be the order of $\pi/2$, the coupling of the diffusion and relaxation should be taken into account.

Non-Fickian effects such as film thickness dependence, two stage, and sigmoidal sorption kinetics can be described by this model, and even cases in which the sorption curves pass through a maximum and then decrease ($m<0$) such as in the case of solvent induced crystallinity can be described with the above model.

3.6 References

1. J. Crank and G. S. Park, eds., "Diffusion in Polymers" Academic Press, New York 1968.

2. J. Crank, "The Mathematics of Diffusion" 2nd ed. Oxford University Press, London & New York, 1975.

3. R. A. Assink, J. Polym. Sci., Polym. Phys. Ed., 13, 1665 (1975).

4. M. D. Sefcik and J. Schaefer, J. Polym. Sci., Polym. Phys. Ed., 21, 1055 (1983).

5. H. Fujita, Chap. 3 in Ref. 1.

6. T. Alfrey, E. F. Gurnee, and W. G. Lloyd, J. Polym. Sci., C12, 249 (1966).

7. H. L. Frisch, Polym. Eng. and Sci., 20 (1), 2 (1980).

8. C. H. M. Jaques, H. B. Hopfenberg, and V. T. Stannett, in "Permeability of Plastic Films and Coating" (Ed. by H. B. Hopfenberg), P. 73, Plenum Press, New York (1974).

9. W. R. Vieth, J. M. Howell, and J. H. Hsieh, J. Membrane Sci., 1, 177(1976).

10. H. B. Hopfenberg and H. L. Frisch, J. Polym. Sci., B7, 405(1969).

11. J. S. Vrentas, C. M. Jarzebski, and J. L. Duda, AICHE J., 21, 894 (1975).

12. J. S. Vrentas and J. L. Duda, J. Polym. Sci., Polym. Phys. Ed. 15, 441 (1977).

13. E. Bagley and F. A. Long, J. Am. Chem. Soc., 77, 2172 (1955).

14. F. A. Long, and D. Richman, J. Am. Chem. Sci., 82, 513 (1960).

15. H. Fujita, Fortschr. Hochpolym.-Forsch., 3, 1 (1961).

16. G. S. Park, in "Diffusion in Polymers", J. Crank and G. S. Park, Eds., Academic Press, New York, 1968, Chap. 5.

17. S. Joshi and G. Astarita, Polymer, 20, 455 (1979).

18. A. R. Berens and H. B. Hopfenberg, Polymer, 19, 489 (1978).

19. R. M. Fedder amd G. S. Hvard, "Methods of Experimental Physics" Vol. 16C, 315 (1980).

20. J. S. Vrentas, J. L. Duda, and Y. C. Ni, J. Polym. Sci.-Phys, 15, 2039 (1977).

21. M. J. Hays and G. S. Park, Trans. Farad. Soc., 51, 1134 (1955).

22. S. Prager, E. Bagley, and F. A. Long, J. Am. Chem. Soc., 75, 1255 (1953).

23. H. Odani, M. Uchikura, K. Taira, and M. Kurata, J. Macromol. Sci., Phys., B17, 337 (1980).

24. J. S. Vrentas, J. L. Duda, and M. K. Lau, J. Appl. Polym. Sci., 27, 3987 (1982).

25. J. S. Vrentas, J. L. Duda, J. Polym. Sci., Polym. Phys. Ed., 15, 403 (1977).

26. J. S. Vrentas, J. L. Duda, J. Polym. Sci., Polym. Phys. Ed., 15, 417 (1977).

27. S. A. Stern and H. L. Frisch, Ann. Rev. Mat. Sci., 11, 523 (1981).

28. J. L. Duda and J. S. Vrentas, in "Encyclopedia of Polymer Science and Technology", Vol. 13, Wiley, New York, 1970, P. 326.

29. J. L. Duda and J. S. Vrentas, in "Encyclopedia of Polymer Science and Engineering", Vol. 5, 2ed. John, Wiely and Sons Inc., New York, 1986, P. 36.

30. H. B. Hopfenberg and V. Stannett, in "The Physics of Glassy Polymers", R. N. Haward, Ed., Wiley, New York, 1973, P. 504.

31. C. E. Roger, in "Physics and Chemistry of the Organic Solid State", Vol. II, D. Fox, M. M. Labes, and A. Weissberger, Eds., Interscience, New York, 1965, Chap. 6.

32. A. Kishimoto and K. Matsumoto, J. Polym. Sci., A2, 679 (1964).

33. H. Odani, J. Polym. Sci., A-2, 5, 1189 (1967).

34. A. Kishimoto, H. Fujita, H. Odani, M. Kurata, and M. Tamura, J. Phys. Chem., 64, 594 (1960).

35. H. Odani, S. Kida, M. Kurata. and M. Tamura, Bull. Chem. Soc., Japan, 34, 571 (1961).

36. H. Odani, J. Hayashi, and M. Tamura, Bull. Chem. Soc., Japan, 34, 817 (1961).

37. H. Odani, S. Kida, and M. Tamura, Bull. Chem. Soc. Japan, 39, 2378 (1966).

38. A. R. Berens, J. Macromol. Sci.-Phys., B14(4), 483 (1977).

39. D. J. Enscore, H. B. Hopfenberg and V. T. Stannett, Polymer, 18, 793 (1977).

40. A. R. Berens, Polymer, 18, 697 (1977).

41. A. R. Berens and H. B. Hopfenberg, J. Polym. Sci.: Polym. Phys. Ed., 17, 1757 (1979).

42. A. R. Berens, Polym. Eng. and Sci. 20 (1), 95 (1980).

43. H. B. Hopfenberg, R. H. Holley, and V. Stannett, Polym. Eng. Sci., 9, 242 (1969).

44. H. B. Hopfenberg, J. Membrane Sci., 3, 215 (1978).

45. H. L. Frisch, T. T. Wang, and T. K. Kwei, J. Polym. Sci. 7 (A2), 879 (1969).

46. T. T. Wang, T. K. Kwei, and H. L. Frisch, J. Polym. Sci. 7 (A2), 2019 (1969).

47. T. K. Kwei and T. T. Wang, in "Permeability of Plastic Films and Coatings", H. B. Hopfenberg, Ed., Plenum Press, New York, 1974, P. 63.

48. A. Peterlin, J. Polym. Sci., B3 1083 (1965).

49. A. Peterlin, Makromol. Chemie., 124 136 (1969).

50. G. Astarita and G. C. Sarti, Polym. Eng. Sci., 18, 388 (1978).

51. G. Astarita and S. Joshi, J. Membrane Sci., 4, 165 (1978).

52. A. Peterlin, Polym. Eng. Sci., 20, 238 (1980).

53. N. L. Thomas, and A. H. Windle, Polymer, 21, 613 (1980).

54. N. L. Thomas, and A. H. Windle, Polymer, 23, 529 (1982).

55. G. C. Sarti, Polymer, 20, 827 (1979).

56. W. J. Koros, D. R. Paul, and A. A. Rocha, J. Polym. Sci.-Polym. Phy. Ed., 14, 687 (1976).

57. A. R. Berens, Angew. Makromol. Chem., 47, 97 (1975).

58. R. T. Chern, W. J. Koros, E. S. Sanders, S. H. Chen, and H. B. Hopfenberg, in "Industrial Gas Separations, ACS Symposium Series 223", T. E. Whyte, C. M. Yon, and E. H. Wagener, Eds., American Chemical Society, Washington, D. C., 1983, P 47.

59. D. Raucher and M. D. Sefcik, in "Industrial Gas Separations, ACS Symposium Series 223", T. E. Whyte. C. M. Yon, and E. H. Wagener, Eds., American Chemical Society, Washington, D. C., 1983, P. 89. and P. 111.

60. K. D. Ziegel, J. Macromol. Sci.-Phys. B5(1), 11 (1971).

61. J. S. McBride, T. A. Massaro, and S. L. Cooper, J. Appl. Polym. Sci., 23, 201 (1979).

62. M. Serrano, Ph.D. Thesis, University of Massachusetts (1986).

63. J. Sax and J. M. Ottino, Polym. Eng. Sci., 23, 165 (1983).

64. R. Goydan, N. S. Schneider, and J. Meldon, Polym. Mater. Sci. Eng., 49, 249 (1983).

65. H. Odani, K. Taira, N. Nemoto, and M. Kurata, Polym. Eng. Sci., 17, 527 (1977).

66. H. Odani, M. Uchikura, K. Taira, and M. Kurata, J. Macromol. Sci.-Phys., B17(2), 337 (1980).

67. K. T. Chiang and M. V. Sefton, J. Polym. Sci.: Polym. Phys. Ed., 15, 1927 (1977).

68. G. T. Caneba, D. S. Soong, and J. M. Prausnitz, J. Macromol. Sci.-Phys., B22(5&6), 693 (1983-1984).

69. Y. S. Kang, J. H. Meldon, and N. H. Sung, Polym. Eng. Sci., 26, 1045 (1986).

C H A P T E R IV

STUDIES OF STRUCTURE AND PROPERTIES IN PHASE SEGMENTED POLYURETHANES

4.1 Introduction

Polyurethane block copolymers which consist of alternating soft and hard segments often exhibit a two-phase morphology because of the segmental incompatibility. The factors which influence the phase separation include segmental polarity difference, segmental length, crystallizability of either segment, intra- and intersegment interaction such as hydrogen bonding, overall composition, and molecular weight. The nature of the segmented polyurethanes depends on the methods and condition of polymerization, sample history, preparation of samples, and constituents of the samples. The elasticity, toughness, and other physical properties of these materials are determined largely by the size, crystallinity, and interconnectivity of the hard domains as well as the nature of the domain interface and the mixing of hard segments in the soft segment phase.

Seymour et al. (1-3) in an IR dichroism study of MDI/BD/PTMO-1000 (1000 MW PTMO) found that an increase in the hard segment content from 24 to 28 wt% MDI changed the hard segment domain microstructure from an isolated to an interconnected morphology.

Abouzahr et al. (4) used wide angle x-ray diffraction to study the crystal structure of MDI/BD/PTMO-2000 polyurethanes, and found no detectable crystalline diffraction for samples with less than 35 wt% MDI. On the basis of small-angle x-ray scattering and stress relaxation studies, Abouzahr et al. also proposed that polyurethanes have an interlocked domain morphology at moderate MDI content (35 and 45 wt%). Bonart (5,6) also examined the packing of MDI/BD hard segments using x-ray scattering and suggested that hard segments were laterally associated forming lamellae with a thickness limited by the average hard segment length. Using electron microscopy and x-ray diffraction analaysis, Schneider et al. (7) proposed that the MDI/BD hard segment domain existed in a micelle-like structure which was made up of a lateral association of hard segment units. Recently, Van Bogart et al. (8), on the basis of x-ray scattering and DSC studies, also concluded that MDI/BD hard segments exist in semi-crystalline domains whose crystallinity increased as the hard segment length increased. It is generally accepted that longer soft segment lengths improve the degree of phase segregation, and that higher hard segment content results in more low molecular weight hard segment dissolved into the soft phase and thus increases the Tg of the soft segment (9-14).

In order to understand the transport properties of segmented polyurethanes, the present study investigated the structure and properties of these materials with different MDI/BD/PTMO ratios as well as different molecular weights of the soft segment (PTMO).

Differential scanning calorimetry (DSC), dynamic mechanical thermal analysis (DMTA), and tensile testing analysis were used to determine the hard and soft segment Tg's, hard segment Tm and crystallinity, storage and loss moduli, and stress-strain behavior.

4.2 Experimental

4.2.1 Materials

Polyurethane samples used in these studies are shown in Table 4.1. The structures for these materials are given in Figure 4.1. Estane is manufactured by B. F. Goodrich, and other polyurethanes were kindly supplied by the Army Materials Technology Lab. Two sets of polytetramethylene oxide (PTMO) polyurethanes were studied, one with 1000 molecular weight (MW) PTMO soft segment, and the other with 2000 MW PTMO. The hard segment consists of diphenyl-methane-4,4'-diisocyanate (MDI) and 1,4-butanediol (BD). All samples were characterized with respect to their soft segment MW, and hard and soft segment content. The designation PU stands for polyurethane, and the number and the symbol S immediately following the system name refer to the molecular weight and the weight fraction of the soft segment. For example, the sample designated with 1S44 in PU1S44 indicates a polyurethane with 1000 MW PTMO and 44% by weight soft segment. The weight fraction of the hard segment was determined by the MW of the hard segment divided by the sum of the

Table 4.1

Composition of PTMO-Polyurethane Block Copolymers

Sample	MDI:BD: PTMO Molar Ratios	Molecular Wt. of PTMO	Hard Segment Wt. Fraction	Soft Segment Wt. Fraction
Estane	2:1:1	1000	0.37	0.63
PU1S52	3:2:1	990	0.48	0.52
PU1S44	4:3:1	990	0.56	0.44
PU2S68	3:2:1	1934	0.32	0.68
PU2S44	8:7:1	2033	0.56	0.44
PU2S34	12:11:1	2033	0.66	0.34

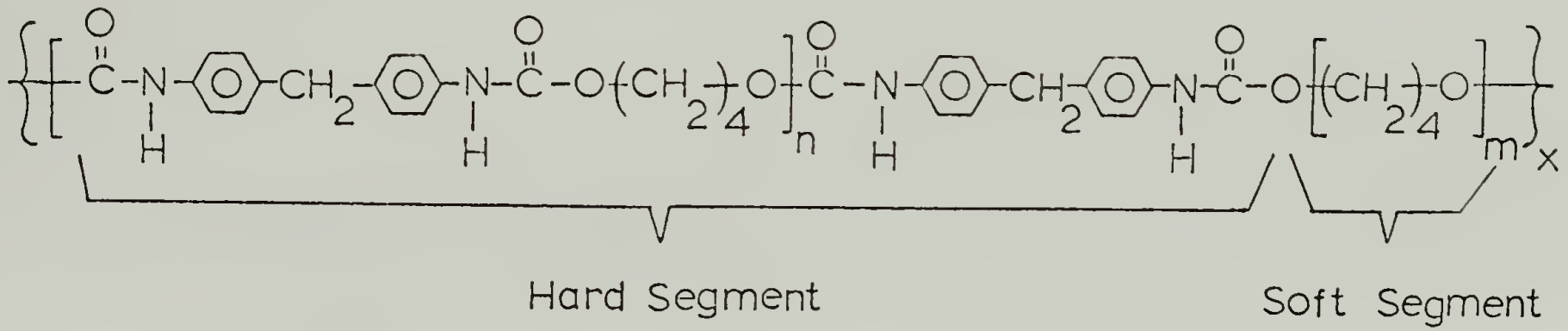

Figure 4.1 The chemical structures of PTMO-polyurethane samples; n and m are the molar ratios.

hard and soft segment molecular weights. For example, the molar ratio of MDI/BD/PTMO for the PU1S44 sample is 4:3:1, and the molecular weight of the hard segment (H) is equal to (4x MDI MW + 3x BD MW). Thus, the weight fraction of the hard segment is H/(H+1000). It is to be noted that some hard segments may be dissolved in the soft phase, but they are still designated as hard segments. The symbols, n and m, shown in Figure 4.1, indicate the number of the constituents. For instance, if the molar ratio is 3:2:1, then, n=2 and m=1.

4.2.2 Preparation of Samples

Film samples were prepared by solvent casting from a DMF solution on the specially designed glass dishes which provide a flat surface and a connection to a vacuum system. After samples were dried at room temperature under vacuum in the dishes for several days, the dried samples were peeled off and brought into a vacuum oven at 80°C for two days to complete solvent removal, and then were stored in a desiccator at room temperature. The high purity DMF was purchased from the Aldrich Chemical Company and used as received.

4.2.3 Instrumentation

(A) Differential Scanning Calorimetry (DSC)

DSC thermograms over the temperature range from -110°C to about 230°C were recorded on a Perkin-Elmer DSC-7 interfaced with a thermal analysis data station. Calibration was done by using indium and cyclohexane as standards. The experiments were carried out at a heating rate of 20°C/min under helium purge in the sample holder. Two samples, APU1S44 and APU2S34, were annealed at 155°C for two days before conducting DSC experiments.

(B) Dynamic Mechanical Thermal Analysis (DMTA)

DMTA data were obtained at 1 Hz by using a Polymer Lab. DMTA, which was controlled automatically by a HP computer. Film samples, with t-w-l of 0.5x7x1 mm in size, were tested under liquid nitrogen from -150°C to 200°C at a heating rate of 4°C/min. Two samples, APU1S44 and PU1S44, were tested.

(C) Tensile Testing

Uniaxial stress-strain measurements at room temperature were made by using an Instron 4202 tensile testing machine with a crosshead speed of 10 mm/min. The instrument was controlled by a HP computer which automatically provides a complete data analysis.

4.3 Results and Discussion

4.3.1 Differential Scanning Calorimetry (DSC)

The results of DSC studies on the polyurethane samples are shown in Figures 4.2-5, and are summarized in Table 4.2. All samples were annealed at 80°C in a vacuum oven for two days except for APU1S44 and APU2S34, which were annealed at 155°C for two days. Figures 4.2 and 4.3 show the DSC results of the soft segments for both 1000 MW and 2000 MW PTMO polyurethanes. It is generally accepted that samples with higher hard segment content may result in a better phase separation and thus a low soft segment Tg. However, for 1000 MW soft segment polyurethanes, it was found that samples with higher hard segment content lead to higher soft segment Tg's due to the short length hard segments dissolved in the soft phase. This was confirmed in this study, as shown in Figure 4.2. The Tg's of the soft segment for all three samples is about -40°C; no detectable decrease in Tg was observed for samples with higher hard segment content. Compared with the Tg of PU1S44, the Tg of APU1S44, -47°C, is about 10°C lower, reflecting an annealing-induced phase separation. Similar results were found by Miller et al. (5) who observed the soft segment Tg dropped from -29°C to -46°C in a PTMO based polyurethane containing 60% hard segment after annealing at 130°C for 5 hours.

Figure 4.3 shows the DSC results for the soft segments of polyurethane samples with 2000 MW PTMO. The soft segment Tg decreases from -61°C to -68°C as the hard segment content increases, indicating an improved phase segregation in this series of samples. In addition, compared with the soft segment Tg's of 1000 MW PTMO

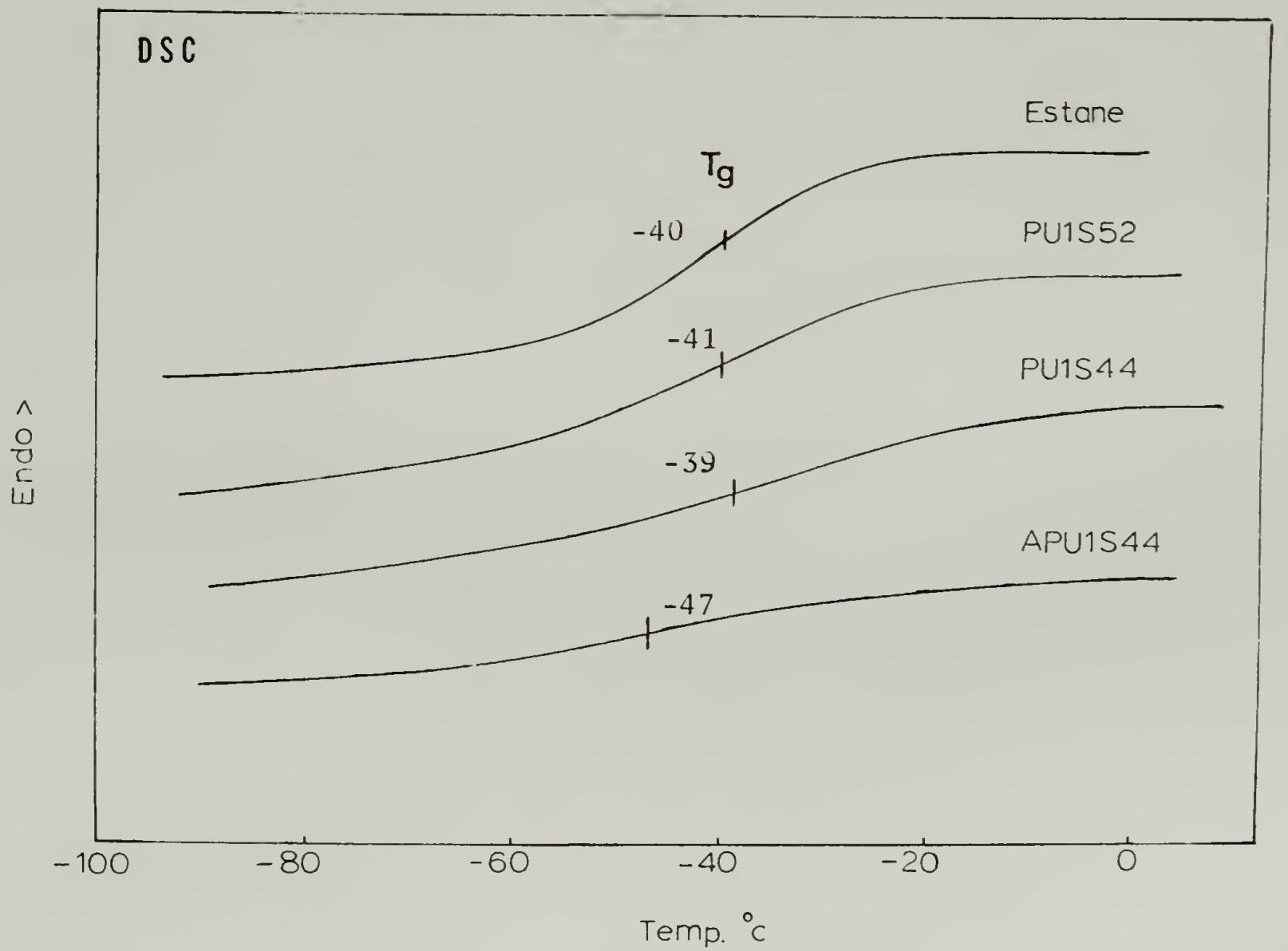

Figure 4.2 DSC traces of soft segment in PTMO-1000 polyurethanes.

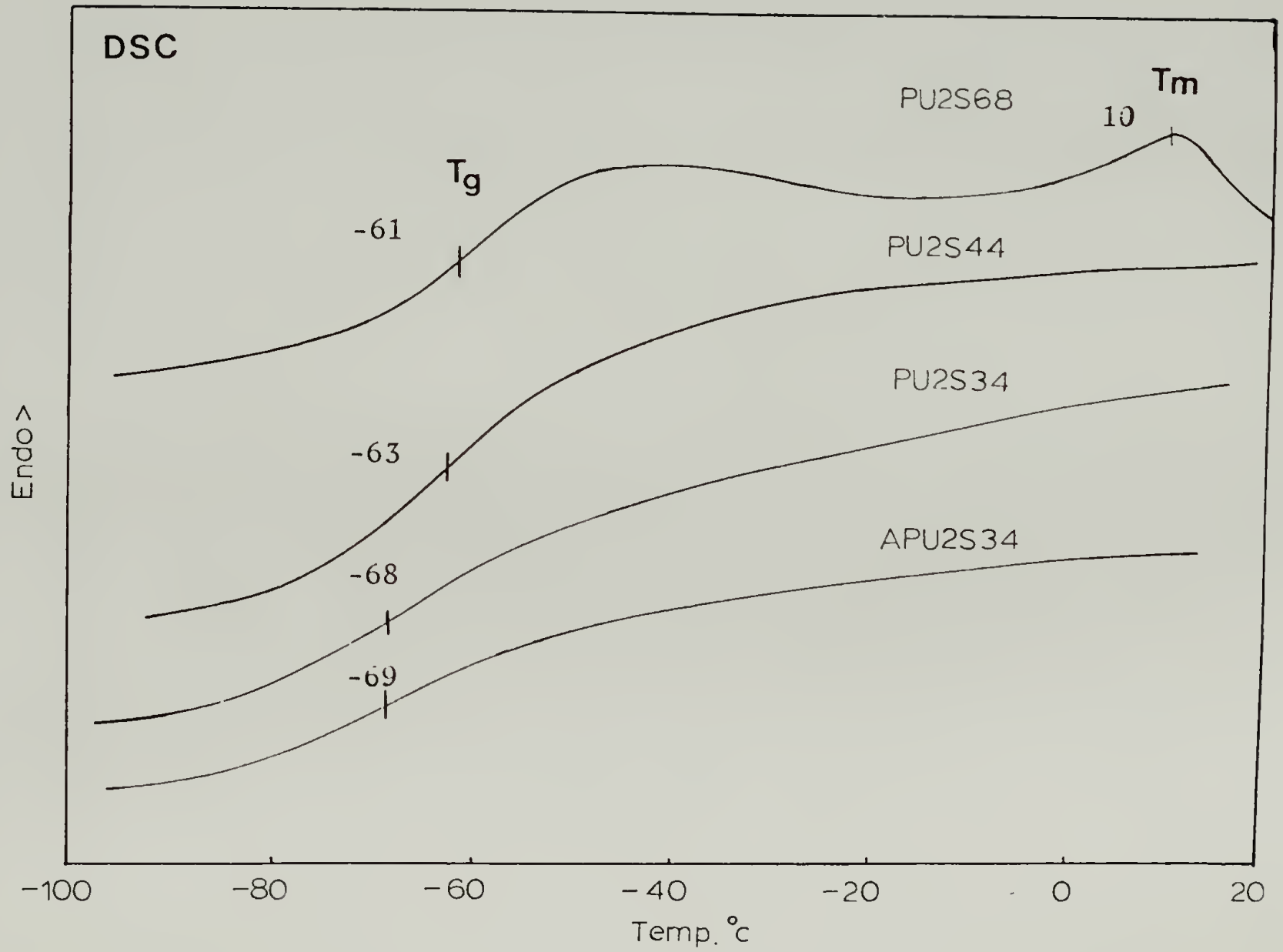

Figure 4.3 DSC traces of soft segment in PTMO-2000 polyurethanes.

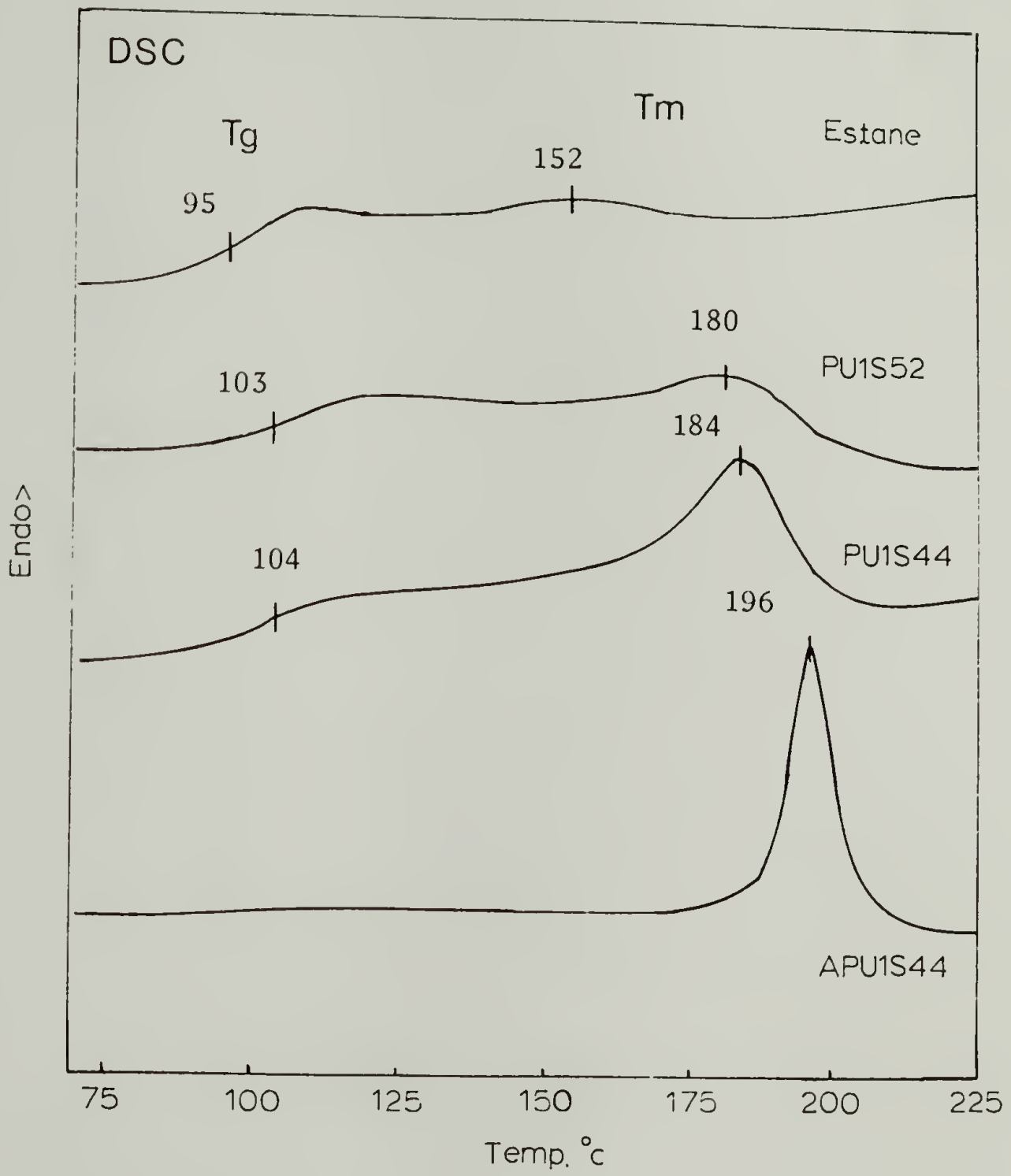

Figure 4.4 DSC traces of hard segment in PTMO-1000 polyurethanes.

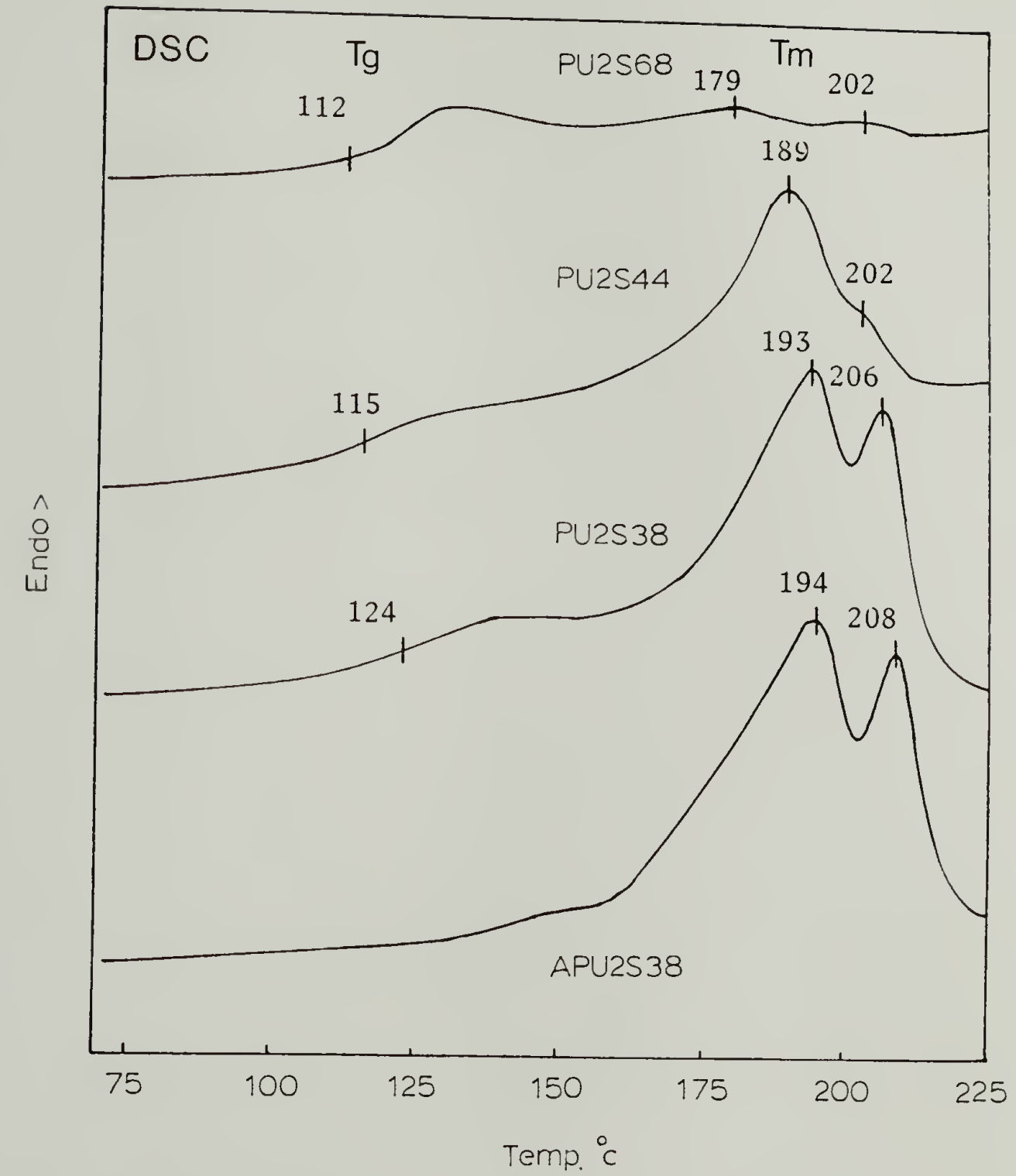

Figure 4.5 DSC traces of hard segment in PTMO-2000 polyurethanes.

Table 4.2

DSC Results of PTMO-Polyurethane Samples

Sample	Tg °C Soft Segment	Tg°C Hard Segment	Tm°C Hard segment	Δ H(J / g) Hard Segment
Estane	-40	95	152	1.9
PU1S52	-41	103	180	4.0
PU1S44	-39	104	184	12.0
APU1S44[a]	-47	—	196	19.0
PTMO-1000[b]	-82			
PU2S68	-61	112	179,202	1.4
PU2S44	-63	115	189,202	16.2
PU2S34	-68	124	193,206	22.8
APU2S34[a]	-69	—	194,208	32.4
PTMO-2000[b]	-79			
Pure-H[c]			192,213	52.0

[a]Annealed PU1S44 and PU2S34 at 155°C for two days

[b]Pure soft segments, taken from Wang and Cooper (16)

[c]Pure hard segment

samples, the soft segment Tg's of 2000 MW PTMO samples are about 20°C lower. This observation suggests that the 2000 MW PTMO samples have better phase separation than the 1000 MW PTMO samples. Moreover, Wang and Cooper (16) showed that the pure soft segment Tg's for 1000 and 2000 MW PTMO's were -82°C and -79°C, respectively, as shown in Table 4.2. The soft segment Tg's in the first series of samples (PTMO-1000) are substantially higher than that in a pure PTMO-1000 sample, indicating a strong interaction between hard and soft phase. This results in a certain degree of hard and soft phase mixing. However, for the second series of samples (PTMO-2000), the soft segment Tg's are much closer to the Tg of the pure PTMO-2000 sample which reflects a better phase separation in this series. The APU2S34 sample yields about the same soft segment Tg as the PU2S34 sample, indicating that annealing does not affect phase separation. A small melting endotherm observed for PU2S68 indicates a small amount of crystallinity present in the soft phase due to the higher soft segment content.

The DSC results for the hard segments of the polyurethane samples are shown in Figures 4.4 and 4.5. Both Tg and Tm were observed for these samples. In Figure 4.4, the hard segment Tg's for PU1S52 and PU1S44 are about the same, while the Tg of the Estane sample is 95°C, which is about 8°C lower than those of PU1S52 and PU1S44. In addition, a small melting endotherm peak (Tm) was observed at 152°c in the Estane sample. This Tm is much lower than that in PU1S52 and PU1S44 samples, 180°C and 184°C, respectively.

The values of heat of fusion ($\triangle H$) shown in Table 4.2, which reflects the crystallinity of the hard segment, increase with increasing hard segment content. These observations indicate that the Tm and the crystallinity increase as the hard segment content increases. The significantly lower Tg, Tm, and heat of fusion in the Estane sample is probably due to the presence of plasticizer in this commercial sample. Compared with the DSC result of PU1S44, APU1S44 shows a higher heat of fusion and a much higher Tm. These results indicate that the amount of crystallites in the hard phase is increased at the annealing temperature above the Tg of the hard segment, resulting in a better phase separation.

Figure 4.5 shows the DSC results for the hard segment in the second series of samples. Both Tg and two endotherm peaks (Tm's) were observed for all the samples. Again, the Tg, Tm, and $\triangle H$ increase with increasing hard segment content, suggesting better phase separation. The appearance of two endotherm peaks rather than one can be explained either by the presence of crystalline lamellae with different thicknesses or by the presence of hard segment crystallites with different crystal structures (7,17). A higher heat of fusion but without significant increase in Tm was observed for APU2S34. This provides another indication of the existence of good phase separation in PU2S34 sample. The absence of detectable hard segment Tg's for APU1S44 and APU2S34 is probably due to the presence of high crystallinity.

4.3.2 Dynamic Mechanical Thermal Analysis (DMTA)

Figure 4.6 shows the dynamic mechanical response of the PU1S44 and APU1S44 samples. As can seen from Figure 4.6, the shift of the tan δ peak toward lower temperatures for APU1S44 can be attributed to the presence of higher phase separation in this sample. The storage modulus is higher for APU1S44 than for PU1S44 due to the higher crystallinity in APU1S44 sample. Both observations are consistent with the DSC results.

4.3.3 Stress-Strain Analysis

The stress-strain curves for both series samples are shown in Figures 4.7 and 4.8, and the values of the Young's modulus are given in Table 4.3. It should be noted that the end points for all the curves except for the curve of PU2S34 are not the breaking points. As can be seen from Table 4.3 for both series of samples, the substantial increase in modulus with increasing hard segment content is attributed to an increase in the degree of interconnectivity of hard domains as the material changes from a predominantly soft segment matrix material to a predominantly hard segment one. In Figure 4.8, it is interesting to note that the yield point and breaking point observed for PU2S34 is probably due to phase inversion. Since PU2S34 has a high hard segment content, 66%, the hard segment is probably the continuous phase.

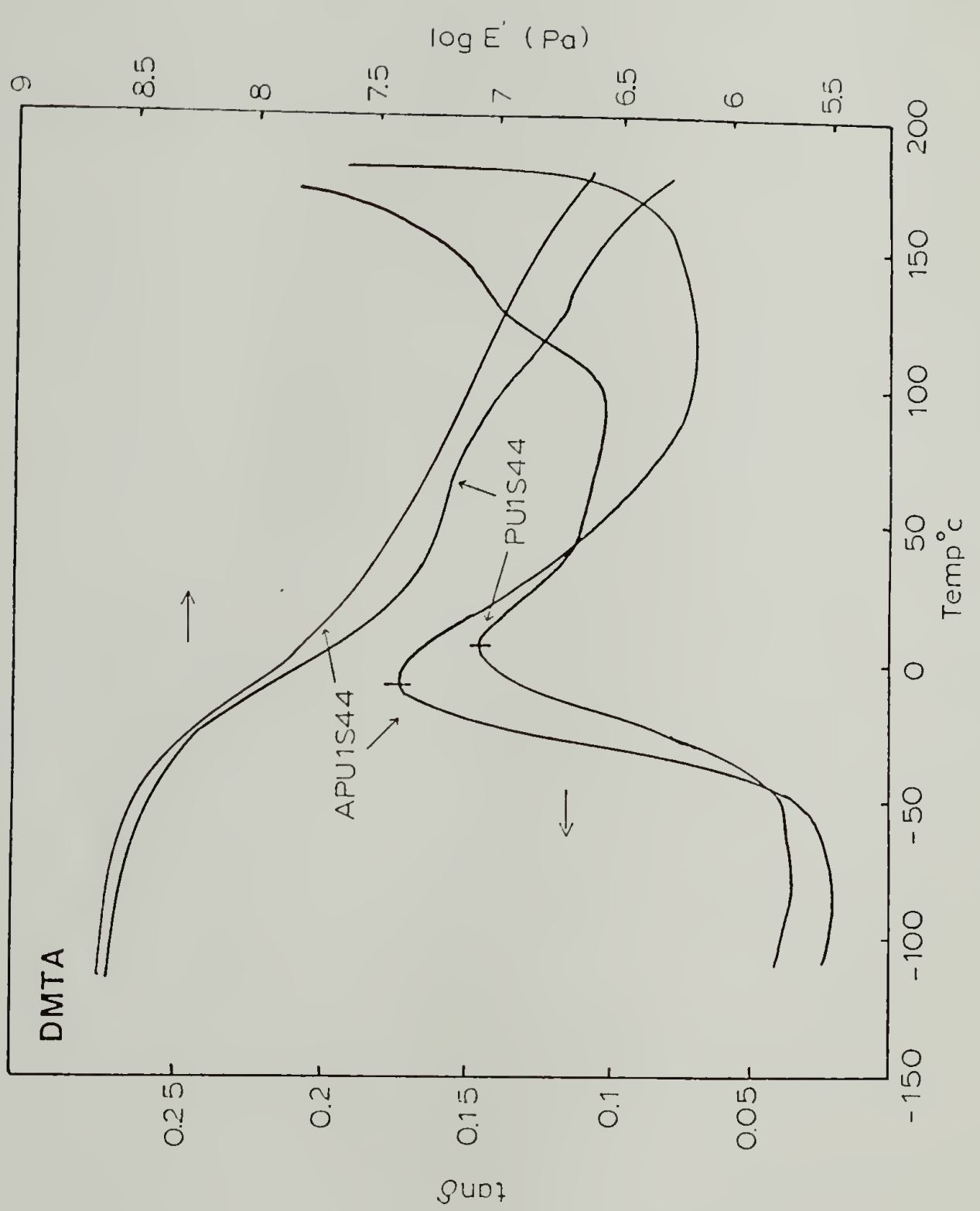

Figure 4.6 Dynamic mechanical properties of PU1S44 and APU1S44.

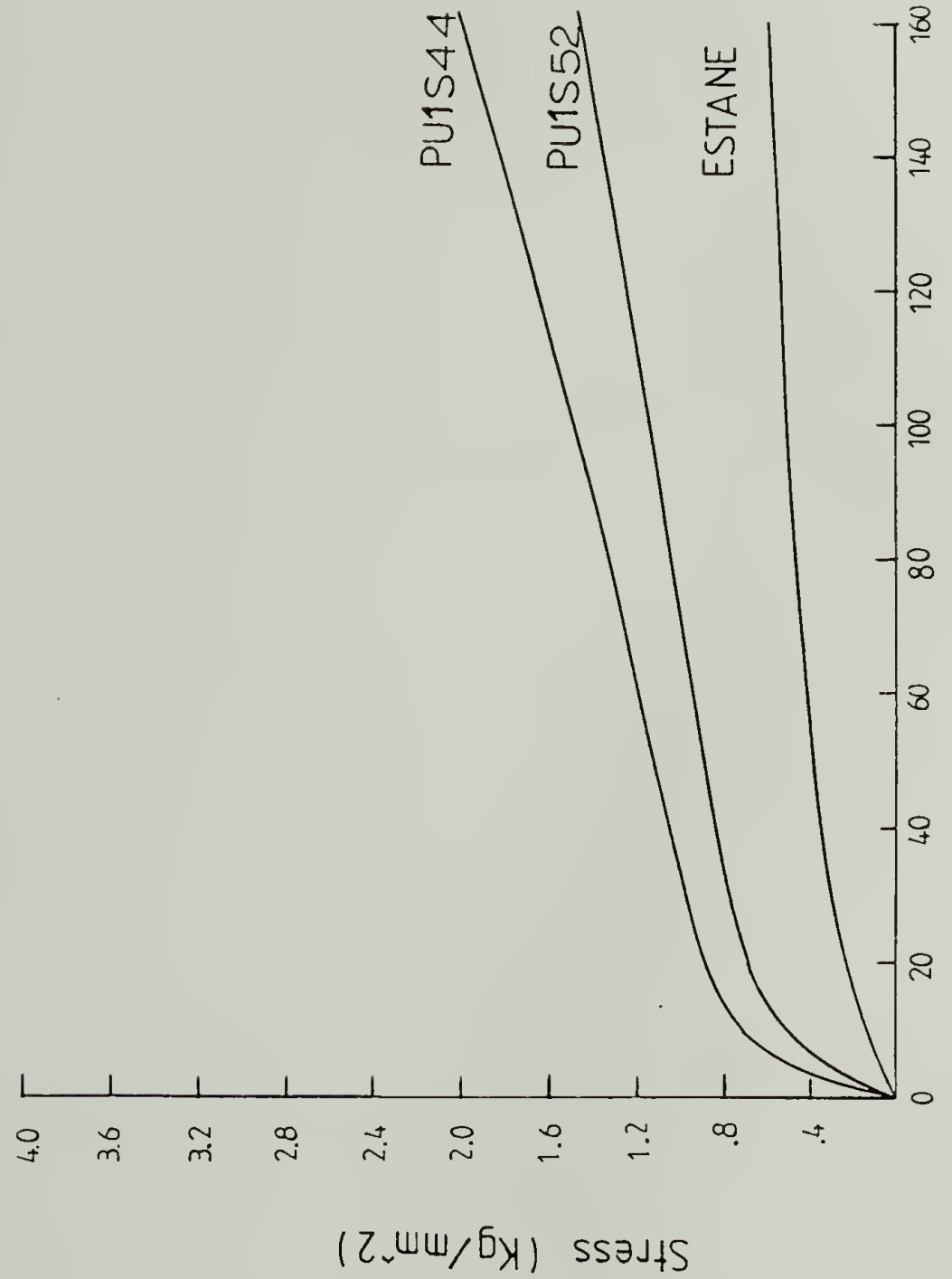

Figure 4.7 Stress-strain behavior of PTMO-1000 polyurethanes.

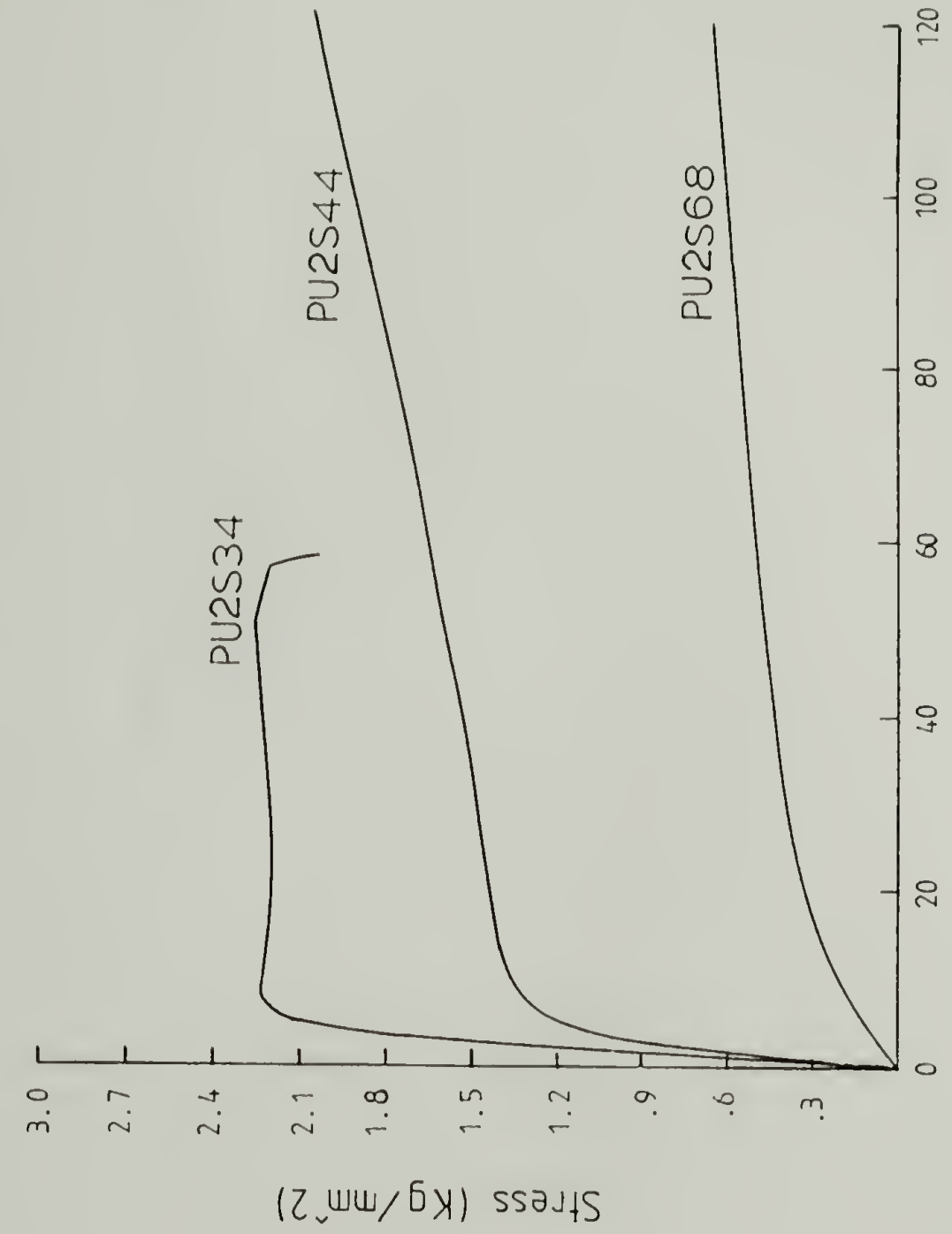

Figure 4.8 Stress-strain behavior of PTMO-2000 polyurethanes.

Table 4.3

Young's Modulus of PTMO-Polyurethane Samples

Sample	Modulus (Kg / mm^2)
Estane	1.5
PU1S52	6.0
PU1S44	10.0
PU2S68	2.5
PU2S44	35.0
PU2S34	46.0

4.4 Conclusions

The structure and properties of the polyurethane samples have been determined by DSC, DMTA and tensile testing analysis. The results of DSC studies indicate that the glass transition temperature of soft phase in the second series of polyurethanes is about 20°C lower than that in the first series of polyurethane samples (PTMO-1000), suggesting a better phase separation occurred in longer soft segment length polyurethanes. An improved annealing-induced phase separation was observed for annealed sample at 155°C, APU1S44, and a sample with PTMO of 2000 MW (PU2S34) exhibits an almost complete phase separation. Hard segment Tg, Tm, and ΔH increase with increasing hard segment content in both series. The appearance of two endotherm peaks rather than one in the second series of samples (PTMO-2000) is probably due to either the presence of crystalline lamellae with different thicknesses or the presence of hard segment crystallites with different crystal structures. The heat of fusion is higher for annealed samples at 155°C in both series, reflecting a higher crystallinity.

A lower temperature tan δ peak and a higher storge modulus in the annealed sample (APU1S44), determined by the DMTA experiments also suggest better phase separation and enhanced crystallinity.

The results of the stress-strain analysis showed that Young's modulus increases with increasing hard segment content in both

series of polyurethanes. The brittle fracture and the yield point which appeared in the PU2S34 sample can be explained either by the phase inversion where the hard phase changes from the dispersed phase to the continuous phase, or by the presence of bicontinuous phases.

4.5 References

1. R. W. Seymour, A. E. Allegrezza, Jr., and S. L. Cooper, Macromolecules, 6, 896 (1973).

2. R. W. Seymour and S. L. Cooper, J Polym. Sci., 46(C), 69 (1974).

3. R. W. Seymour and S. L. Cooper, Rubber Chem. Technol., 47, 19 (1974).

4. S. Abouzahr, G. L. Wilkes and Z. Ophir, Polymer, 23, 1077 (1982).

5. R. Bonart, J. Macromol. Sci., Phys., B2, 115 (1968).

6. R. Bonart, L. Morbitzer, and G. J. Hentze, J. Macromol. Sci., Phys., B3(2), 337 (1969).

7. N. S. Schneider, C. R. Desper, J. L. Illinger, A. O. King, and D. J. Barr, J. Macromol. Sci., Phys., B11, 527 (1975).

8. J. W. C. Van Bogart, P. E. Gibson, and S. L. Cooper, J. Polym. Sci., Polym. Phys. Ed., 21, 65 (1983).

9. C. S. P. Sung and N. S. Schneider, J. Mat. Sci., 13, 1689 (1978).

10. T. R. Hesketh, J. W. C. Van Bogart and S. L. Cooper, Polym. Eng. Sci., 20, 190 (1980).

11. N. S. Schneider, and C. S. P. Sung, Polym. Eng. Sci., 17, 73 (1977).

12. C. S. P. Sung, T. W. Smith, and N. H. Sung, Macromolecules, 13, 117 (1980).

13. J. W. C. Van Bogart, A. Lilaonitkul, L. E. Lerner, and S. L. Cooper, J. Macromol. Sci.-Phys., 17, 267 (1980).

14. C. B. Hu, R. S. Ward, Jr., and N. S. Schneider, J. Appl. Polym. Sci., 27, 2167 (1982).

15. J. A. Miller, B. Lin, K. K. S. Hwang, K. S. Wu, P. E. Gibson, and S. L. Cooper, Macromolecules, 18, 32 (1985).

16. C. B. Wang and S. L. Cooper, Macromolecules, 16, 775 (1983).

17. R. M. Briber and E. L. Thomas, J. Macromol. Sci.-Phys., B22(4), 509 (1983).

C H A P T E R V

TRANSPORT STUDIES IN PHASE SEGREGATED POLYURETHANES

5.1 INTRODUCTION

A substantial amount of work has shown that the physical properties and morphology of polyurethane materials depends on the composition and chemical nature of the hard and soft segment. However, the influence of the heterophase structure of segmented polyurethanes on small molecule transport behavior has received little attention. Most of the reported work on studying the transport properties are restricted to the homopolymers. The theories and models for rubbery polymers have been well established, and have provided a consistently accurate representation in most of the cases. A large body of experimental work and theoretical predictions have been devoted to studying the transport properties of gas and solvent vapor in glassy polymers. The glassy state is a non-equilibrium state and glassy polymers generally exhibit non-Fickian diffusion behavior.

Duda and Vrentas (1) have divided diffusional transport into three different types, viscous diffusion, elastic diffusion and viscoelastic diffusion, in terms of the Deborah number. When the polymer-solvent system behaves like a purely viscous fluid, the

diffusion process is described by the classical law of diffusion and is classified as viscous diffusion. A commonly accepted premise (2-4) is that an elastic diffusion process can be analyzed by using the classical diffusion equation with a diffusion coefficient which is independent of concentration, even though such a system is clearly not a purely viscous fluid mixture. For example, Meares (5,6), Zhurkov and Ryskin (7), Kishimoto, Maekawa, and Fujita (8), and Berens (9) obtained diffusion data for low penetrant concentration below the polymer glass transition temperature and all of these investigators concluded that the diffusional transport could be described by the equations of the classical theory with a mutual diffusion coefficient which was independent of concentration. Hence, it appears that, for sufficiently low penetrant concentrations below Tg, the elastic diffusion process can be considered to be Fickian even though no definitive theoretical justification for this hypothesis is available.

When the mass transfer process exhibits a number of features which cannot be explained by the classical theory of diffusion, the diffusion process can be classified as a viscoelastic diffusion, which normally exhibits non-Fickian anomalous curves, such as sigmoidal shapes, pseudo-Fickian behavior, two-stage sorption, case II and super case II diffusion, and dual mode sorption. All these anomalous or non-Fickian phenomena observed in the study of difusional transport in polymer-penetrant systems have been described in detail by a number of investigator (2,10-15).

Because of the relatively complicated structure of the heterophase polymers, a limited number of studies on the transport behavior of block copolymers have been reported. The polymers which were extensive studied were styrene-butadiene (SB) and styrene-butadiene-styrene (SBS) block copolymers which have rather well defined mophologies. Odani et al., Chiang and Sefton, Ceneba et al. and Kang et al. (16-20) have investigated the effect of solvent vapor on transport behavior of SB or SBS block copolymers. In general, two non-Fickian features were observed: (1) the thickness anomaly in the reduced sorption and desorption curves, and (2) the two-stage and sigmoidal curves at a certain concentration.

For segmented polyurethanes, most of the reported work has involved gas diffusion. Ziegal (21) has investigated four types of commercial thermoplastic polyurethane elastomers using a gas flow method. Two step transient behavior was observed with the larger-sized penetrants, namely Ar and N_2. It appears that these penetrants can distinguish between the soft and hard phases of polyurethane block copolymers. The dependence of gas diffusion on temperature in a series of polyurethane block copolymers was examined by McBride et al (22). A discontinuity was observed in the Arrhenius plots for some materials, and this discontinuity was found to be related to the onset of the Tg in the hard domains. Serrano (23) studied the transport of small molecules in a series of well characterized random segmented polybutadiene polyurethanes to determine the diffusivity of these materials experimentally and to

model the effective diffusion coefficient with effective medium theory (24). Recently, Goydan et al. (25) have studied the incremental vapor sorption and desorption for a commercial polyurethane, Estane, with ortho-dichlorobenzene as a solvent. Two-stage sorption curves were observed at intermediate and higher vapor concentrations, but this behavior was generally absent in the desorption runs (Figure 5.1). The two-stage sorption curves are related to the relaxation of the hard segment induced by the presence of the solvent, and can be fitted by the Berens-Hopfenberg (26) model of Fickian diffusion combined with a relaxation process. To understand this non-Fickian two-stage behavior, further studies on the solvent vapor sorption and diffusion in segmented polyurethanes are clearly needed.

The goal of this chapter is to examine the effect of the solvent, 1,2-dichloroethane, on the diffusion and sorption behavior in a variety of linear polyurethanes with different MDI:BD:PTMO ratios as well as different molecular weights of the soft segment. The structure and properties of these polyurethane materials have been described in chapter IV. Incremental vapor sorption and diffusion measurements have been carried out to determine the sorption isotherms and the behavior of the diffusivity as a function of concentration, and to define the extent of any relaxation effects. Hysteresis studies and the effect of film thickness and sample thermal history on the diffusion behavior have also been undertaken to define the origin of the relaxation process. In

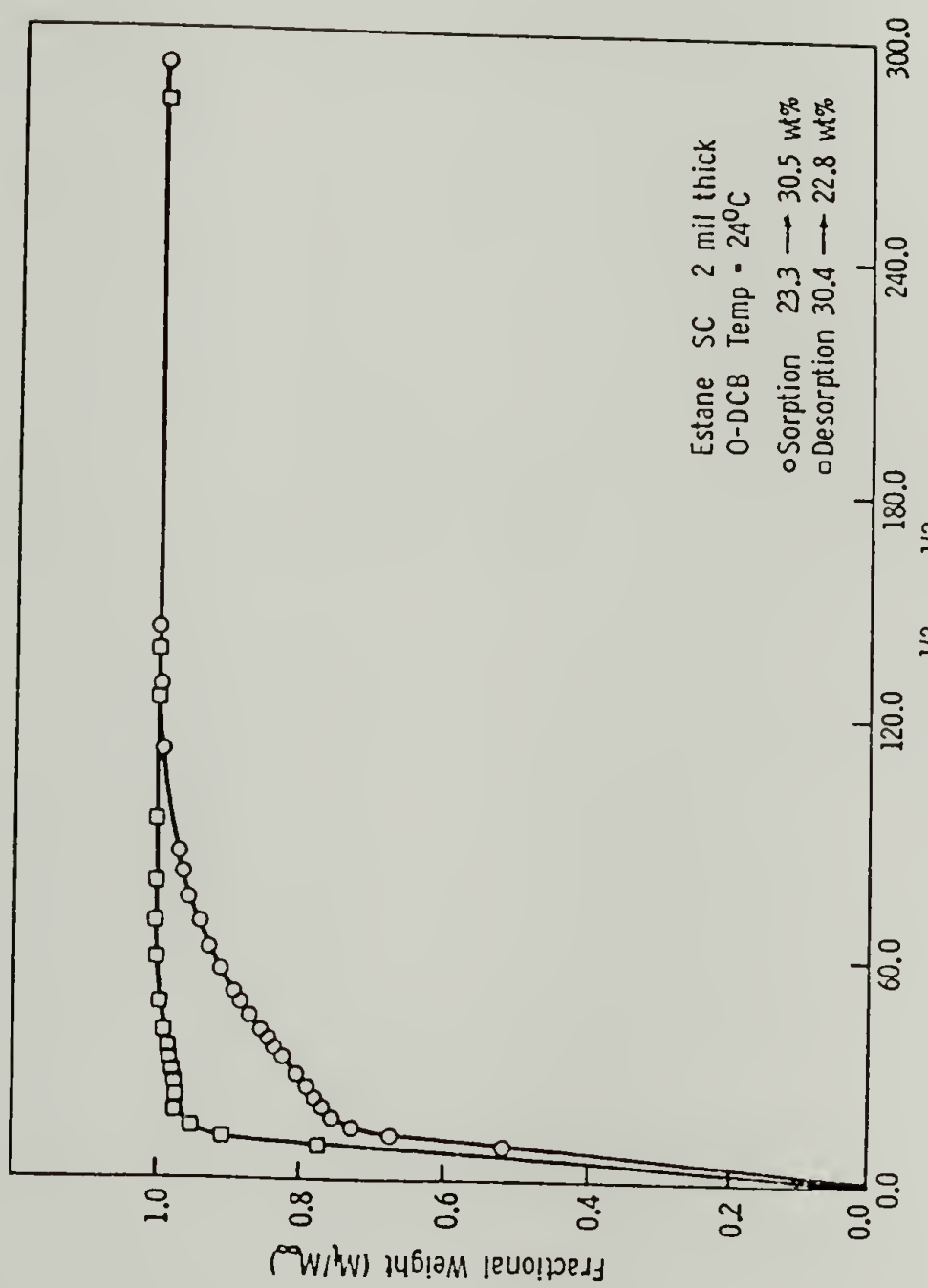

Figure 5.1 Sorption and desorption curves of ortho-dichlorobenzene in Estane sample.

addition, the diffusivity was determined by the initial slope method for curves showing Fickian behavior, while, for anomalous sorption curves, the Joshi-Astarita equation (27) was used to fit the experimental data and to calculate the diffusion coefficient.

5.2 Experimental

5.2.1 Materials and Preparation of Samples

Polyurethane materials used in this study are described in Table 4.1 and Figure 4.1, and the characteristics of these materials as determined by DSC, DMTA and tensile testing are discussed in chapter IV. The method for preparation of film samples with different thicknesses, 0.05 mm, 0.11 mm, and 0.23 mm, was also described in chapter IV. The dimensions of film samples in the incremental vapor sorption and desorption experiments is about 2x2 cm to eliminate any errors resulting from edge effect. The solvent or penetrant used in this study is 1,2-dichloroethane, which was purchased in high purity form from Aldrich Chemical Company and used as received.

5.2.2 Experimental Methods

A good review on the experimental methods of the permeation and sorption studies is given by Felder and Hvard (28). The diffusion

apparatus, procedures, and methods for calculation of diffusivity described in this section are restricted to this study.

(A) Diffusion Apparatus

The apparatus for incremental vapor sorption and desorption experiments is shown in Figure 5.2, and is ususlly called a McBain balance. The glass apparatus was placed in a wood cabinent, in which the temperature was maintained at 30°C and controlled by a bulb heater and circulating fans with a temperature controller. The pump used in this system was a mechanical pump which gives a vacuum of 10^{-4} torr. The MKS pressure transducer and indicator were connected to the system to monitor the pressure of the system from 0 to 100 mm Hg with accuracy of $\pm$0.001 mm Hg. The sensitivities of the thermostated quartz springs used to determine the weight uptake of the sample were 20, 5, and 2 mg/cm depending on the sorption ability of the samples. These quartz springs were calibrated before doing the sorption experiments.

To maintain a constant temperature in the sample container, the cyclindrically shaped glass chamber was surrounded by a water jacket which provides a constant temperature of 24$\pm$0.1°C. Since a decrease in the vapor pressure in the system results when a film absorbs solvent vapor, a large solvent vapor resorvior was designed to connect to the system to minimize this effect. The weight uptake of the sample was determined by the displacement of the spring which was measured within 0.01 mm using a Gaertner cathetometer. Sorption

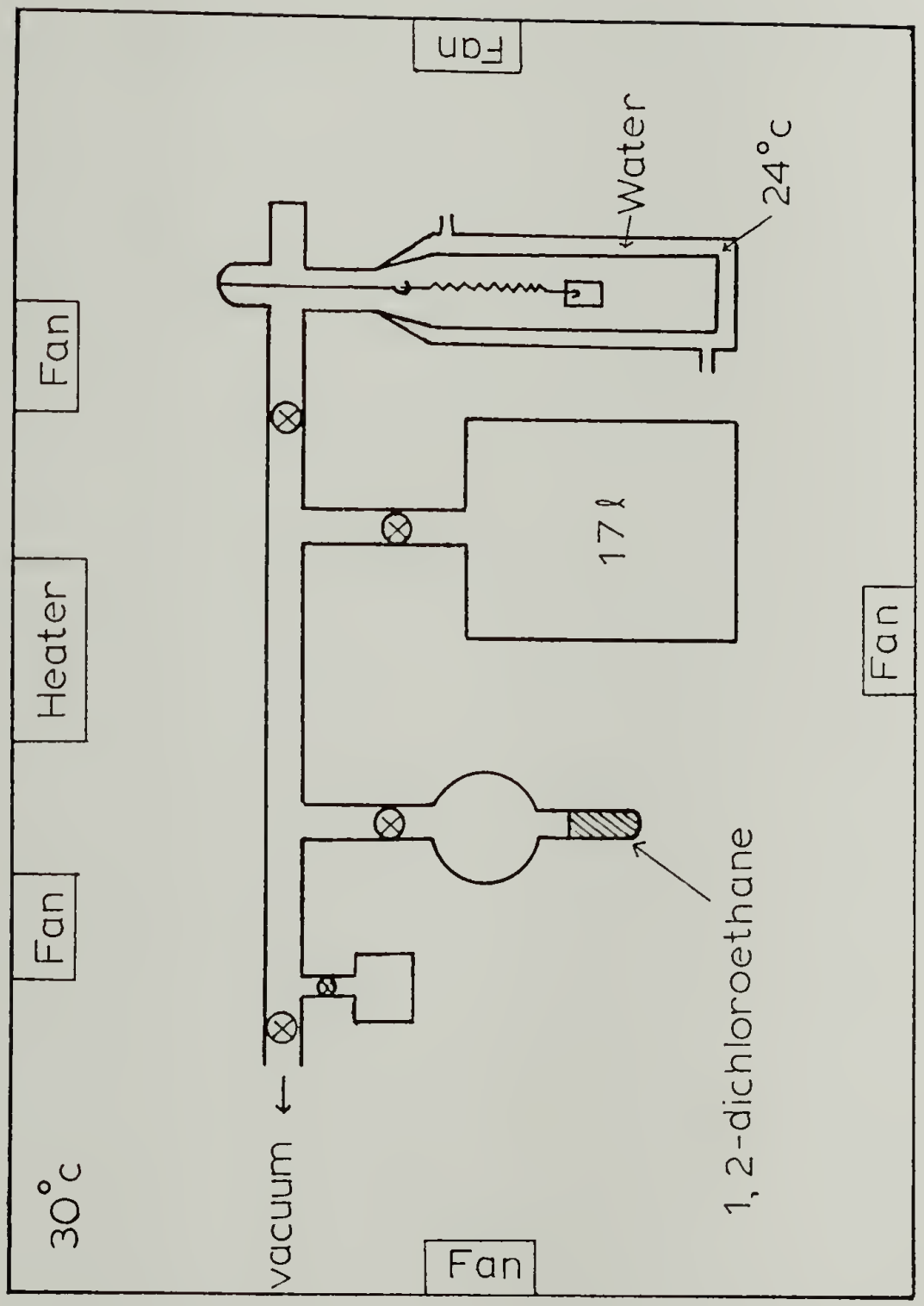

Figure 5.2 Sorption apparatus.

and desorption experiments were conducted at 24°C using 1,2-dichloroethane as a solvent which has a saturated vapor pressure P_0=74.8 mm Hg at 24°C.

(B) Procedures

This study is called incremental vapor sorption and desorption experiments, which were carried out in a vacuum system. Beginning with the dry film the procedure involved equilibrating the film with solvent at some vapor activity, P_i/P_0, exposing the film to a step change in activity, P_f/P_0, and recording the weight changes as a function of time until the equilibrium corresponding to this new activity was achieved. The procedure was repeated in activity increments of about 0.1 until the full range was covered. Due to long term changes in sample weight, each such determination usually required one day, or more, to attain equilibrium. After completing the set of sorption measurements, the procedure was reversed and desorption experiments were performed beginning with the film equilibrated at high activity. Once again, the full activity range was traversed by exposing the film to step decreases in activity and recording the weight loss as function of time.

(C) Calculations

Based on Hooke's law, $w=k\,\Delta x$, the weight gain or loss is the product of the spring constant k and the displacement of the spring Δx. In the sorption or desorption experiments, the Δx was recorded

as a function of time t, and, therefore, w can be calculated with a given spring constant by using Hooke's law. A plot of M_t/M_∞ as a function of square root of time $t^{1/2}$ is made for each set of experiments. Here, M_t is the weight gain or loss at time t, and M_∞ is the equilibrium weight at long times. The sorption isotherm curves were obtained by plotting the final equilibrium solvent concentration, determined by the total weight uptake of the solvent divided by the dry sample weight, vs. solvent vapor activity, P_f/P_0. In an attempt to compare the sorption behavior for samples with different thicknesses, the reduced sorption curves were made by plotting M_t/M_∞ vs. $t^{1/2}/L$, where L is the thickness of the dry film.

Assuming Fickian diffusion and a constant diffusion coefficient, solutions of the diffusion equation (Fick's second law) may be used to estimate the effective diffusion coefficient. Four methods are usually used to determine the diffusivity. These are half-time method, initial-slope method, moment method, and limiting-shope method. Crank (15) has given the detailed mathematical derivations and descriptions for these four methods. The only method used in this study to determine the diffusion coefficient is the initial slope method. For a film sample or a plane sheet at small time t with a thickness L, a graph of M_t/M_∞ vs. $t^{1/2}$ is linear and the initial slope, m, is propotional to the square root of the diffusion coefficient D. Thus, the equation for this method is given as follows:

$$M_t/M_\infty = m\ t^{1/2} \qquad (5.1)$$

where $$m = 4D^{1/2}/\pi^{1/2}L \qquad (5.2)$$

and then, $$D = \pi m^2 L^2/16 \qquad (5.3)$$

It should be noted that there exists a certain amount of solvent in the sample before starting each set of incremental sorption or desorption experiments. The thickness correction is clearly needed due to swelling. Assuming that the swelling is isotropic and induces no volume change on mixing, the diffusivity is given by the following equation:

$$D' = D/\phi_2^{2/3} \qquad (5.4)$$

Here, ϕ_2 is the final volume fraction of the polymer, and D' is the corrected diffusion coefficient, which represents the diffusion coefficients in all the D-C curves.

For anomalous sorption curves, the two-stage and S-shaped curves, the Joshi and Astarita (27) equation is used to fit the experimental data and to calculate the apparent diffusion coefficient. The detailed mathematical description of this equation was given in section 3.5 in chapter 3. The results of the derivations are shown below:

$$W = M_t/M_\infty = f_D(t) - m[f_{DR}(t) - (\tan\phi/\phi)(1-\exp -t\phi^2/\Theta_D)] \qquad (5.5)$$

where

$$f_D(t) = 2 \sum_{n=1}^{\infty} 1-\exp[(-a_N^2 t/\Theta_D)]/[a_N^2] \qquad (5.6)$$

$$f_{DR}(t) = 2 \sum_{n=1}^{\infty} 1-\exp[(-a_N^2 t/\Theta_D)]/[a_N^2-\phi^2] \qquad (5.7)$$

$$a_N = \pi(n-0.5) \qquad (5.8)$$

$$\Theta_D = L^2/D \qquad (5.9)$$

$$\phi^2 = \Theta_D/\Theta_R = L^2/D\Theta_R \qquad (5.10)$$

Three parameters appear in equation 5.5, namely m, ϕ, and Θ_D, where m is the fraction of the relaxation; ϕ^2 is the ratio of the characteristic times for diffusion and relaxation precesses, shown in equation 5.10; Θ_D is the diffusion time, shown in equation 5.9, and Θ_R is the relaxation time. These three parameters were determined with a non-linear regression program, which is called BMDP3R, along with a subroutine program resulting from the first derivative of equation 5.5 with respect to these parameters, respectively. The university computer (Cyber) was used to do all the curve fitting and calculations. The subroutine program and the method to connect to the main program (BMDP3R) are described in Appendix A.

5.3. Results and Discussion

Figure 5.3 shows the scheme of the incremental vapor sorption and desorption studies, including sorption isotherms, the incremental diffusion-time behavior, hysteresis phenomenon, thickness and annealing studies, curve fitting, determination of diffusivity, and the behavior of the diffusivity as a function of solvent concentration. The results of these studies are described and discussed in the following sections.

5.3.1 Sorption Isotherms

Figure 5.4 shows the sorption isotherm of 1.2-dichloroethane for the Estane sample. The sorption isotherm is determined by performing incremental vapor sorption and desorption experiments with the three film thicknesses, 0.05mm, 0.11mm and 0.23mm. The final concentration was calculated by the total weight uptake of the solvent at certain activity divided by dry sample weight. The activity, a, is determined by the ratio of P_f/P_o, where P_f and P_o are the final vapor pressure and the saturated vapor pressure of the 1.2-dichloroethane at 24°C, respectively. As can be seen from Figure 5.4, all points fall on one curve, which shows an initial linear region and then bends sharply upwards in a manner typical of a swelling solvent. This observation indicates that the sorption isotherm for the Estane sample is thickness independent, and no

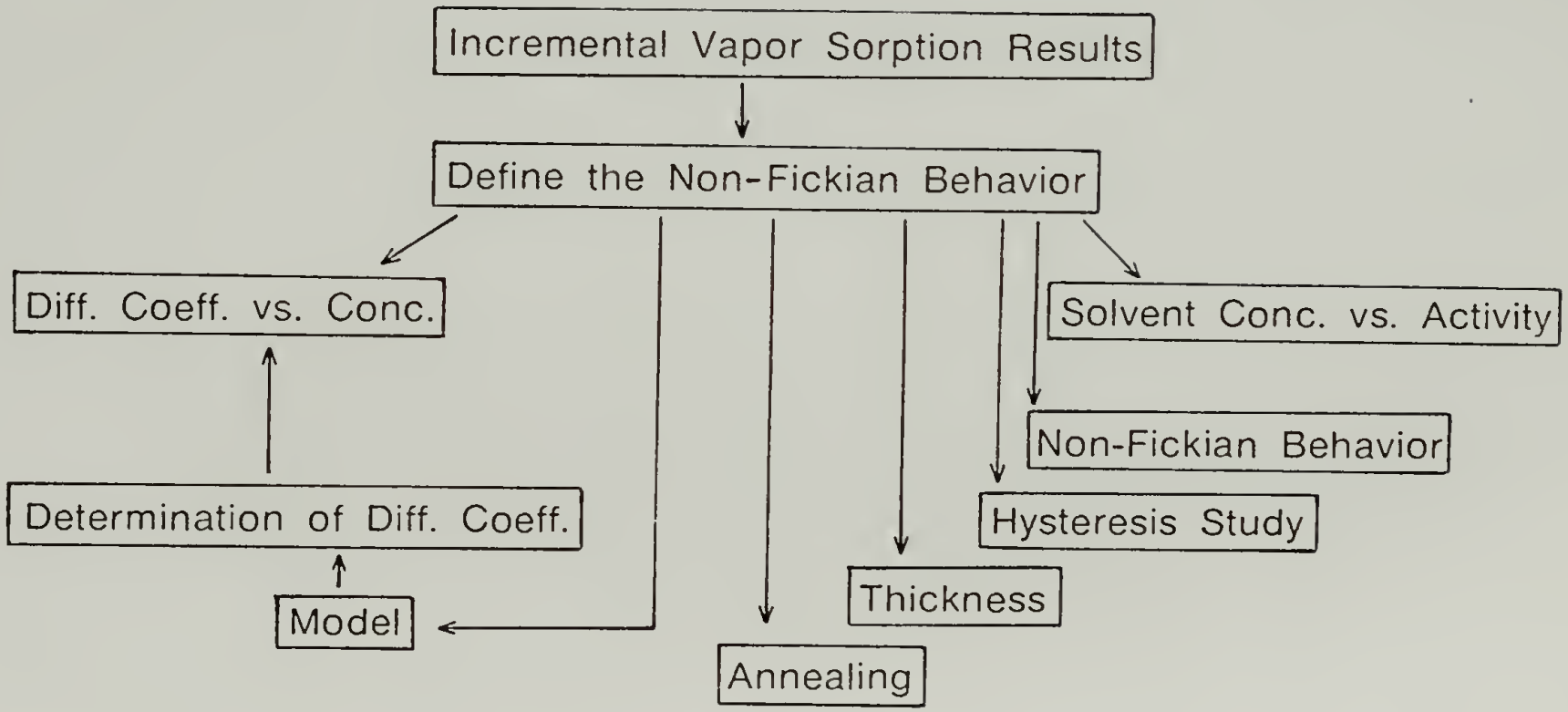

Figure 5.3 The scheme of the transport studies.

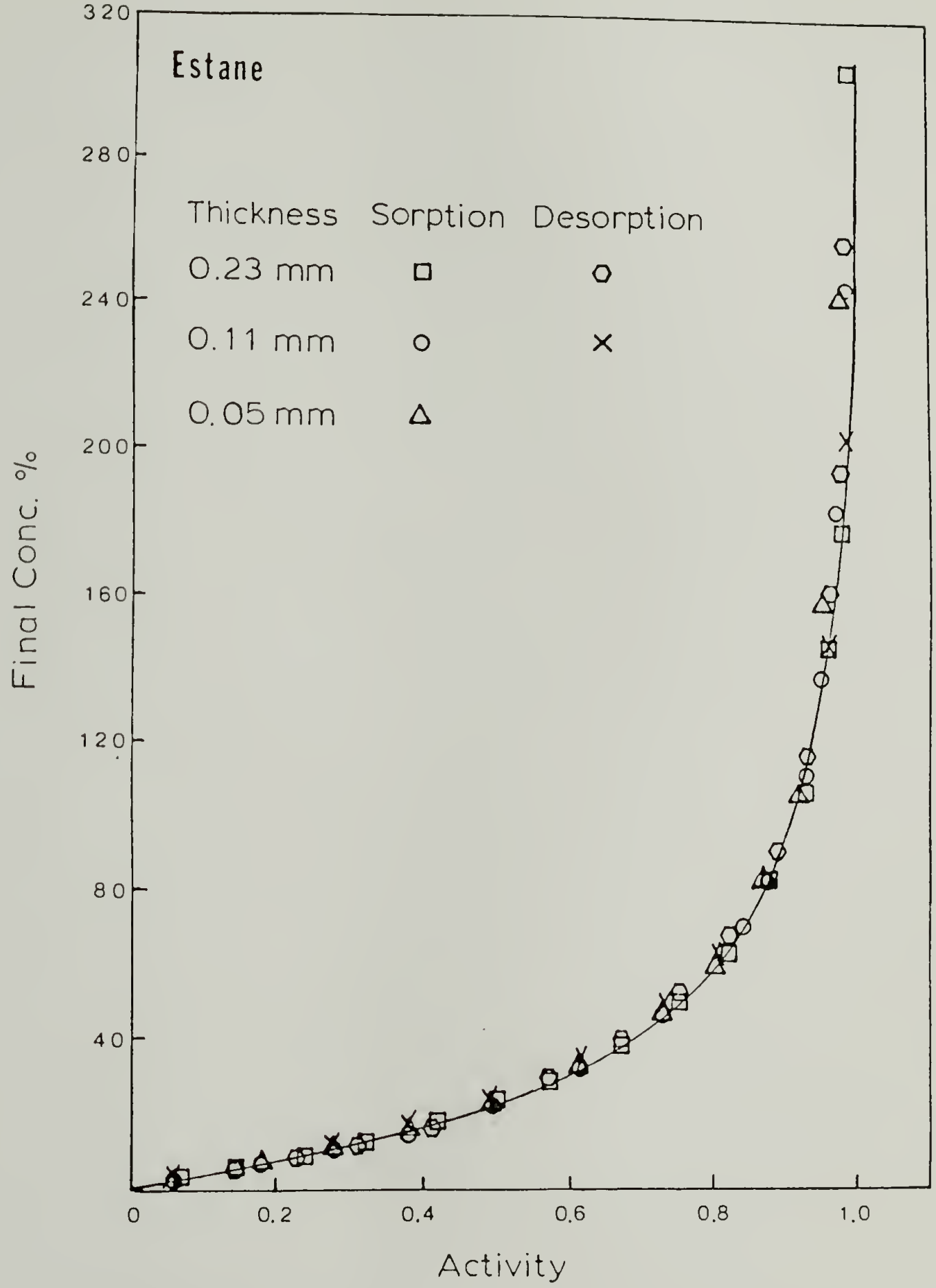

Figure 5.4 Sorption isotherm curves of 1,2-dichloroethane in Estane with different film thicknesses at 24°C.

detectable hysteresis exists. The behavior of the curve seems to follow the Flory-Huggins equation (29), though the initial region obeys Henry's law. It should be noted that the maximum immersion uptake of 1.2-dichloroethane in Estane is about 450 wt%. If the curve is extrapolated virtually to unit activity, the value of the solvent vapor uptake would be consistent with the 450 wt% immersion uptake. A similar behavior was found for an Estane sample with ortho-dichlorobenzene as a solvent, which gives only 230 wt% immersion uptake (25). The sorption isotherms of first sorption, desorption, and second sorption curves for PU1S44 are shown in Figure 5.5. As can be seen from this figure, the final concentration is always higher in the desorption curve than that in the first sorption curve, and the second sorption curve appears to be in between the desorption and the first sorption curves. These results may be explained in terms of the relaxation process which can be induced either by the swelling of the soft segment resulting in an increase in the mobility of the hard segment due to the enhancement of the flexibility of the soft segment, or by the direct interaction between 1,2-dichloroethane and the amorphous hard segment phase and/or interphase. It should be noted that the crystalline phase of the hard segment is assumed not to be penetrated by 1.2-dichloroethane vapor. As solvent is removed from the sample, the relaxed structure arising from the sorption-induced relaxation of the polymer molecules persists, resulting in an extra free valume after sorption run. Hence, the equilibrium concentration for desorption

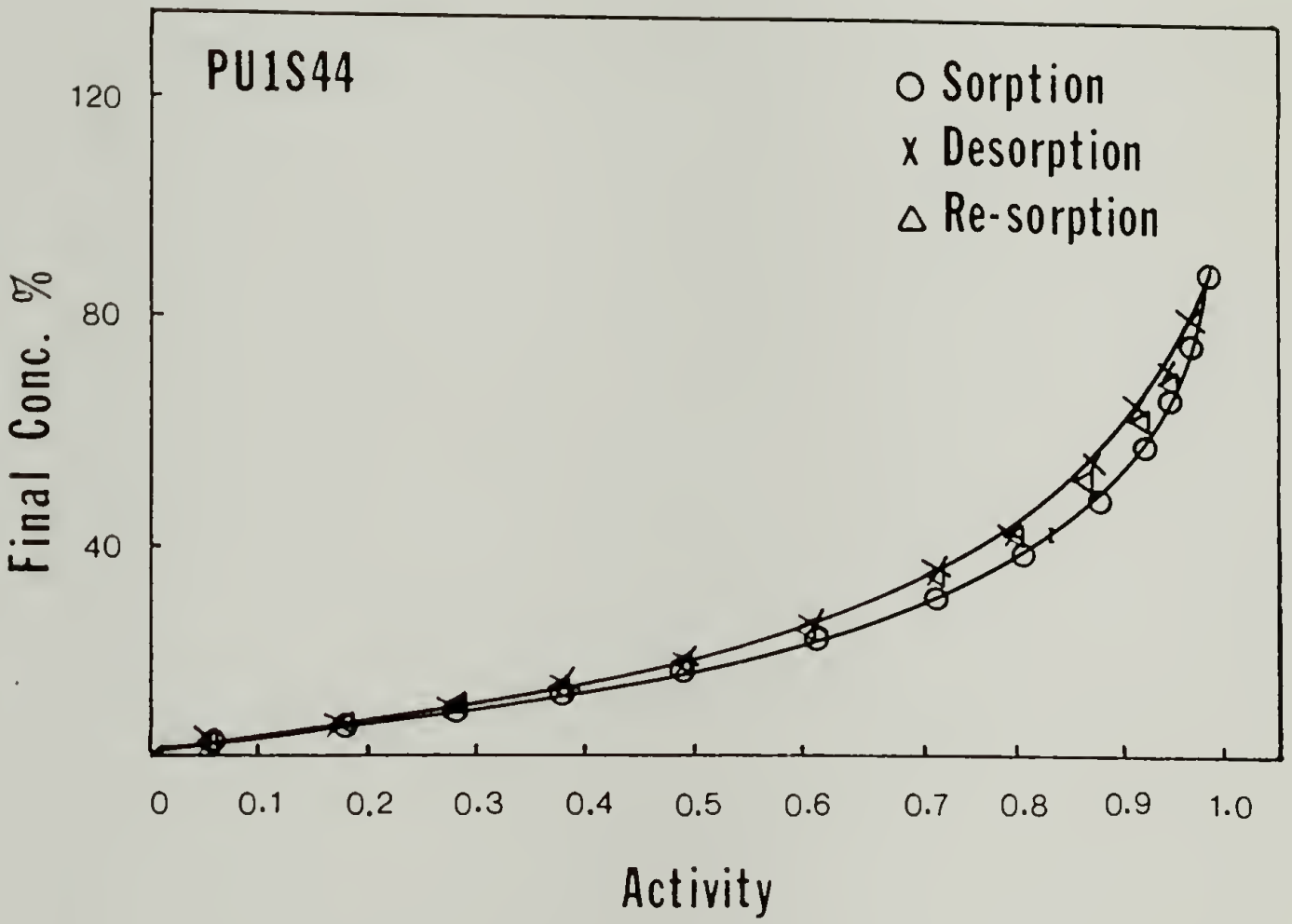

Figure 5.5 Sorption isotherm curves of 1,2-dichloroethane in PU1S44 with film thickness of 0.11 mm at 24°C.

is higher than that for the first sorption. In addition, the second sorption curve does not superimpose on the first sorption curve, indicating that the relaxed structure is retained after desorption run and does not return to the original state. Thus, a higher final concentration was observed in the second sorption curve. This hysteresis behavior was not shown in the case of Estane sample. It is to be noted that much higher swelling occured in the Estane sample, which has a relatively high soft segment content, resulting in a faster relaxation rate of polymer molecules upon solvent removal. Therefore, no detectable hysteresis was observed for Estane sample. The hysteresis behavior was observed for PU1S52 and PU2S68 (Figures 5.6 and 5.7) but was not significant due to the characteristics of their high soft segment content and relatively high solvent swelling. Figures 5.8 and 5.9 shows the sorption isotherms of 1,2-dichloroethane for PU2S44 and PU2S34, respectively. As can be seen from these figures, lower solvent swelling and hysteresis behavior were observed for both samples containing higher hard segment content. This hysteresis beharior appears to be significant for samples which contain higher hard segment content, resulting in a low solvent sorption. Figure 5.10 shows the final concentration as a function of solvent vapor activity for PU2S68, PU2S44, and PU2S34 in the desorption runs. The equilibrium concentration decreases with increasing hard segment content, suggesting that the solubility of 1,2-dichloroethane in soft segment is much higher than that in the hard segment phase. Compared with

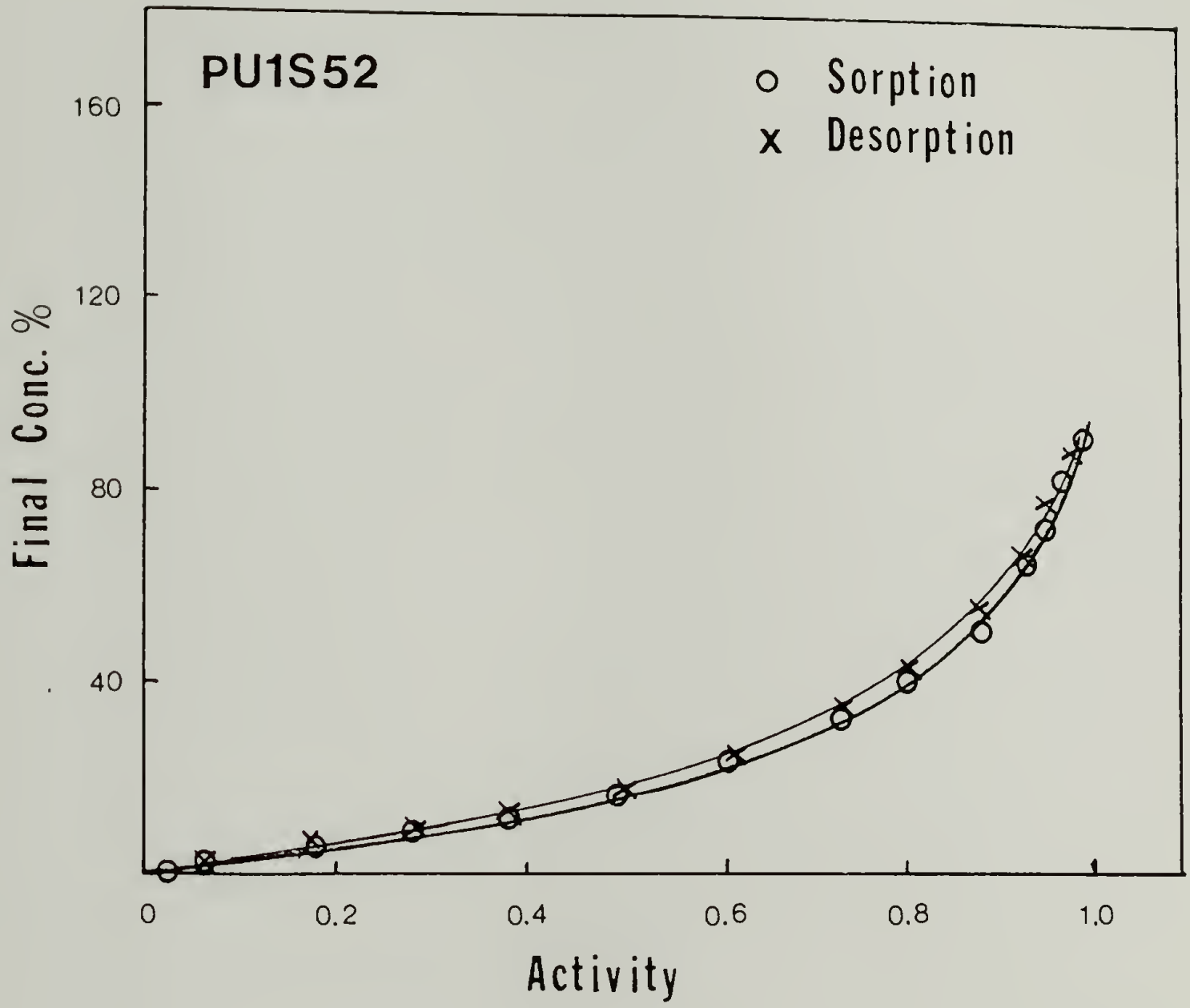

Figure 5.6 Sorption isotherm curves of 1,2-dichloroethane in PU1S52 with film thickness of 0.11 mm at 24°C.

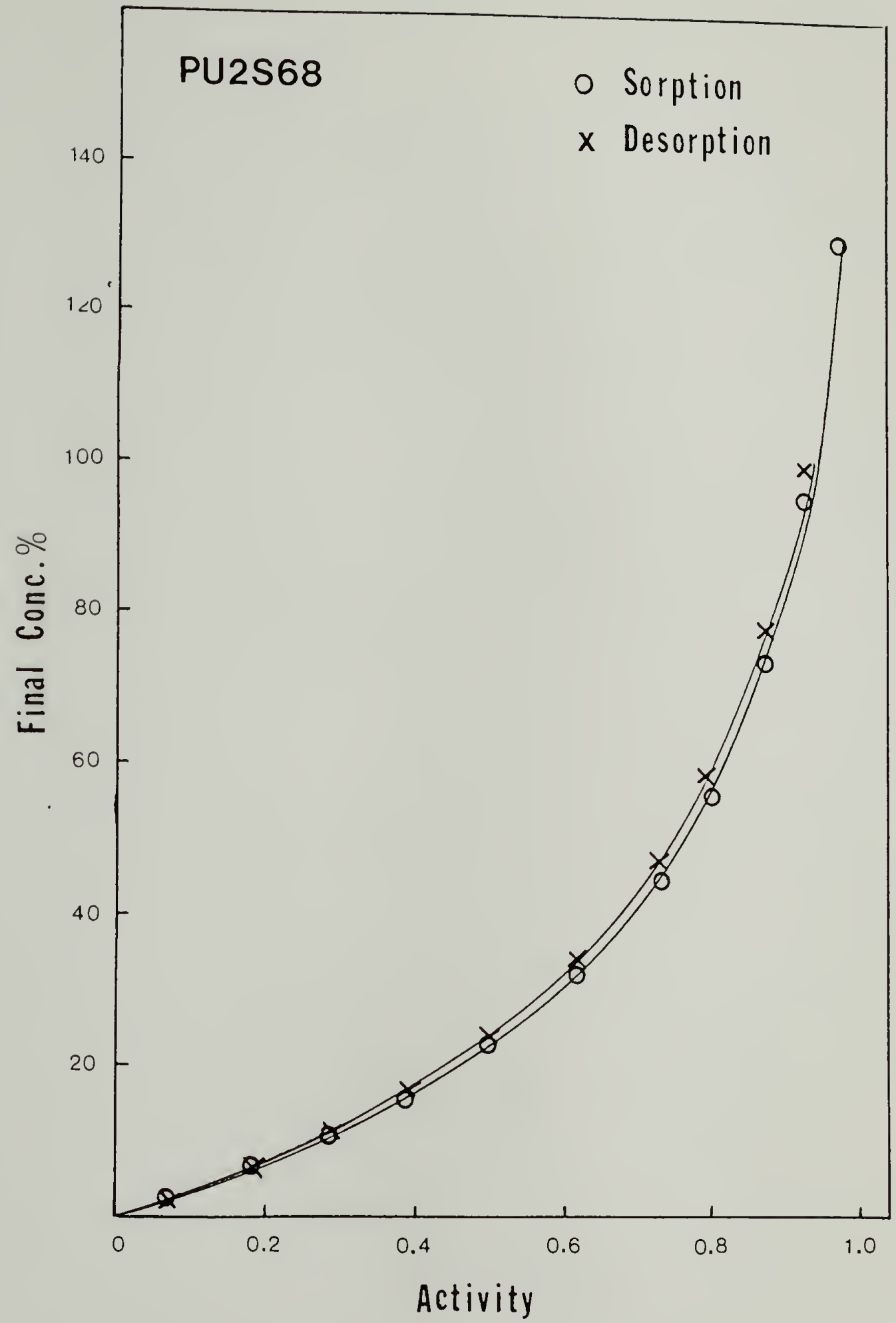

Figure 5.7 Sorption isotherm curves of 1,2-dichloroethane in PU2S68 with film thickness of 0.11 mm at 24°C.

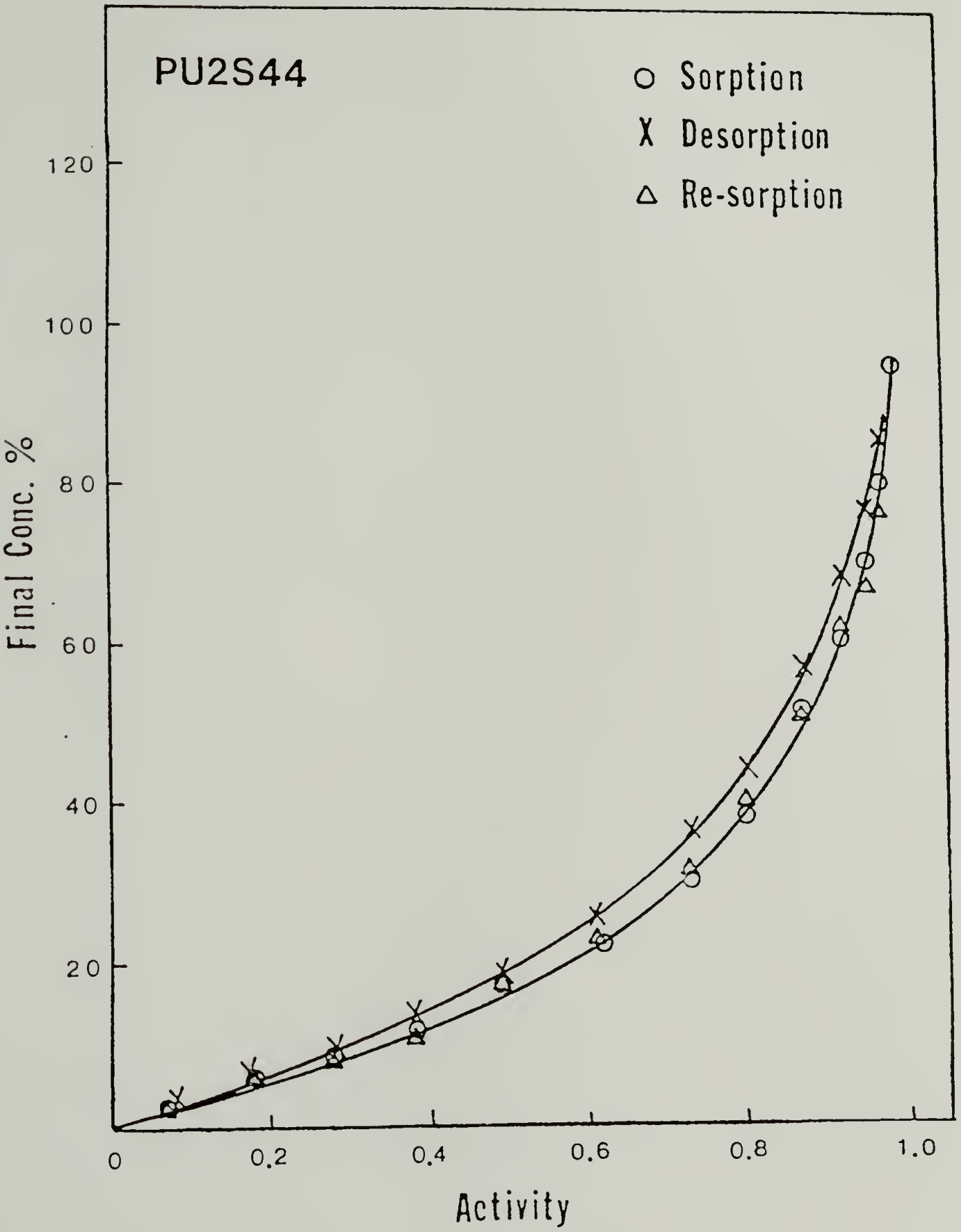

Figure 5.8 Sorption isotherm curves of 1,2-dichloroethane in PU2S44 with film thickness of 0.11 mm at 24°C.

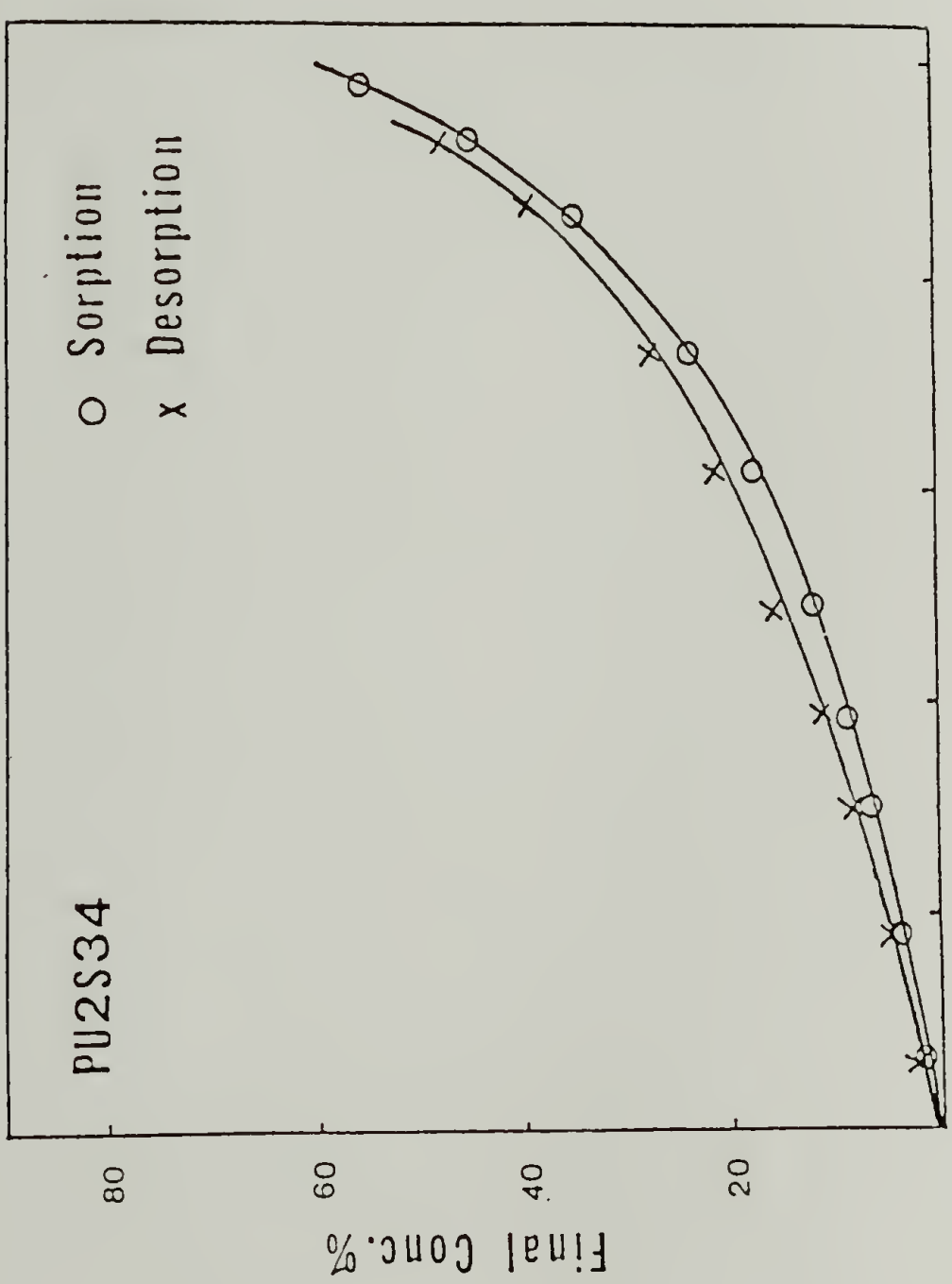

Figure 5.9 Sorption isotherm curves of 1,2-dichloroethane in PU2S34 with film thickness of 0.11 mm at 24°C.

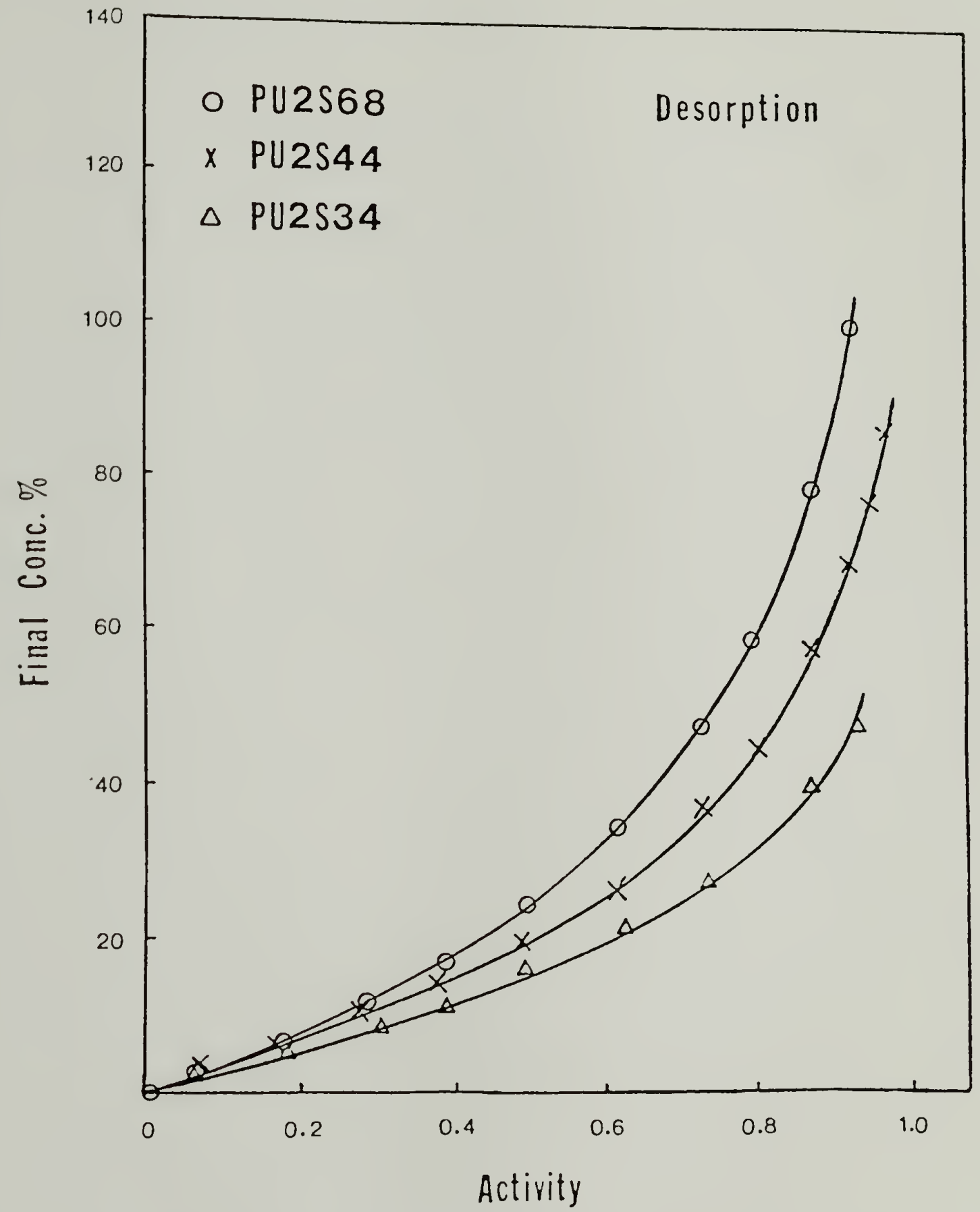

Figure 5.10 A comparison of sorption isotherm behavior,determined from desorption experiments, for 1,2-dichloroethane in PU2S68, PU2S44, and PU2S34 with film thickness of 0.11 mm at 24^{o}C.

the amount of sorption in the soft phase, the amount of sorption in the glassy hard phase is almost negligible.

Figures 5.11 and 5.12 show the sorption isotherms for PU1S44 and APU1S44, and PU2S34 and APU2S34, respectively. The final concentration as a function of activity in both figures is higher for annealed samples at 80°C than for annealed samples at 155°C. It was found (26,30) that an annealed poly(vinyl chloride) (PVC) sample contains less free volume than an as-received PVC sample (without annealing) as determined by density measurements. For polyurethane materials, not only does the free volume decrease but also the crystallinity of the hard phase increases for annealed samples at 155°C, and thus, the amount of sorption is lower. Both curves, shown in Figures 5.11 and 5.12, appear to separate from each other at the moderate and higher activities, indicating that the effect of solvent on the glassy hard segment phase and/or interphase becomes significant at higher solvent concentrations. The formation of a more rigid structure in the hard segment phase due to annealing decreases the mobility of the hard block chains and lowers the effect of the flexible soft segment on the hard phase due to annealing-improved phase separation. Thus, the difference between both sorption isotherm curves in Figures 5.11 and 5.12 can be attributed to the morphology changes of the hard phase, and also to a decrease in the amount of a mixed interfacial region.

Two important results were obtained from this study: (1) the appearance of the hysteresis behavior for samples containing high

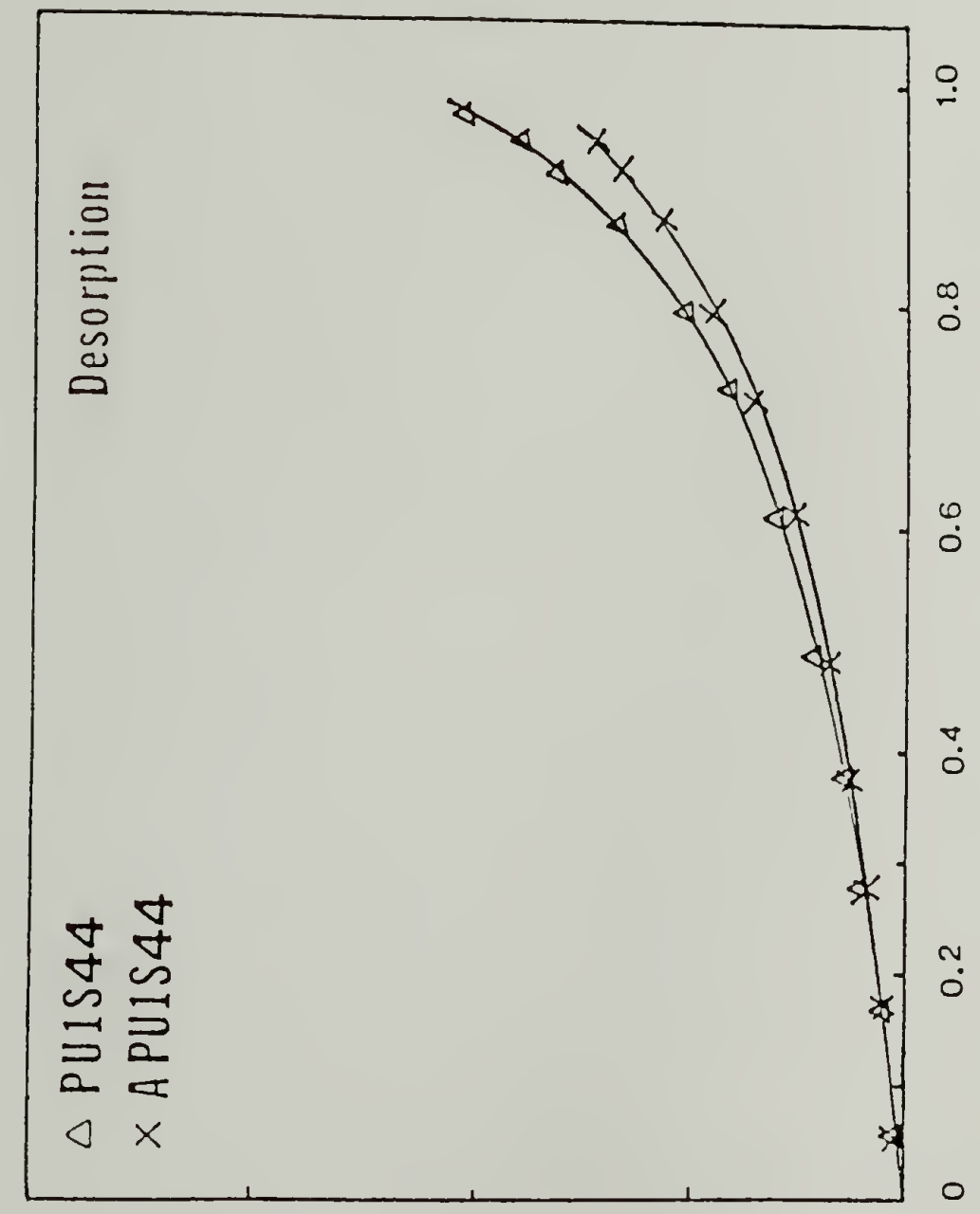

Figure 5.11 Acomparison of sorption isotherm behavior, determined from desorption experiments, for 1,2-dichloroethane in PU1S44 and APU1S44 with film thickness of 0.11 mm at 24°C.

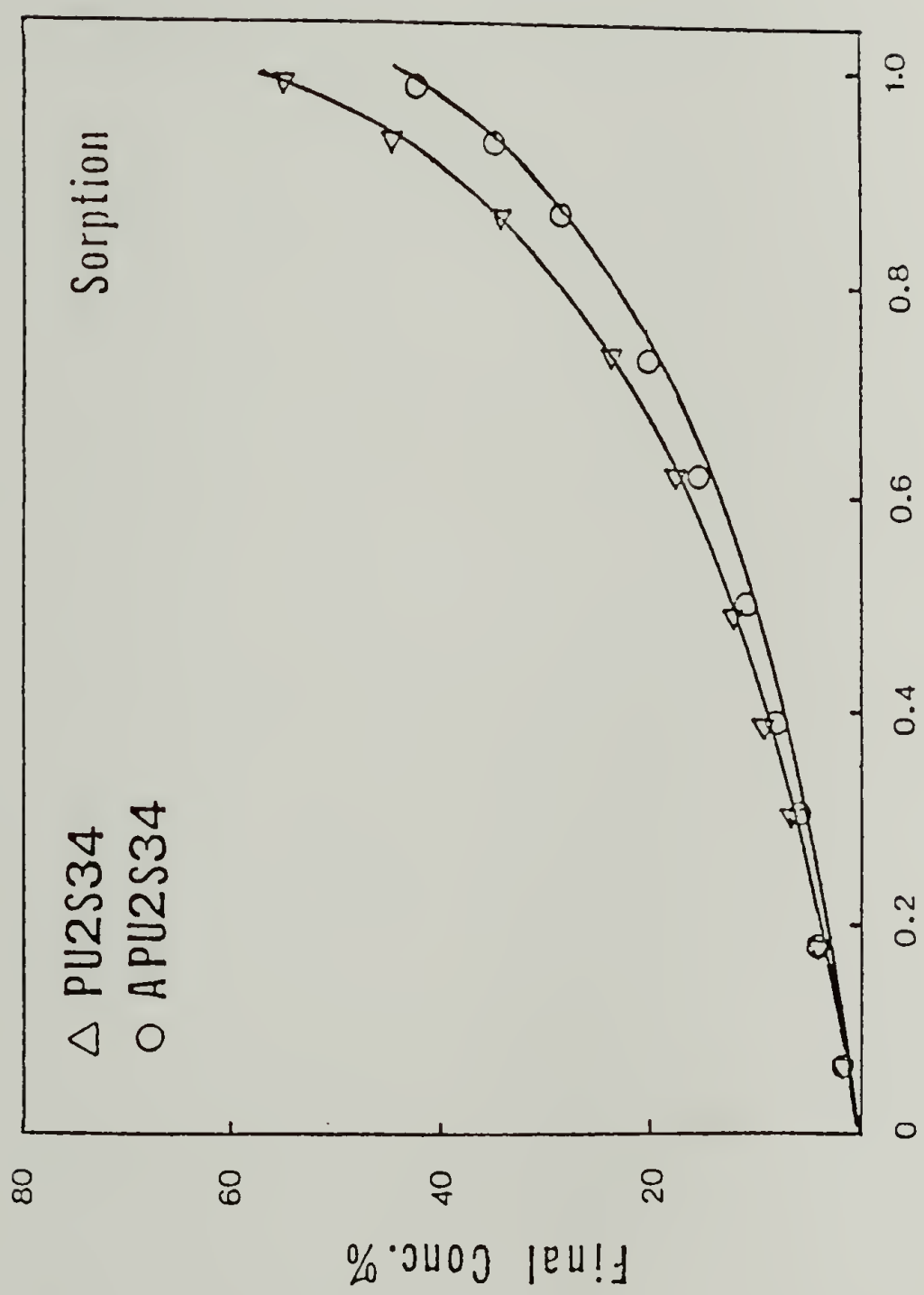

Figure 5.12 A comparison of sorption isotherm behavior, determined from desorption experiments, for 1,2-dichloroethane in PU2S34 and APU2S34 with film thickness of 0.11 mm at 24°C.

hard segment contents suggests a relaxation process present in the glassy hard phase and/or interfacial region induced by the presence of the solvent, and (2) the difference observed in the sorption isotherm curves for annealed samples at 80°C and 155°C is pronounced, implying that the effect of the solvent on the glassy hard phase and/or interfacial region is significant. It will be seen in the following section that the interaction of solvent with the hard phase and/or interfacial region also has a profound effect on the diffusion behavior.

5.3.2 Diffusion Behavior

Two-stage sorption curves were observed for ortho-dichlorobenzene in an Estane sample at moderate and high activities, but were generally absent in desorption runs, while at lower ortho-dichlorobenzene contents, the sorption-time curves appear Fickian in shape, as reported by Goydan et al.(25). However, in this study using 1,2-dichloroethane as a solvent, the sorption and desorption curves show sigmoidal behavior for Estane samples at moderate and high activities. These results are shown in Figures 5.13 and 5.14. The sample thickness used in this study is 0.23 mm. M_t/M_∞ is the weight uptake of solvent vapor at time T divided by that at infinite time, and $T^{1/2}$ is the square root of time. As can be seen from these figures, the sigmoidal curves become pronounced at an activity of about 0.60, below which the curves are Fickian in shape. As

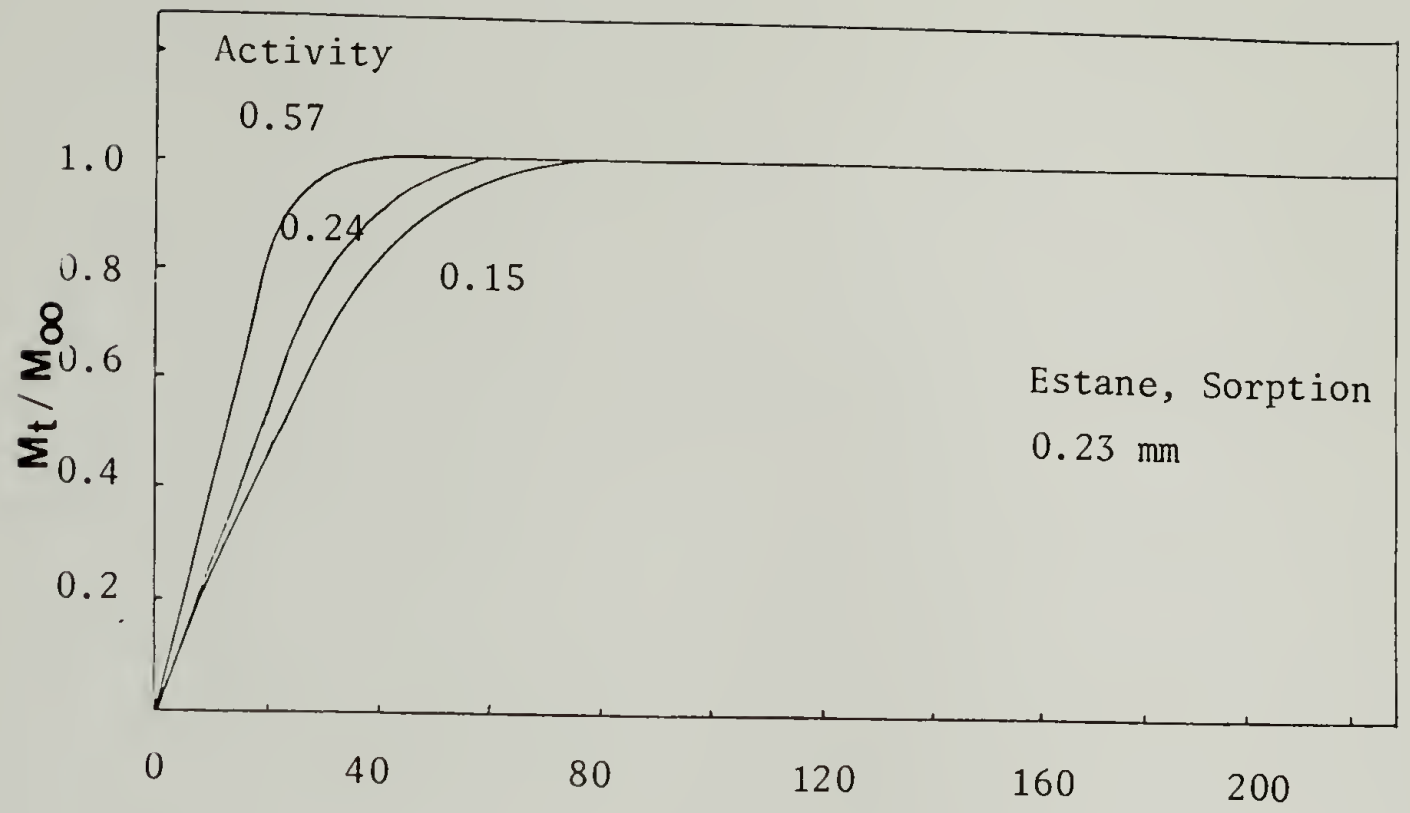

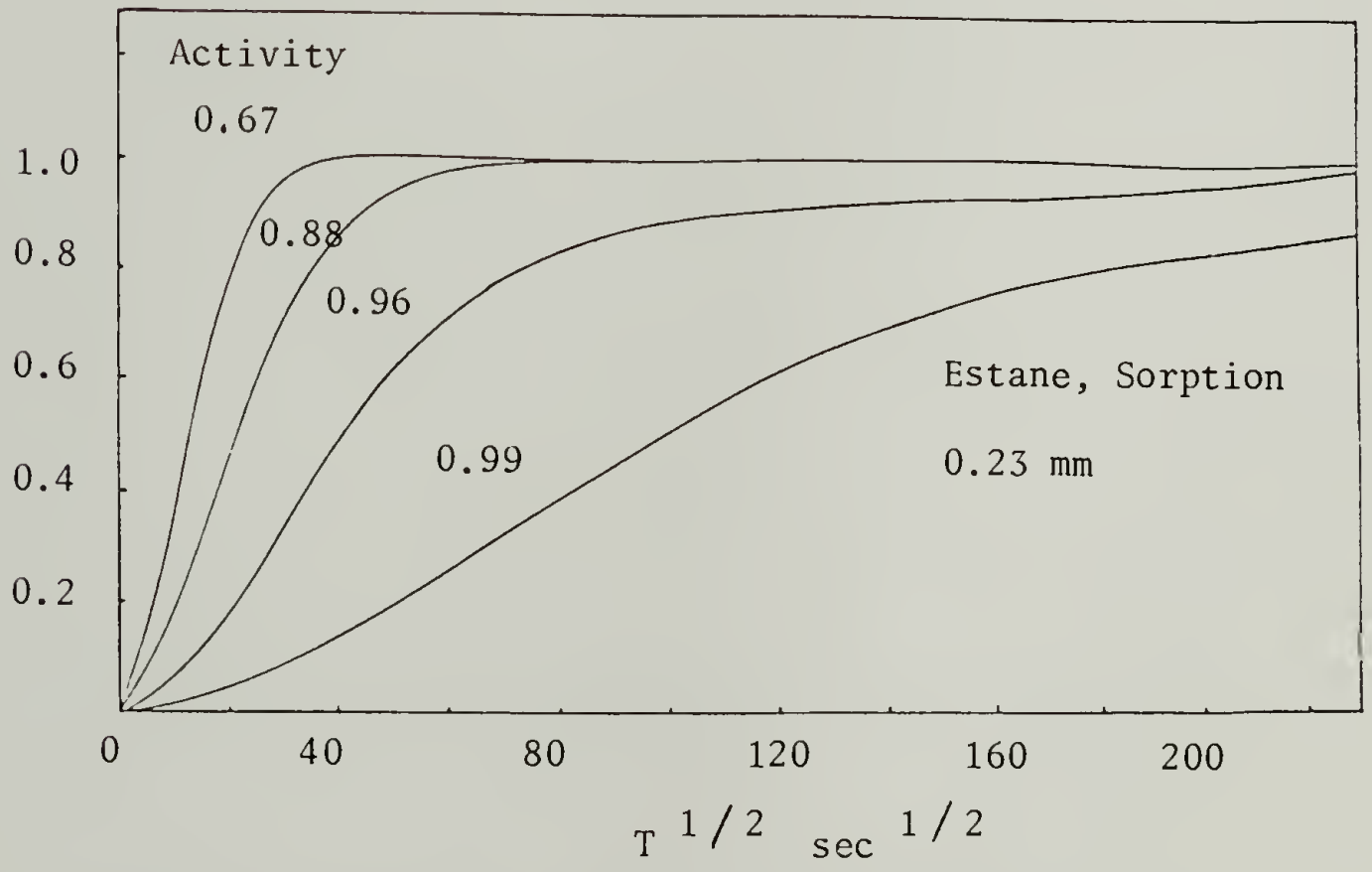

Figure 5.13 Sorption curves of 1,2-dichloroethane in Estane with film thickness of 0.23 mm at different activities.

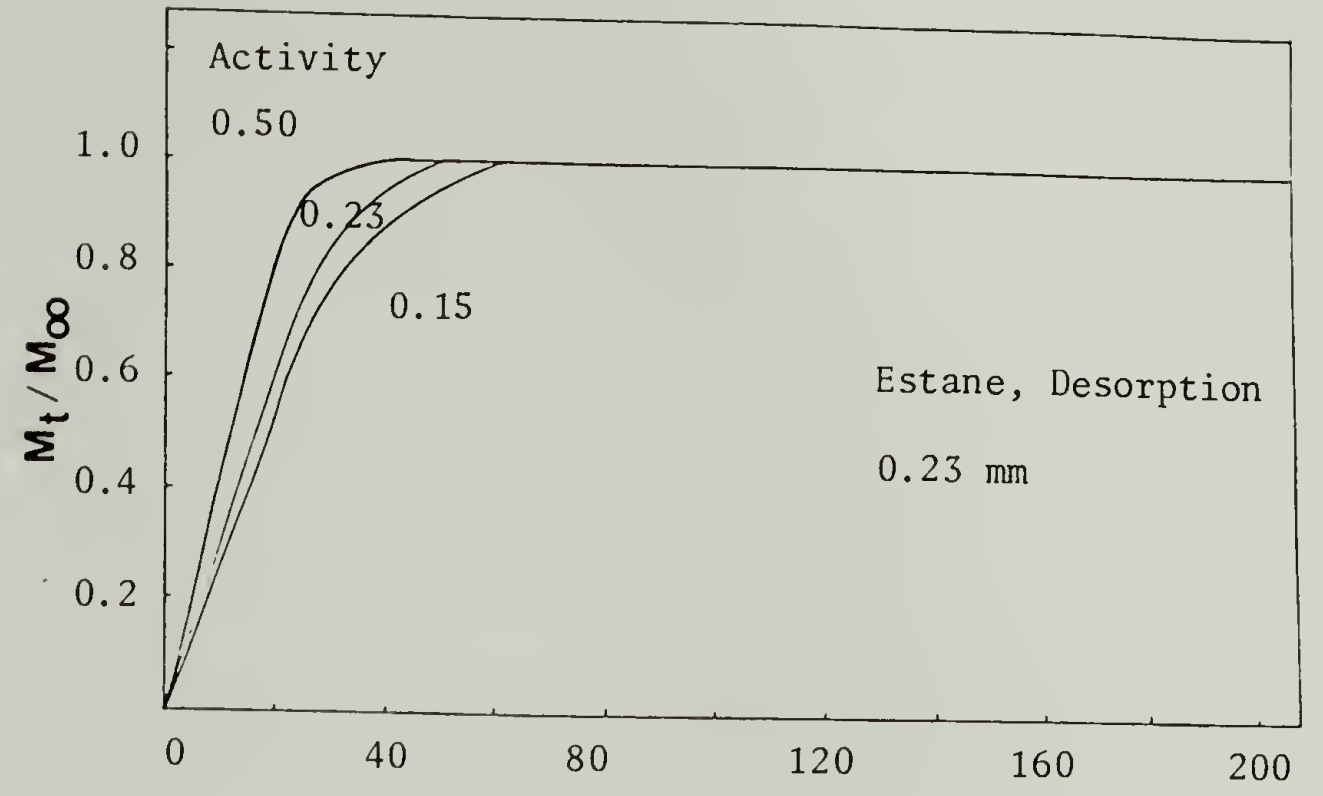

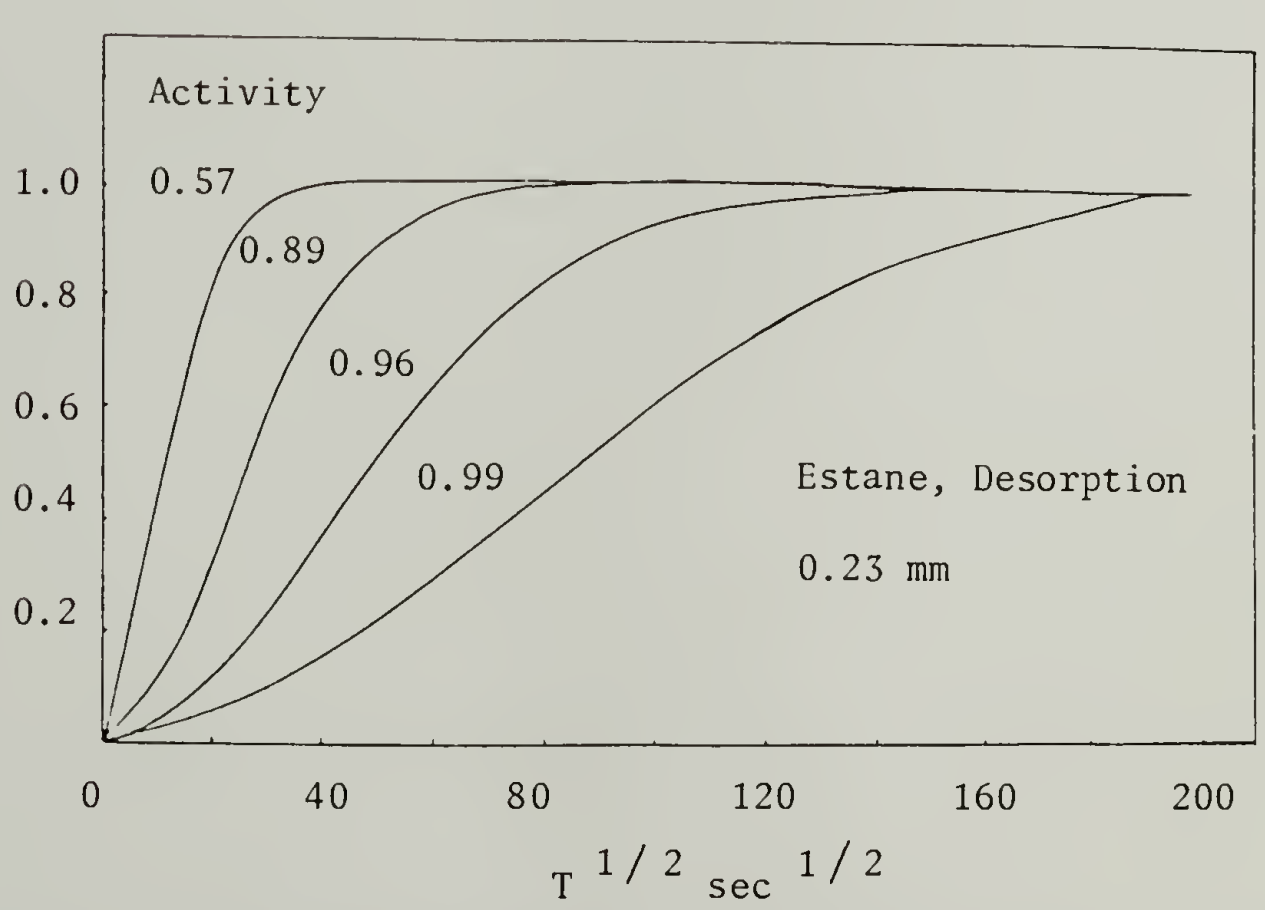

Figure 5.14 Desorption curves of 1,2-dichloroethane in Estane with film thickness of 0.23 mm at different activities.

noted in the previous section, the degree of swelling of 1,2-dichloroethane in Estane is quite high, especially at higher activities, reflecting that the solvent induced relaxation of polymer molecules becomes significant at high activity. This relaxation process results in comparable diffusion and relaxation rates, and thus the S-shape curves were observed. Both sorption and desorption curves exhibit the same behavior, suggesting that the arrangement of the molecules appears to be reversible. Similar results were observed for PU2S68 (but not as pronounced as Estane), indicating that the diffusion curves appear to be S-shaped for samples having higher soft segment contents due to higher degrees of swelling. The relaxation behavior mainly results from the swelling of solvent in the soft segment phase in which the flexibility of soft segment increases, resulting in an increase in the mobility of the hard segment.

Two-stage sorption curves were observed for PU1S52, PU1S44, PU2S44, and PU2S34. Figure 5.15 shows the diffusion curves for PU1S44 sample with a thickness of 0.11 mm at activities 0.62 and higher. As can be seen from this figure, the curve at activity 0.62 is Fickian in shape, while all other curves at activities higher than 0.62 are no longer Fickian in shape and display an initial steeply sloped region followed by a second nearly linear region of reduced slope which levels off to the final equilibrium. It should be noted that the sorption curves at activities below 0.62 show Fickian behavior, and the desorption curves show Fickian shapes over

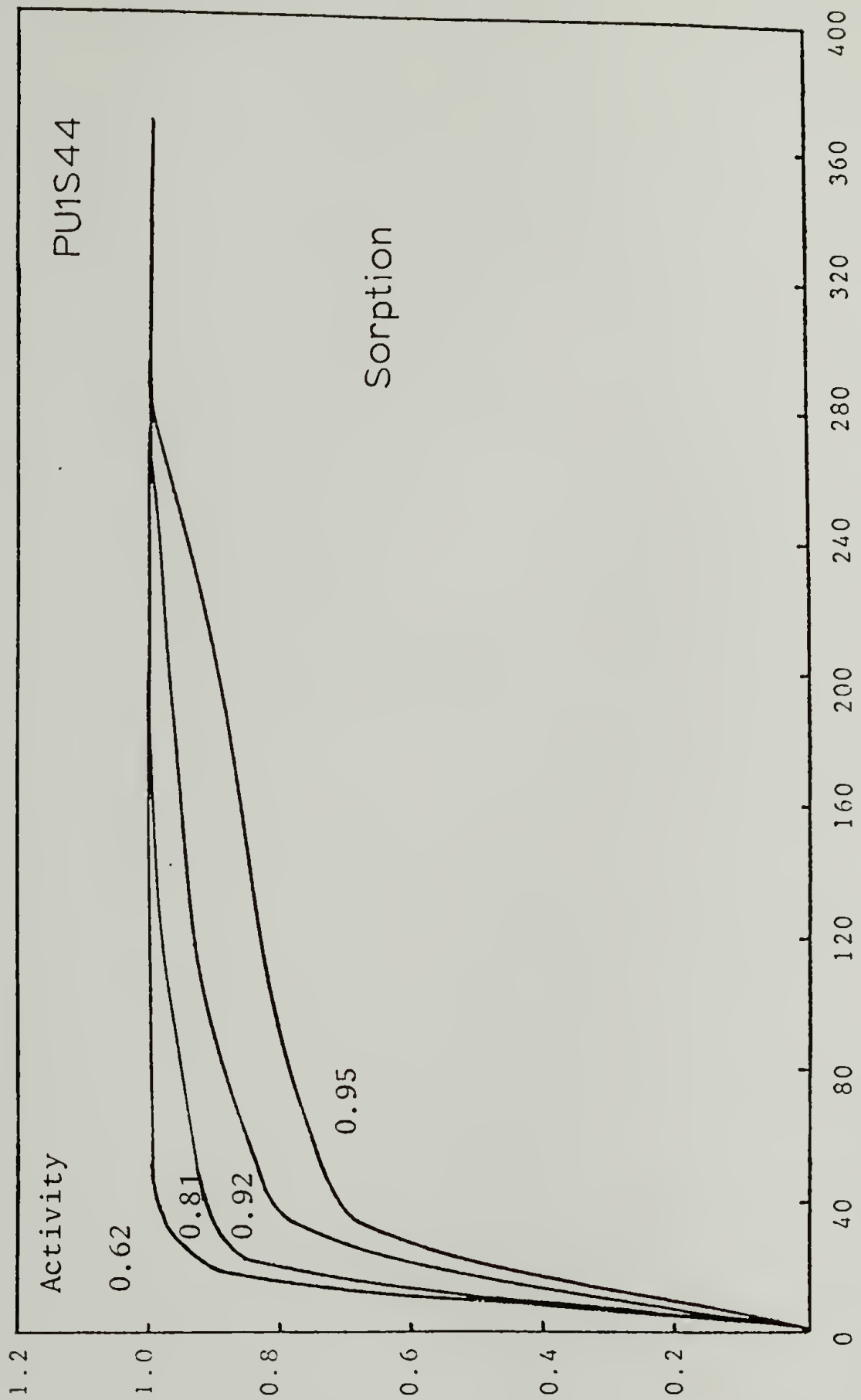

Figure 5.15 Sorption curves of 1,2-dichloroethane in PU1S44 with film thickness of 0.11 mm at different activities.

the entire activity range. In Figure 5.15, the contribution of the second stage become pronounced as activity increases. At the temperature of our experiments, the rate of transport of 1,2-dichloroethane in polyurethanes is governed primarily by the mobility of the PTMO matrix. This mobility is affected by the extent to which the hard and soft block chains mix with each other, and by the blocking effect of the crystalline phase in the hard segment. In addition, the slow diffusion of solvent in the hard phase and/or interfacial phase resulting in a relaxation process also gives a pronounced effect on the entire transport behavior. At low vapor activities or solvent concentration, the solvent vapor is mainly present in the soft phase, and the relative small amount of solvent in the interfacial phase and/or hard phase is not enough to induce the relaxation process of the rigid phase. Thus, the transport behavior of the solvent is dominant in the soft phase, resulting in a Fickian shape. At higher activities, as shown in Figure 5.15, the sorption of the solvent still primarily occurs in the soft phase and the curves show a first-stage linear relationship with $T^{1/2}$, while, due to an increase in the contribution of solvent vapor in the hard phase and/or interfacial phase, the mobility of the hard block chains are increased inducing the relaxation process, and giving rise to the second-stage behavior in the sorption runs. Since similar observations were obtained for PU1S52, PU2S44 and PU2S34, it is generally concluded that polyurethanes with higher hard segment contents ($\sim$>50 wt% hard segment) show two-stage

sorption behavior while for samples with hard segemnt content less than 50% by weight sorption curves exhibit sigmoidal behavior at the intermediate and higher vapor activities.

The two-stage sorption behavior appears to result from a relaxation process. This is primarily due to the sorption of solvent in the interphase and/or glassy hard phase. To further examine this two-stage diffusion behavior, the following three types of experiments, hysteresis, thickness, and annealing studies, were performed to define this second-stage behavior which arises from the relaxation process of the glassy hard phase and/or interphase induced by the presence of the solvent.

(A) Hysteresis Studies

The diffusion behavior of sorption, desorption, and second sorption of 1,2-dichloroethane in PU1S44 and PU2S44 at certain activity intervals are shown in Figure 5.16 and 5.17, respectively. In Figure 5.16, the second stage curve was observed in the first sorption run, but has disappeared in the desorption and second sorption runs which appear to be Fickian in shape. It should be noted that the two-stage anomalous diffusion behavior is generally absent in desorption and sorption runs over the entire activity range for the PU1S44 sample. These diminished two-stage curves in desorption and second sorption runs indicate that the rearrangement of the polymer molecules induced by the presence of the solvent is a non-reversible process. This hysteresis phenomenon explains that

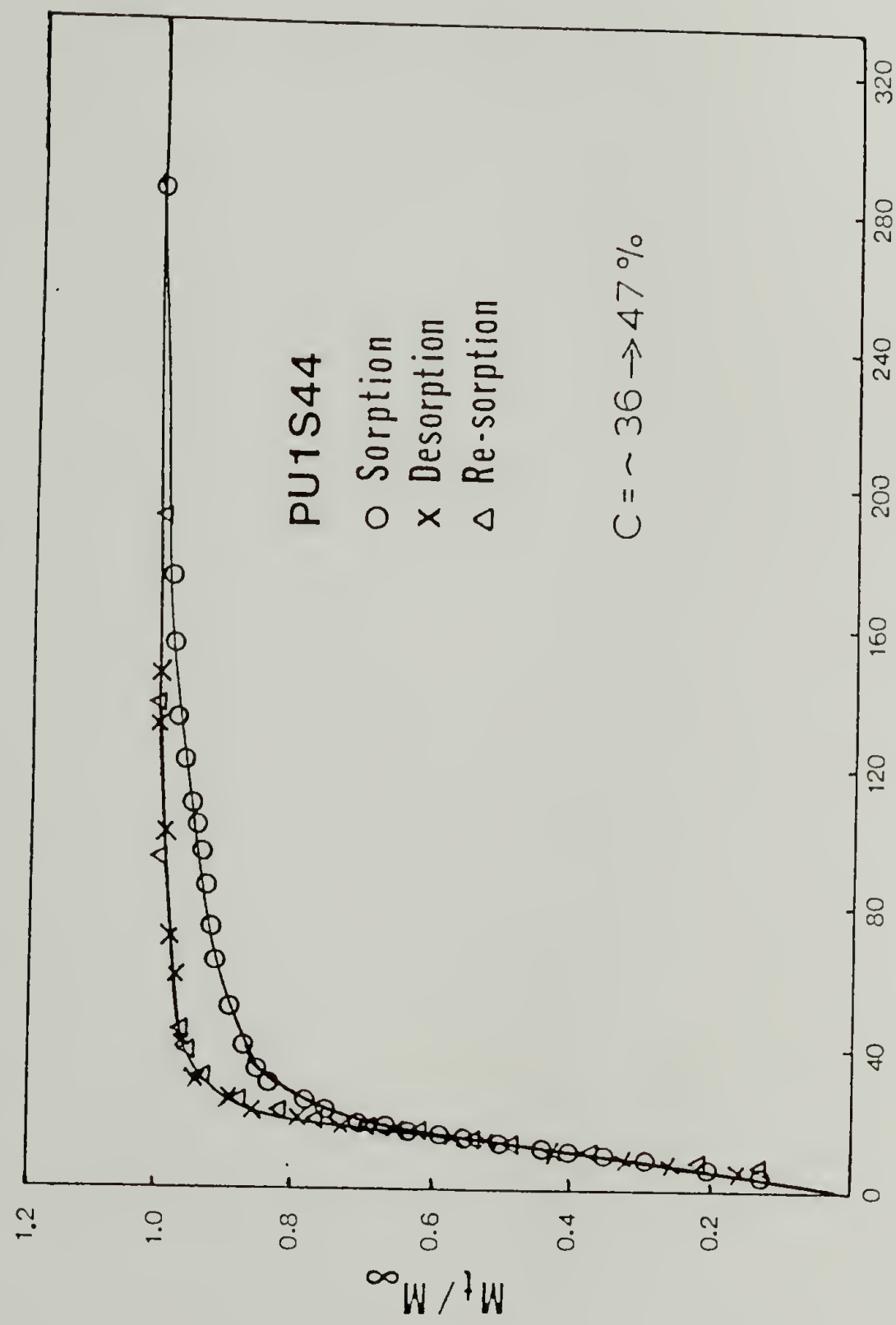

Figure 5.16 Sorption, desorption, and second sorption curves of 1,2-dichloroethane in PU1S44 with film thickness of 0.11 mm at concentration interval of 36 → 47%.

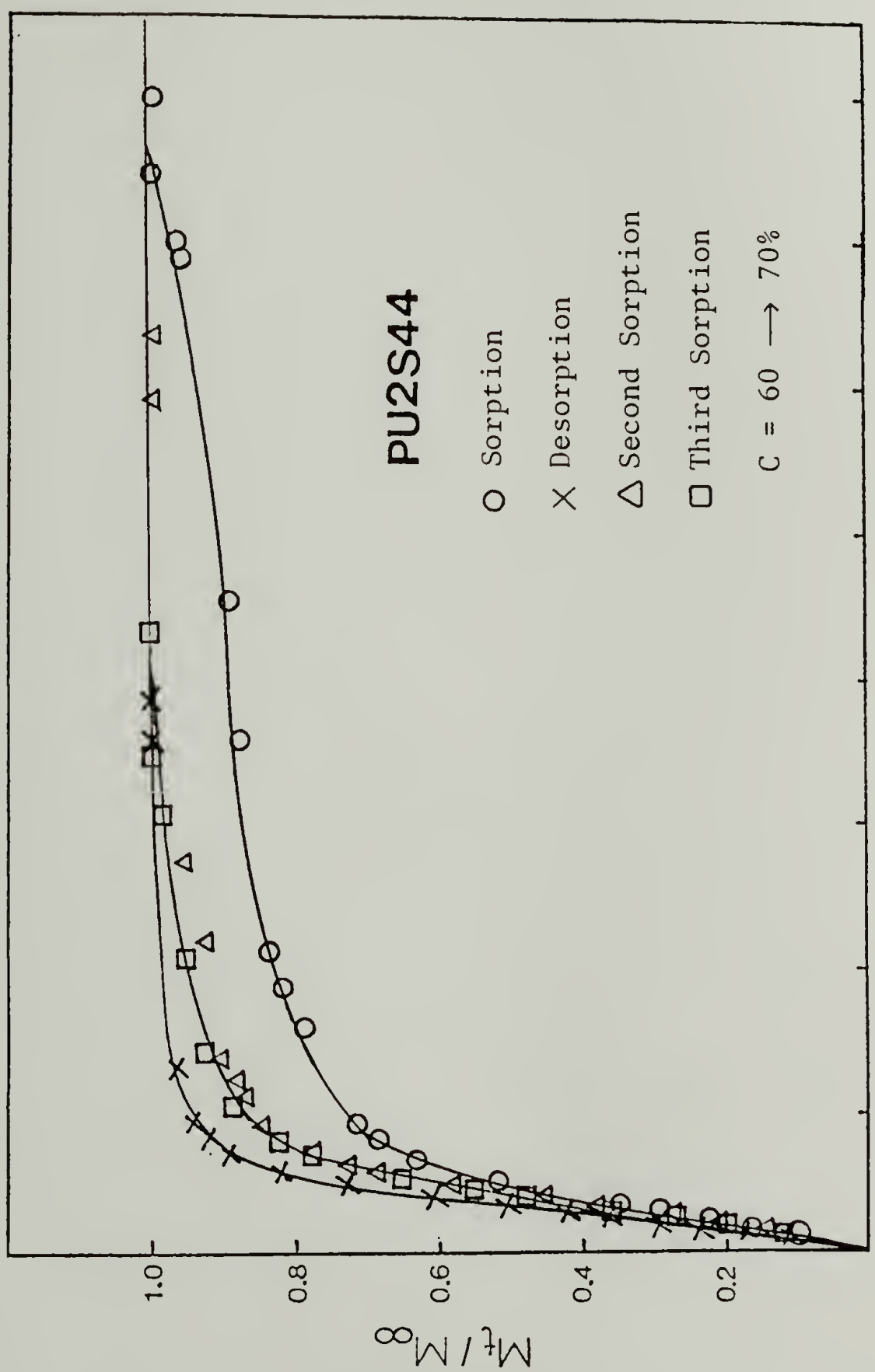

Figure 5.17 Sorption, desorption, second sorption and third sorption curves of 1,2-dichloroethane in PU2S44 with film thickness of 0.11 mm at concentration interval of 60 → 70%.

the relaxed structure resulting from the presence of the solvent persists after the first sorption run and creates the extra free volume in the polymer either by the solvent itself or by the relaxation process. As solvent is removed from the polymer, the extra free volume remains and the evaporation rate of the solvent is much faster than the relaxation rate corresponding to the polymer molecules attempting to relax back to the original state, and thus the relaxation is relatively slow under desorption and no detectable second stage behavior was observed. The second sorption experiments were carried out often about two days under vacuum after the desorption run. The second sorption curve is almost superimposed on the desorption curve, indicating that the morphology of the polymer after the desorption run persists and is different from the morphology of the polymer before the first sorption run, and hence the sorption behavior is similar to the desorption curve. It should be noted that the sample thermal history is different for the first (annealed at 80°C for two days) and second sorption runs, giving one more possible explanation for the difference in the first and second sorption behavior. However, even though the sample thermal history for both sorption runs is the same, the sorption behavior is still different, as shown in Figure 5.17, which shows the hysteresis study of PU2S44 sample. This sample in the third sorption run was prepared with the same sample thermal history as in the first sorption run. This means that the sample was brought into a vacuum oven at 80°C for two days after the second sorption experiments, and

then, the third sorption experiments were conducted. As can be seen from Figure 5.17, the third sorption curve appears to coincide with the second sorption curve but not with the first sorption curve, indicating that, to return the relaxed structure to the original state, the controlling factor is time. The appearance of the hysteresis behavior in both PU1S44 and PU2S44 samples clearly indicates that the two-stage sorption behavior is the result of a relaxation process.

(B) Thickness Studies

Figures 5.18 and 5.19 show a series of reduced sorption curves for films of different thicknesses for Estane and PU1S44 samples, respectively. These curves do not appear to reduce to a single curve as is normally found in Fickian sorption, indicating a non-Fickian system. These figures also show that sorption proceeds relatively more quickly in thicker films, and for both samples the non-Fickian curves become less pronounced as film thickness increases. The tendency of the curves to approach Fickian behavior and to coincide can be observed with the thicker films. These results suggest that the diffusivity D becomes less time dependent and shifts toward pure concentration dependence as thickness is increased. This occurs because, for very thick films, diffusion may be so slow that D has time to approach the equilibrium diffusion coefficient closely at all concentration, and hence D appears to be concentration dependent only. In addition, the relaxation time is

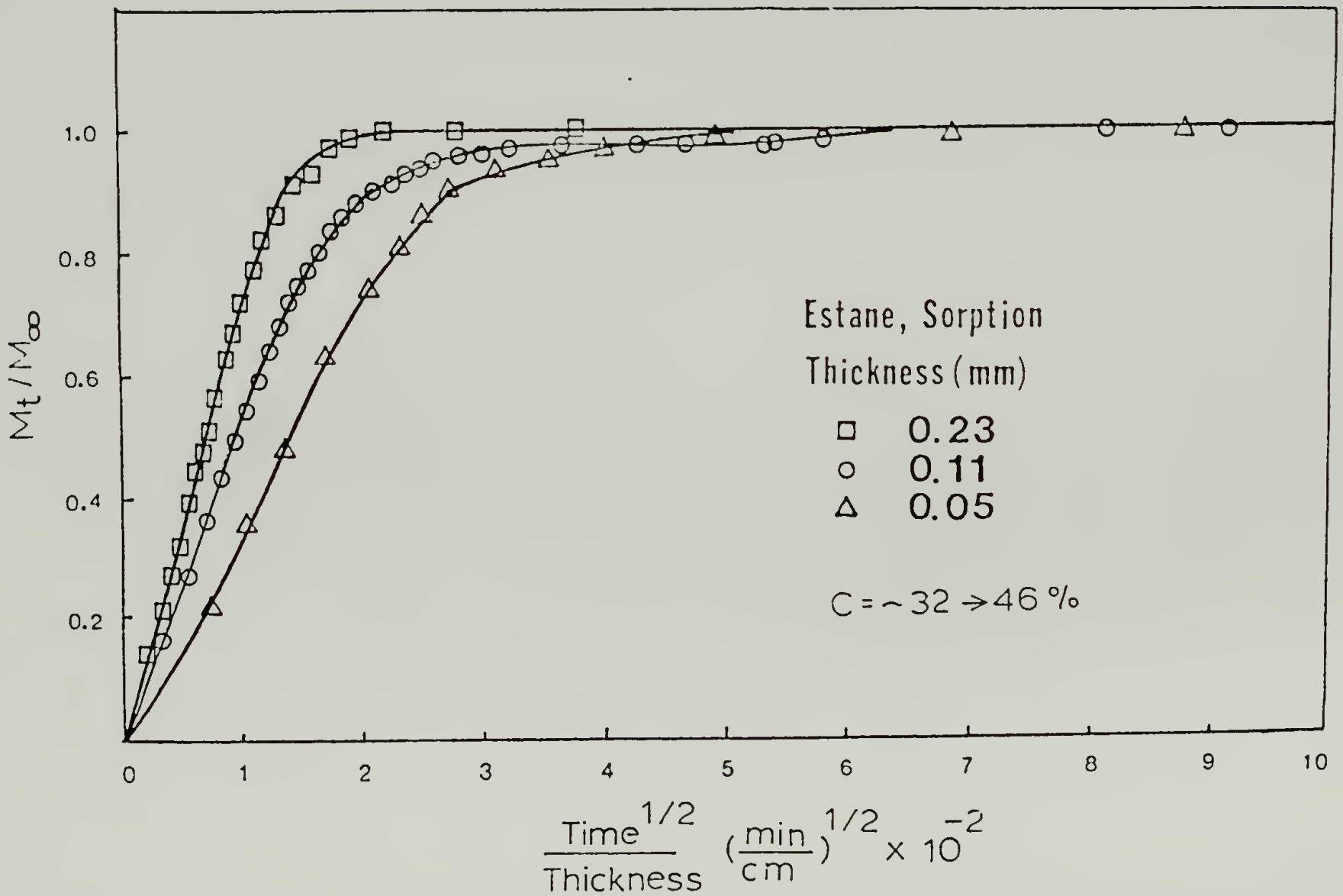

Figure 5.18 Reduced sorption curves for 1,2-dichloroethane in Estane with different film thicknesses at the same concentration interval.

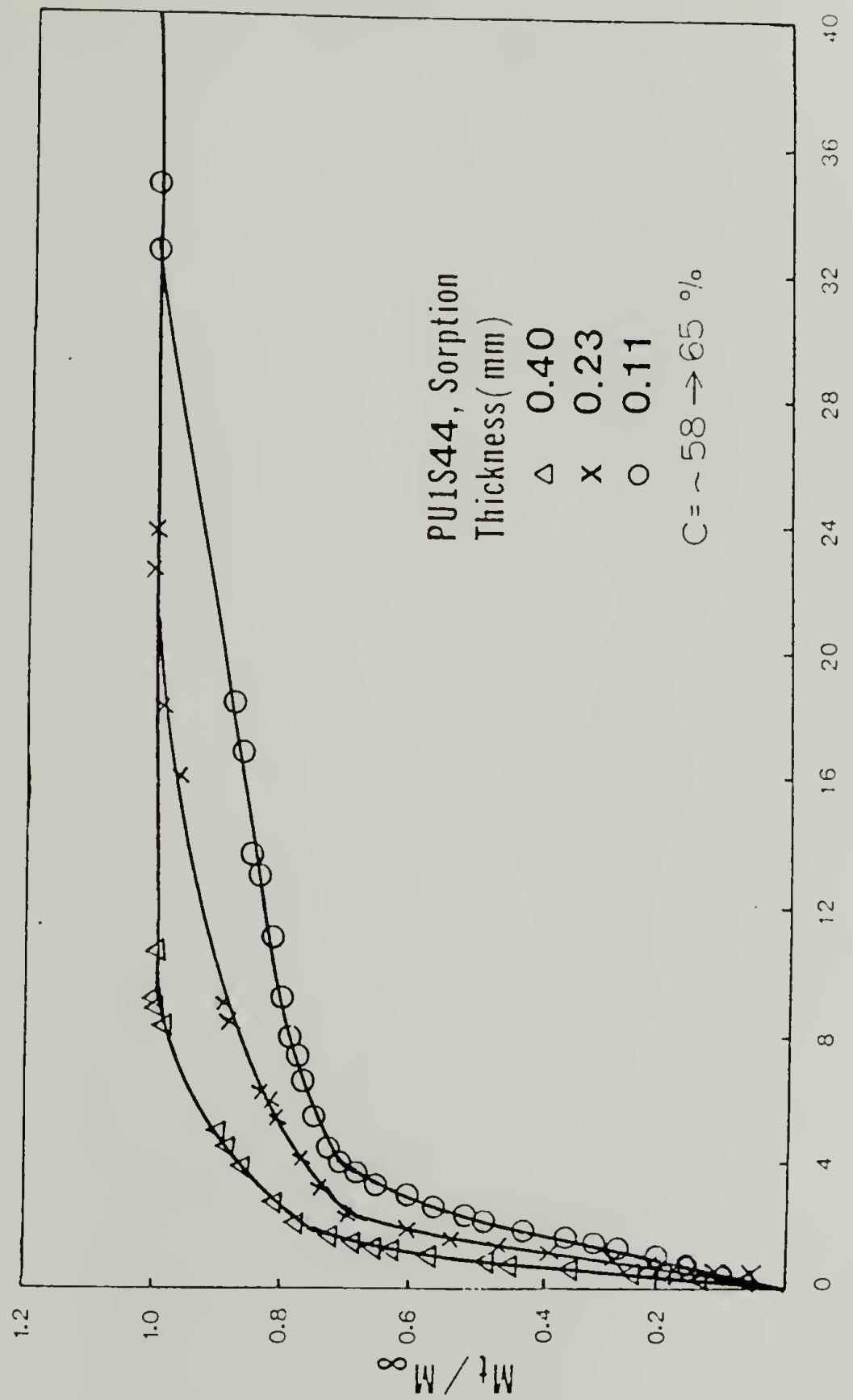

Figure 5.19 Reduced sorption curves of 1,2-dichloroethane in PU1S44 with different film thicknesses at the same concentration interval.

assumed to be independent of the film thickness. As the film thickness increases, the diffusion time increases but relaxation time remains the same, resulting in a much longer diffusion time than relaxation time. Thus, the contribution to the relaxation process becomes relatively small, and the non-Fickian sorption behavior appears to diminish as thickness increases. On the basis of this study the appearance of the anomalous sorption behavior may be attributed to the relaxation processes.

(C) Annealing Studies

Figure 5.20 shows the sorption curves for PU2S34 and APU2S34 at the same concentration interval, 35-45 %. As can be seen from this figure, compared with the sorption curve of PU2S34, the contribution of the second-stage curve is more pronounced for APU2S34. Berens and Hopfenberg (26,30) have studied the sorption experiments for heat treated poly(vinyl chloride) (PVC) sample with n-hexane, and a significant relaxation process or second stage behavior was observed for annealed PVC samples. This observation was explained by a decrease in the free volume of the heat treated sample. For annealed polyurethane sample, not only does the free volume of the amorphous hard phase decrease but also the crystallinity of the hard phase increases. In addition, the amount of interfacial mixing also relatively decreases. The increase in the crystalline phase may result in an increase in the blocking effect for the penetration of solvent in the hard phase and/or

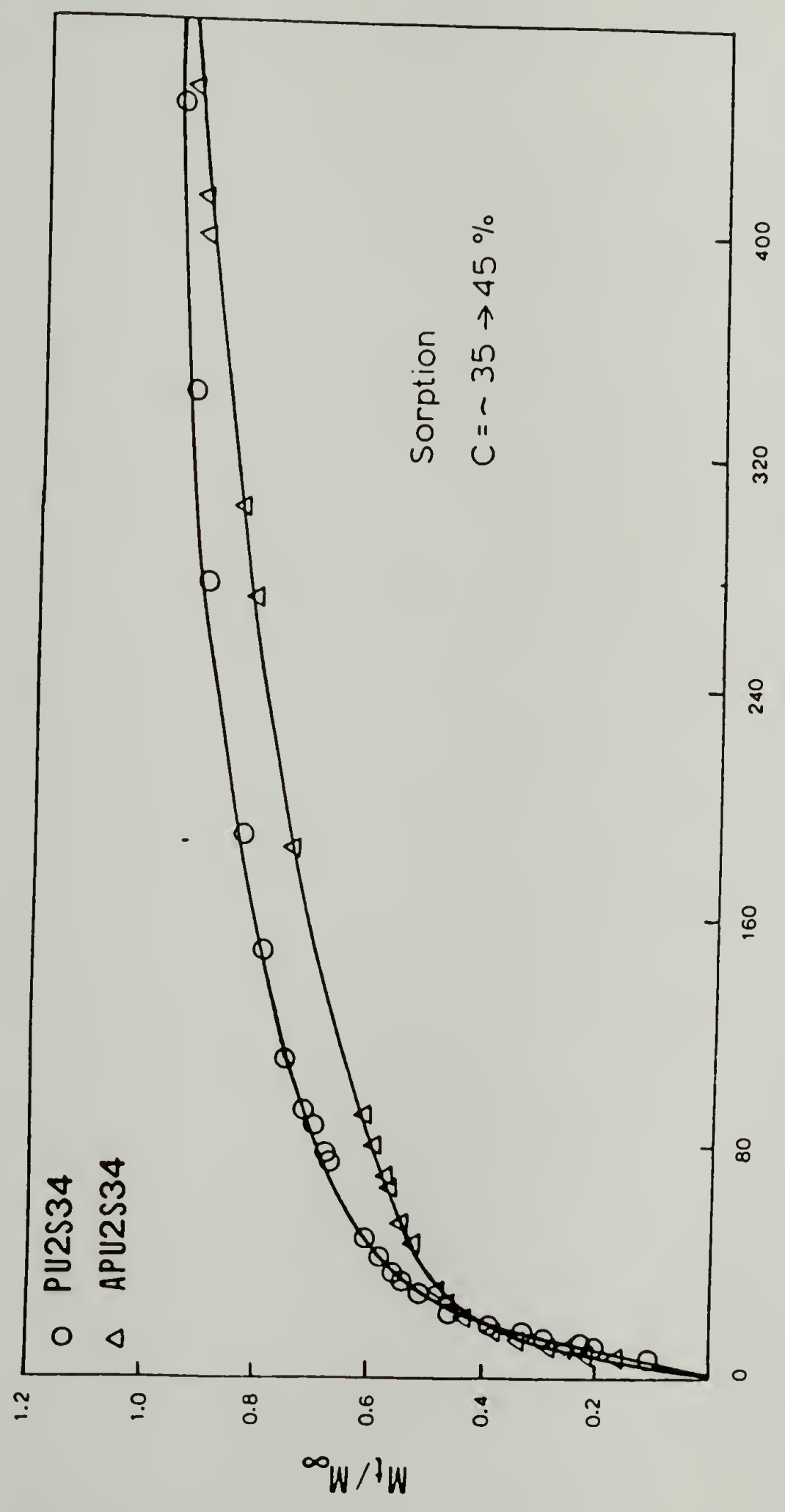

Figure 5.20 A comparison of sorption curves of 1,2-dichloroethane in PU2S34 and APU2S34 with the same film thickness of o.11 mm at the same concentration interval.

interfacial phase. Thus, the relaxation process in the hard phase and/or interfacial phase becomes relatively slow, and a more pronounced two-stage behavior was observed for APU2S34 sample. Silmilar results were observed at other concentration intervals for the same pair of the samples. This study suggests that the second stage behavior likely results from the relaxation of hard phase or interfacial phase induced by the presence of the solvent.

5.3.3 Analysis of Soption-Time Behavior

It was well established that the diffusion of organic vapor into polymers above their glass transition temperature generally obeys Fick's law. As described by Crank (15), the several characteristics of Fickian behavior are that the weight uptake is proportional to the square root of time over approximately the initial 60% of the weight change on sorption and desorption. The sorption and desorption curves will coincide for constant D. For D increasing with concentration, as commonly observed, the sorption curve will lie above that for desorption. Since the rate of weight change is only a function of the variable $(t/l^2)^{1/2}$, sorption-time curves over the same concentration range for a given sample in different thicknesses must reduce to a single curve when plotted as the fractional weight uptake M_t/M_∞ against $(t/l^2)^{1/2}$.

The value of D, if indeed constant, may be calculated from the initial slope, m, of data plotted as fractional weight uptake

against the square root of time. This relationship was described by the equations 5.1-3 in section 5.2.2.3. Our sorption data were obtained by incremental vapor sorption experiments which provided small concentration intervals in each of the sorption experiments. The diffusion coefficient D thus can be assumed to be constant in this small concentration interval, and can be determined by applying equations 5.1-3 for sorption or desorption curves showing Fickian behavior. It should be noted that the thickness correction was made in calculating the D due to swelling (equation 5.4). Since segmented polyurethane is a heterophase polymer, D is thus called the apparent or effective diffusion coefficient. As detailed in the preceding section, the sorption behavior with 1,2-dichloroethane exhibits various departures from the requirements of Fickian behavior specified above. In the low concentration region, this is limited to a reversal in the expected rates of sorption and desorption. At higher concentrations there is the emergence of an increasingly pronounced two stage sorption and sigmoidal behavior, which is uncommon in an elastomeric material.

The distinct two stage sorption curves at the higher solvent concentrations resemble the behavior reported by Berens and Hopfenberg (26) for diffusion in glassy PVC and polystyrene microspheres. They treated the behavior phenomenologically as the sum of independent Fickian and relaxation processes. However, both two-stage and sigmiodal curves were observed in our experiments, and thus, the Joshi-Astarita equation was used to fit the non-Fickian

curves and to determine the diffusivity. This equation was described in equation 5.5. Two typical examples for curve fitting are shown in Figures 5.21 and 5.22, which show the experimental and theoretical curves for PU1S44 and Estane samples, respectively. The theoretical curves were determined by equation 5.5. As can be seen in both figures, the second stage and sigmoidal curves can be fitted very well by using the Joshi-Astarita model, suggesting that the anomalous sorption behavior may be due to a relaxation process or the coupling of the diffusion and relaxation. Three parameters, m, ϕ, and Θ_D, were determined. ϕ, the ratio of the diffusion time to the relaxation time, is much higher for Estane than that for PU1S44, indicating that the relaxation rate in Estane is much faster resulting in a higher value of ϕ. As described in the sorption isotherm section, the degree of swelling in Estane is very high due to the presence of low hard segment content, reflecting a high relaxation rate. It appears that the ϕ values explain the sorption isotherm observations. Based on the experimental observations and theoretical calculations, it can generally be concluded that the sigmoidal behavior occurs for high swelling polyurethanes samples resulting in a high relaxation rate, and the two-stage behavior occurs for low swelling samples which generate low relaxation rate.

5.3.4 Diffusion Coefficient vs. Solvent Concentration

The diffusion coefficient, although assumed constant over each

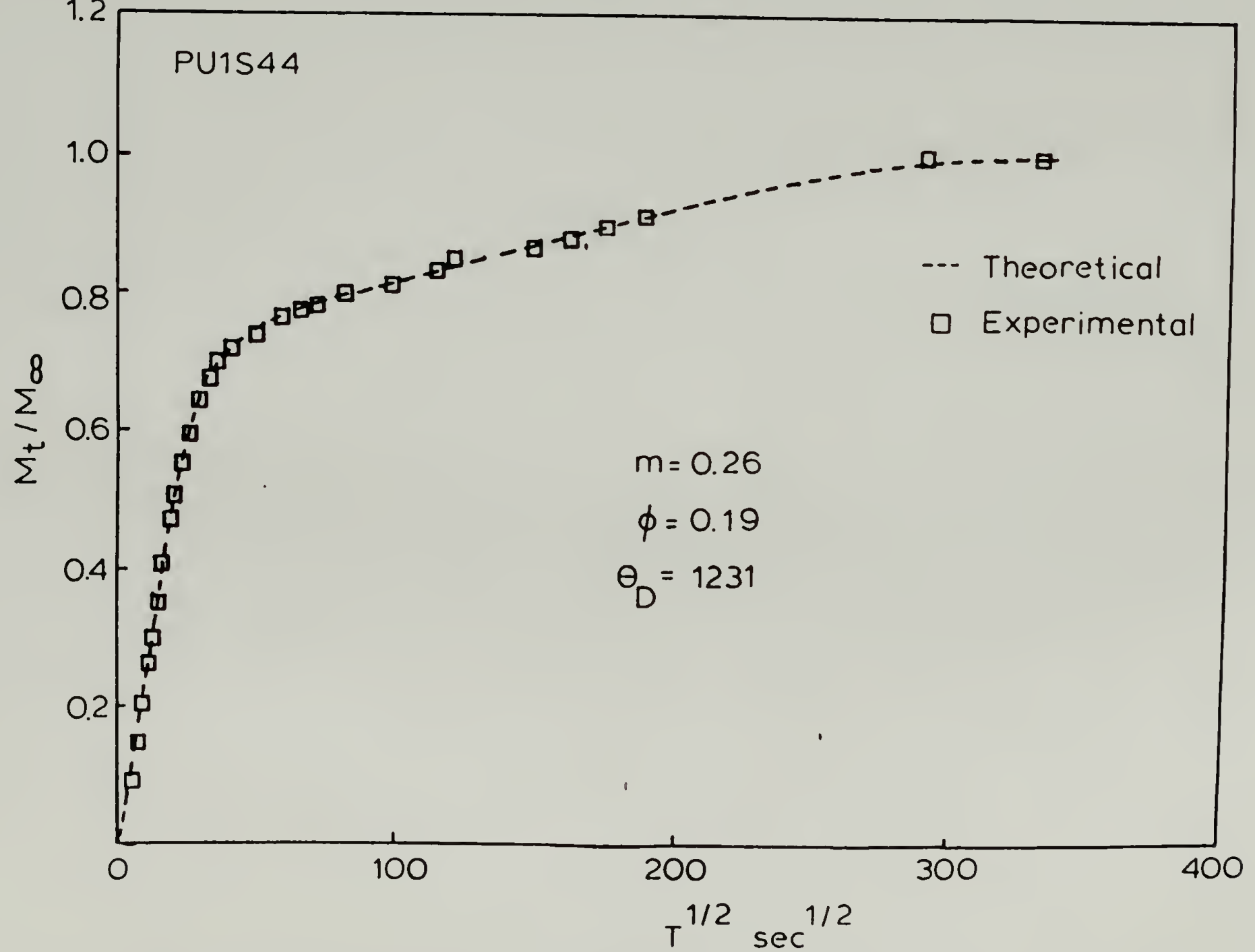

Figure 5.21 Application of Joshi-Astarita equation to the transport of 1,2-dichloroethane in PU1S44 at certain concentration interval.

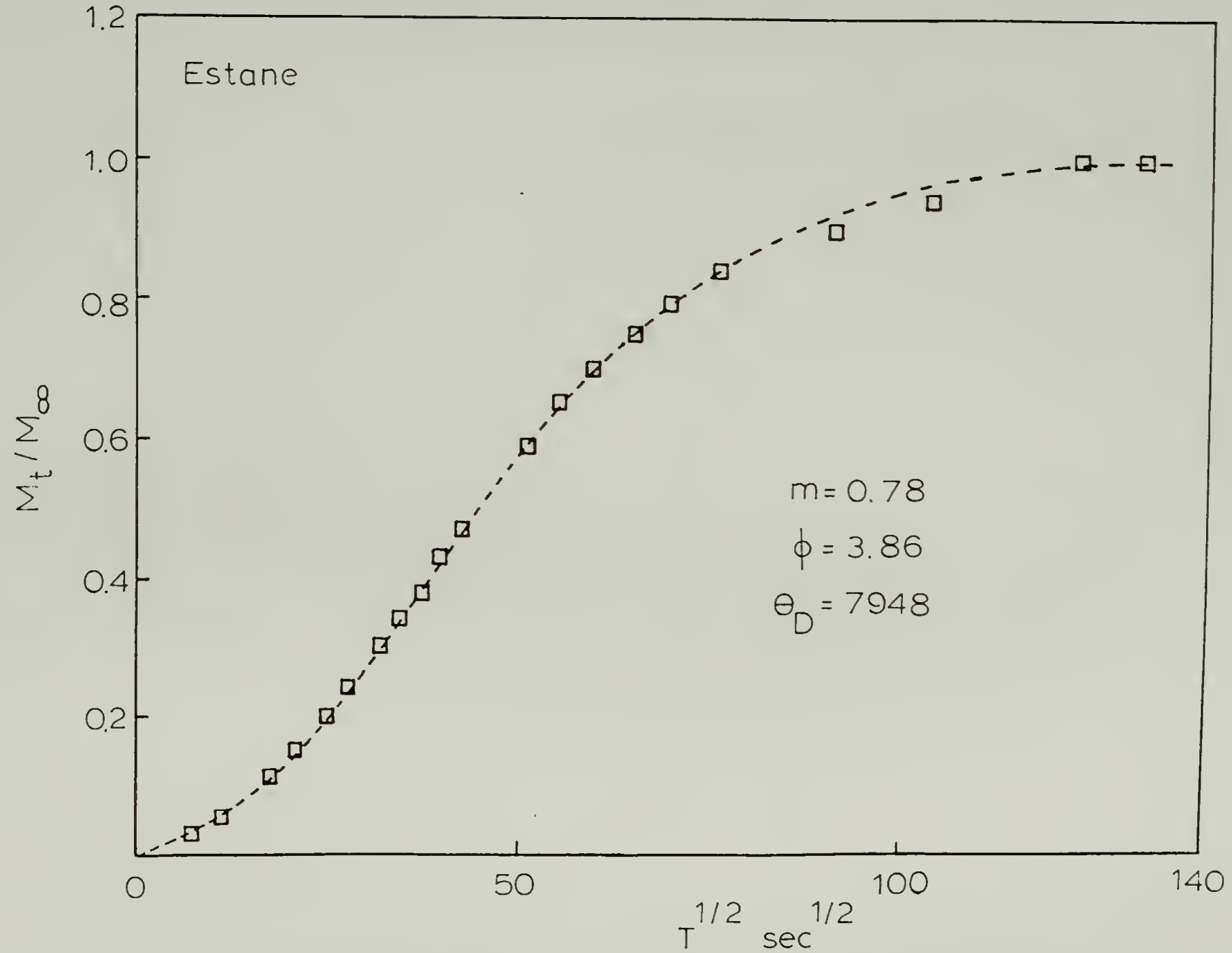

Figure 5.22 Application of Joshi-Astarita equation to the transport of 1,2-dichloroethane in Estane at certain concentration interval.

increment, is a strong function of concentration when considered over the full range of the sorption experiment. Apparent diffusion coefficient were calculated for each of the sorption and desorption steps for all the samples. As described in the previous section, the apparent diffusion coefficient D of a Fickian system is evaluated by the initial slope method. For curves displaying non-Fickian sorption behavior, the D is determined by the Joshi-Astarita equation.

The results of apparent mutual diffusion coefficients for each of the desorption curves for all polyurethane samples as a function of final solvent concentration are shown in Figures 5.23 and 5.24. In both figures, we plotted D against a reduced final solvent concentration, assuming that the 1,2-dichloroethane molecules are absorbed only in PTMO soft matrix, since the amount of solvent absorbed in the hard phase is relatively small, almost negliglble as compared with the amount of solvent absorbed in the soft phase. In each case D initially increases with concentration, reaches a maximum and then drops off with further increases in concentration. For the diffusion of vapors into rubbery polymers, relative maxima in the D-C curves are common because diffusivity is the product of a mobility factor (self-diffusion coefficient) and a thermodynamic factor (31-33). The mobility factor increases with penetrant concentration whereas the thermodynamic factor usually decreases. For polyurethane samples, the swelling of 1,2-dichloroethane in the PTMO soft phase dominates the full solvent concentration range, and

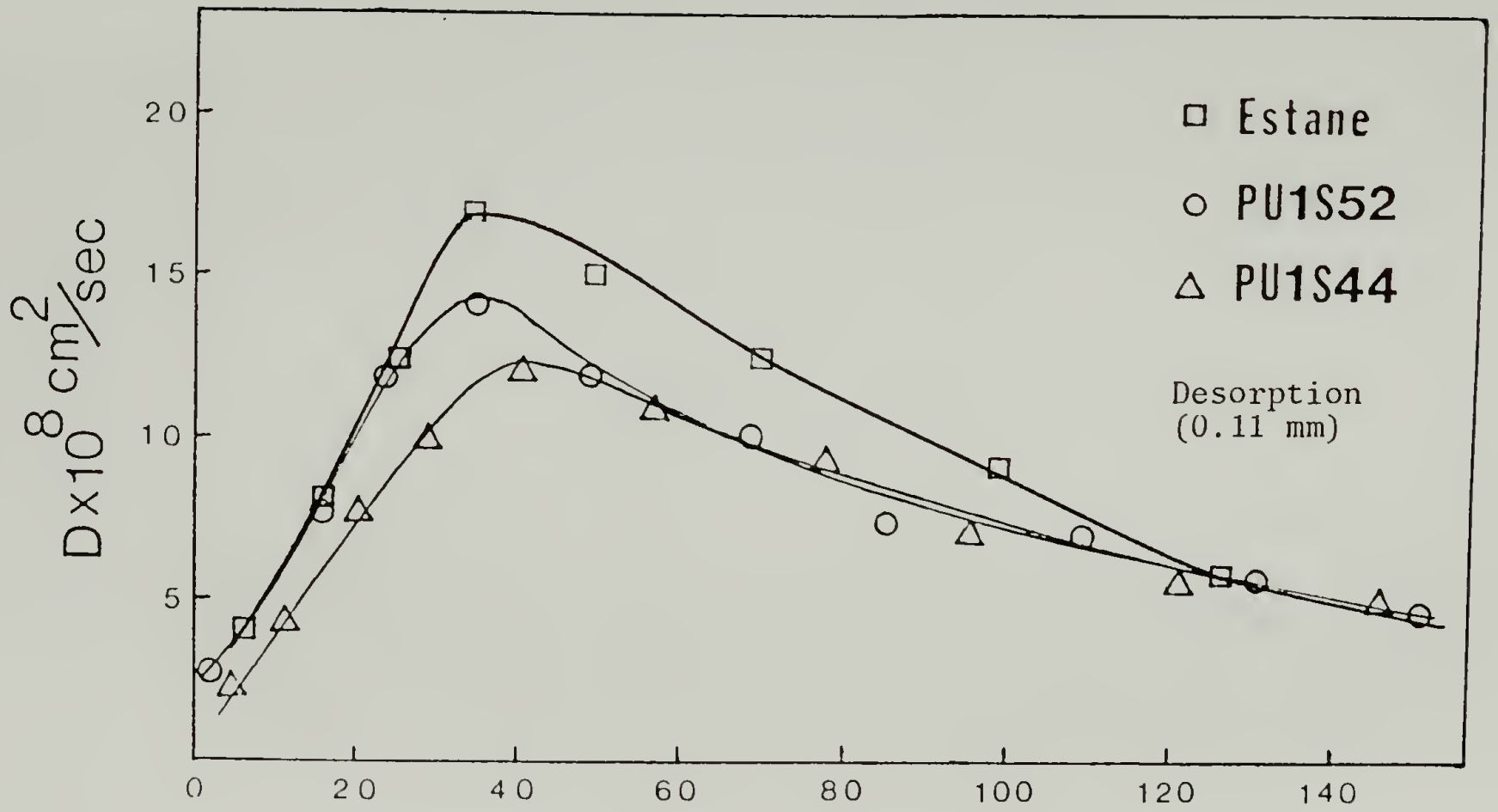

Figure 5.23 D-C curves, determined by the desorption runs, for 1,2-dichloroethane in Estane, PU1S52, and PU1S44.

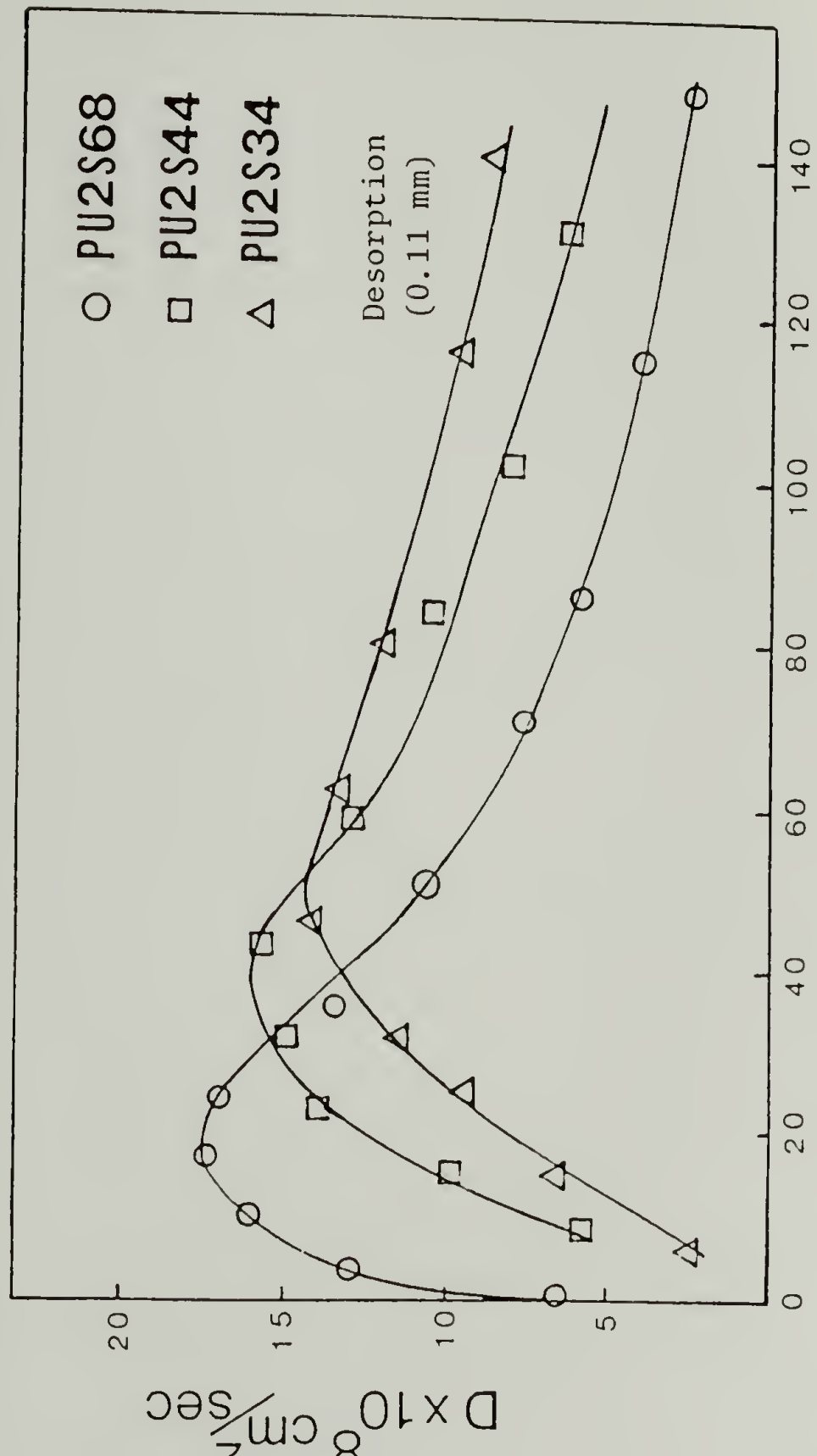

Figure 5.24 D-C curves, determined by the desorption runs, for 1,2-dichloroethane in PU2S68, PU2S44, and PU2S34.

PTMO at our experimental temperature, 24°C, appears to be a rubber. Thus, the maxima in D-C curves were observed. The features of the self-diffusion coefficient will be described in Appendix B.

For samples with 1000 MW PTMO as shown in Figure 5.23, the position of the maximum appears to be the same for the three samples, but D is higher for samples with higher soft segment contents in certain concentration ranges. In Figure 5.24, initially D is higher for higher soft segment content samples, but with further increasing concentration, D passes through a maximum and then drops much faster for PU2S68 than for PU2S44 and PU2S34. The maximum thus shifts to higher concentration for samples with higher hard segment content. These observations may be explained in terms of the domination of the thermodynamic factor for PU2S68 due to the high degree of swelling in this sample. In addition, the relaxation effect is more significant for PU2S44 and PU2S34. At concentration ranges between 30-60%, the relaxation induced free volume in the sample becomes significant for PU2S44 and PU2S34, and thus the D keeps increasing as concentration increases, and finally the D drops off due to the thermodynamic factor.

Figures 5.25, 5.26, and 5.27 show D vs. C curves for PU1S44 and APU1S44, PU2S44 and PU2S68, and PU2S34 and APU2S34. No hysteresis was observed for PU1S44, PU2S34, and PU2S68, but for APU2S44, PU2S34, and APU2S34, D vs. C for desorption curves are generally higher than that for sorption curves. These observations

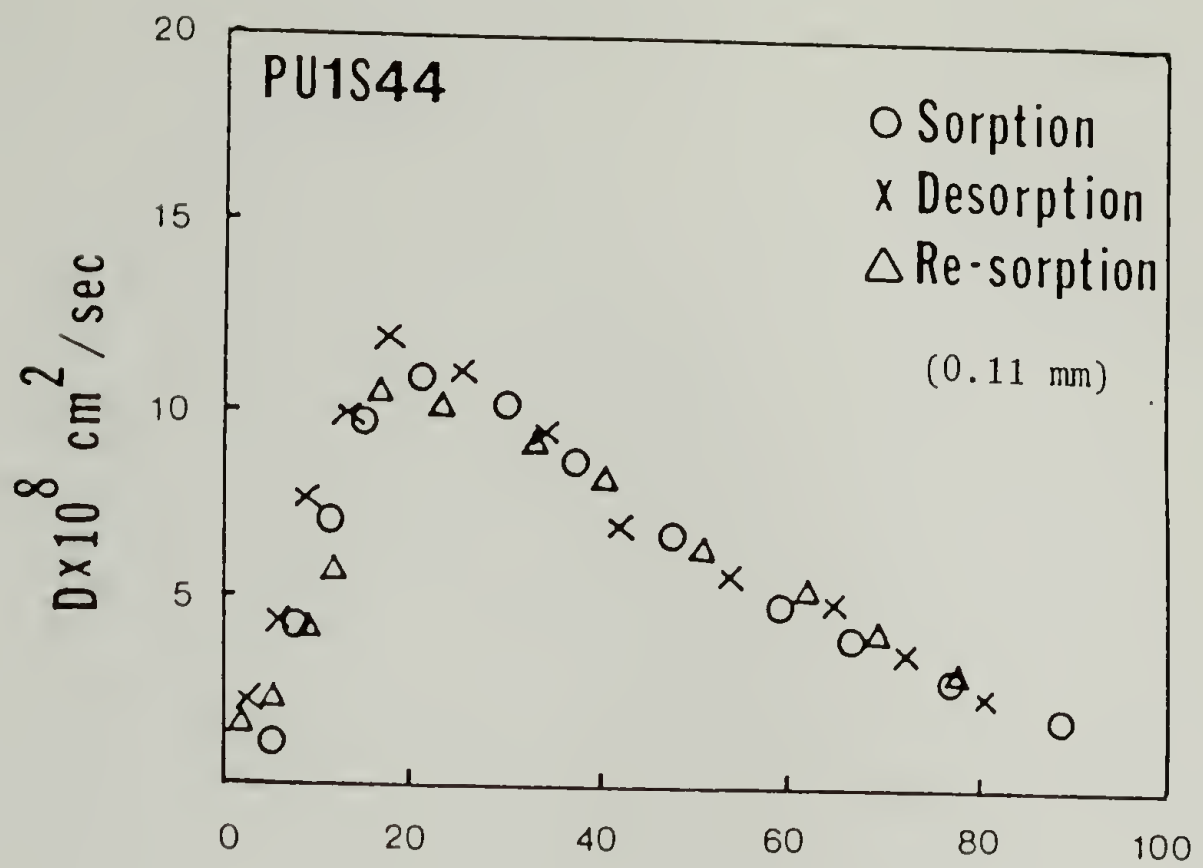

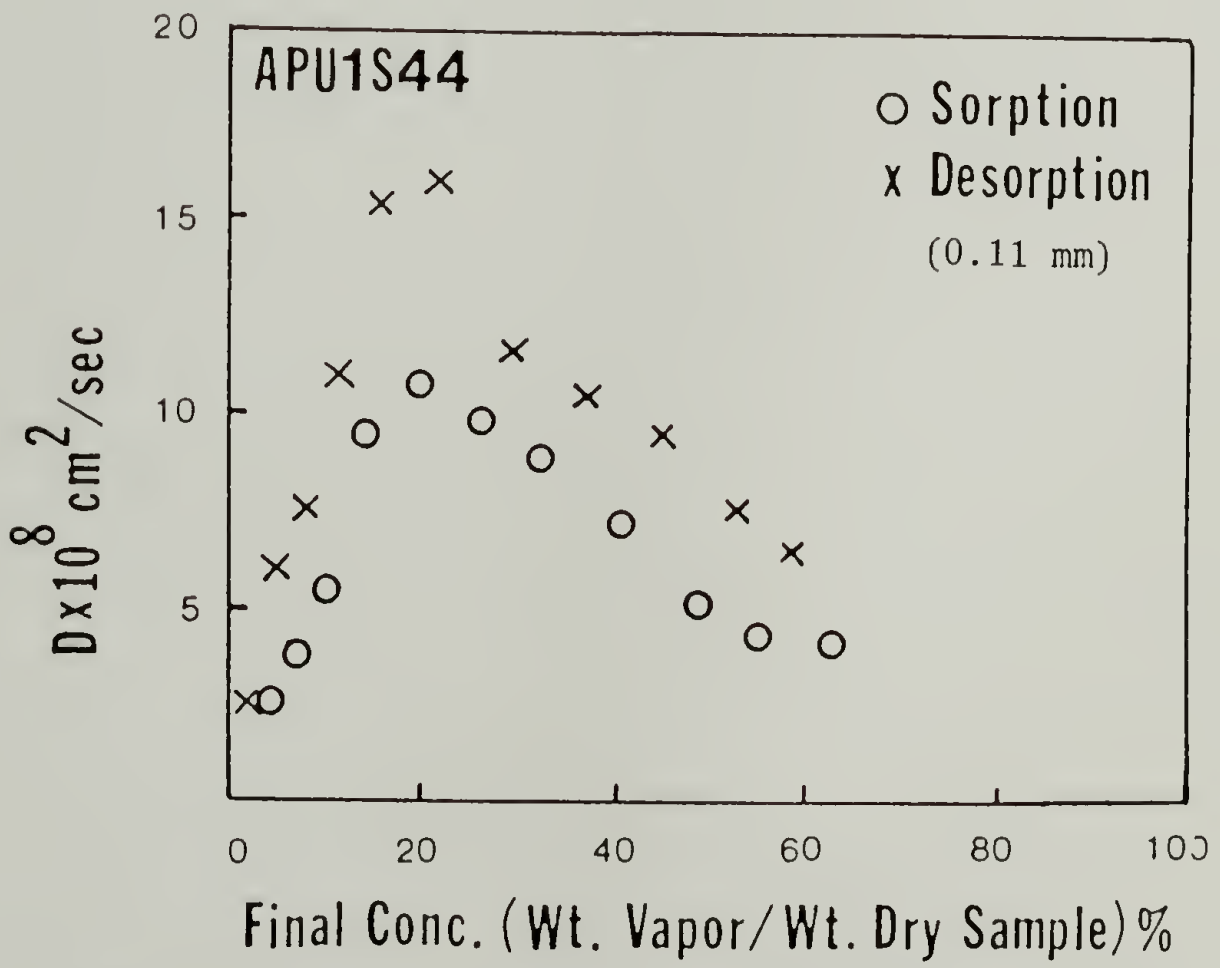

Figure 5.25 D-C curves of 1,2-dichloroethane in PU1S44 and APU1S44.

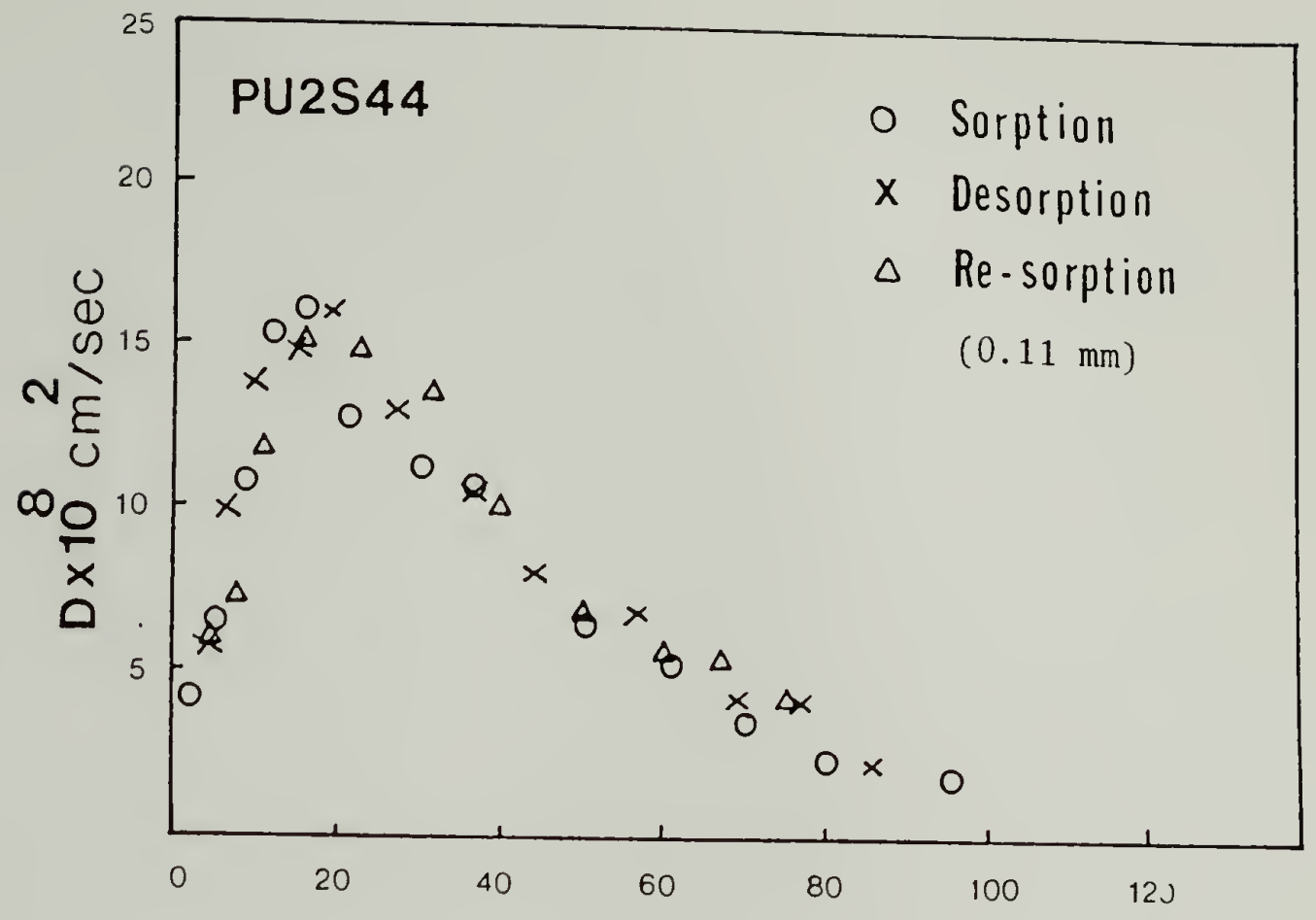

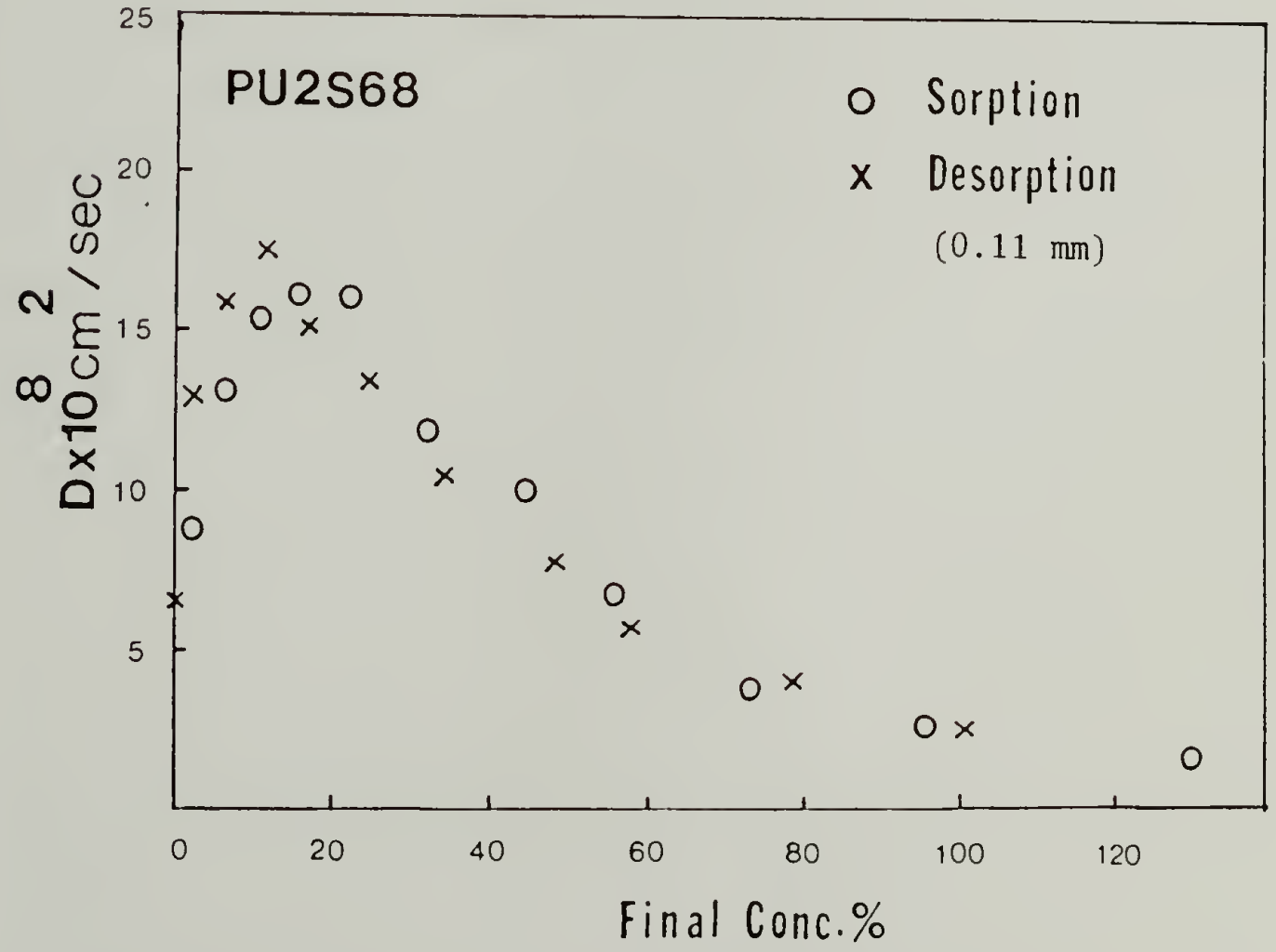

Figure 5.26 D-C curves of 1,2-dichloroethane in PU2S44 and PU2S68

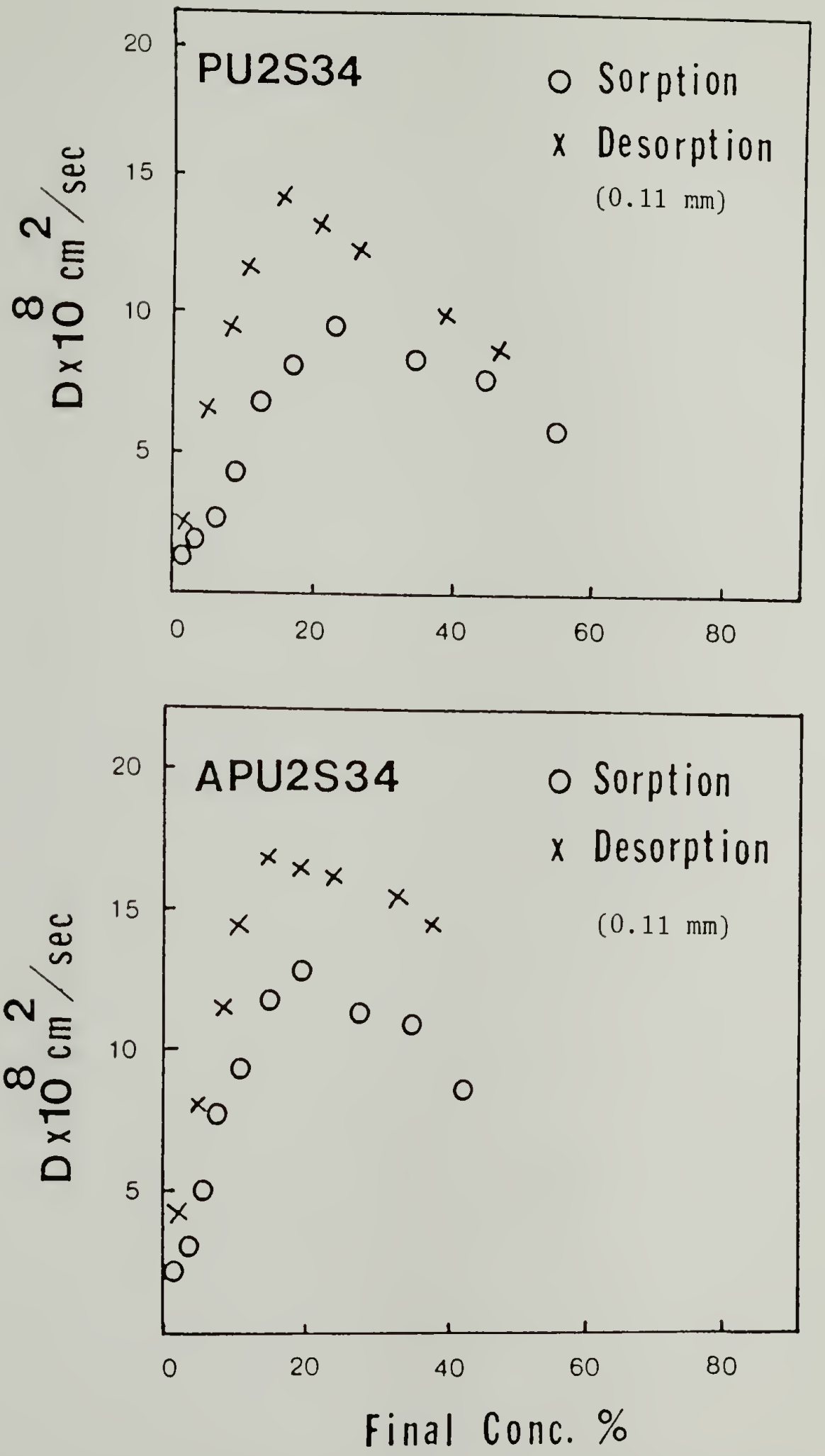

Figure 5.27 D-C curves of 1,2-dichloroethane in PU2S34 and APU2S34.

indicate that better phase separation results in a higher diffusion coefficcient for desorption curves.

Comparison of D vs. C for the annealed sample at 80°C with that for the annealed sample at 155°C shows D to be higher for the latter. These results are shown in Figures 5.28 and 5.29 determined from the desorption experiments and can be attributed to the better phase separation in the annealed sample at 155°C. It is to be noted that the diffusion is dominant in the soft segment, and the better phase separation increases the mobility of the soft segment, resulting in a higher diffusivity for the annealed sample at 155°C.

The results of D vs. C for Estane and PU1S44 at three different thicknesses are shown in Figures 5.30 and 5.31. Diffusion coeffients were calculated from sorption and desorption experiments for Estane and PU1S44, respectively. In both cases, D is higher for thicker samples at a given penetrant concentration range. These results have also been observed by Chiang and Sefton (18) who explained that for a thicker film, sorption of solvent through out the sample requires a longer time than for a thin one, thus resulting in a purely concentration dependent diffusion in films approaching infinite thickness. The diffusion coefficient therefore appears to be higher for thicker samples. Similar explanations can be applied to our results. For a given penetrant concentration profile in PTMO phase, there is more penetration of 1,2-dichloroethane into the glassy hard phase or interface for a thicker film than that for a thin one. It takes longer time to

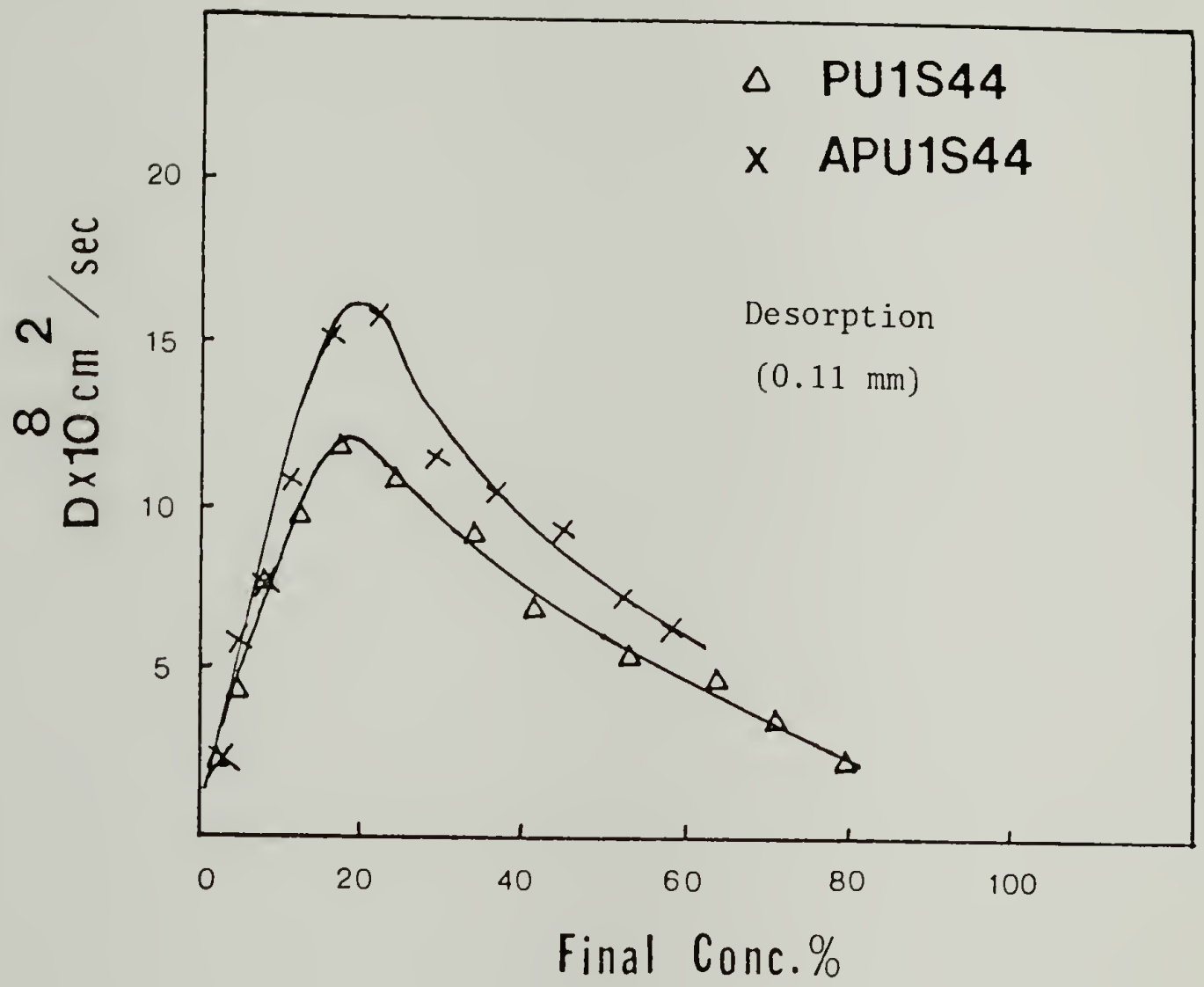

Figure 5.28 A comparison of D-C curves, determined from the desorption runs, for 1,2-dichloroethane in PU1S44 and APU1S44.

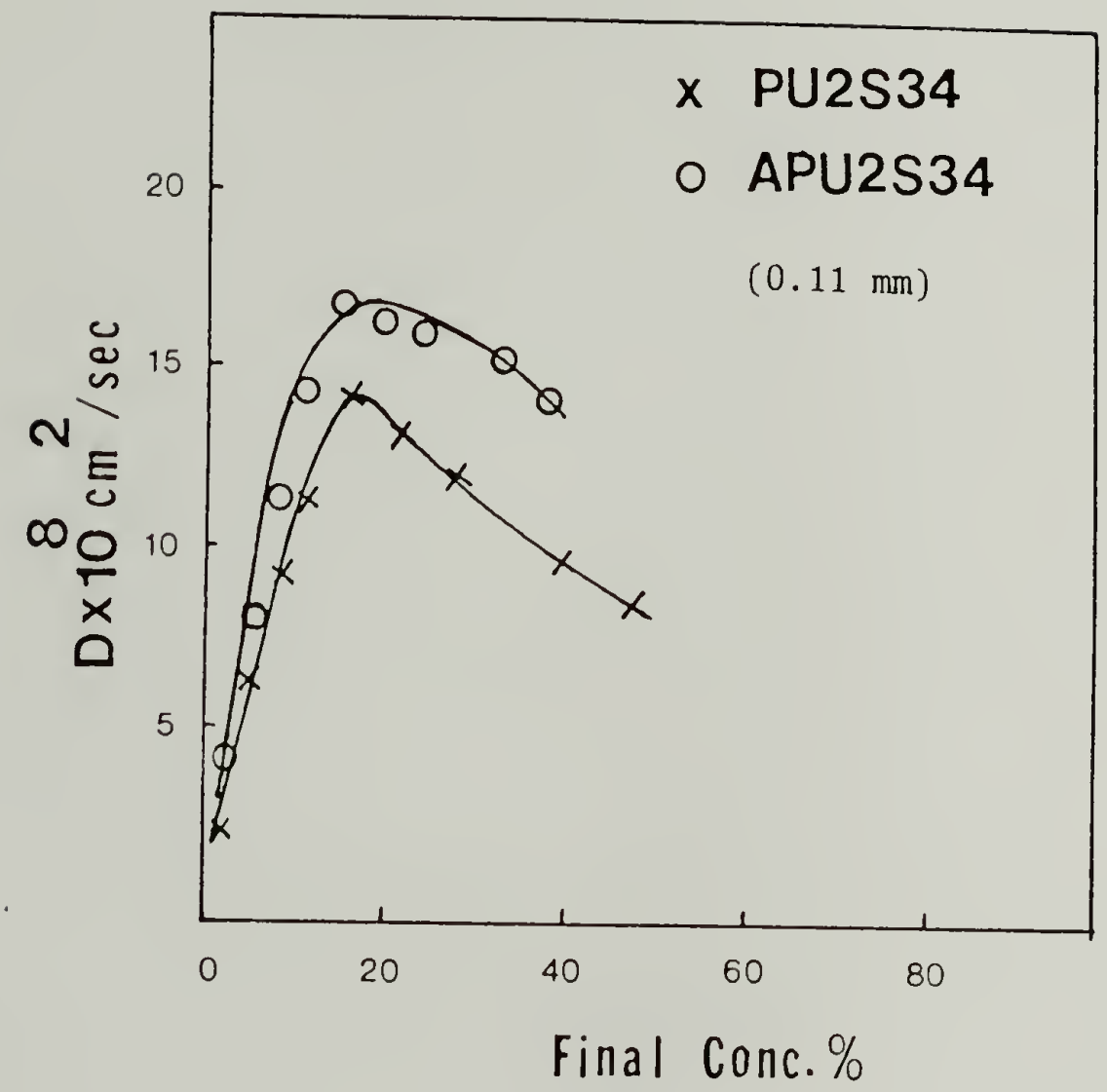

Figure 5.29 A comparison of D-C curves, determined from the desorption runs, for 1,2-dichloroethane in PU2S34 and APU2S34.

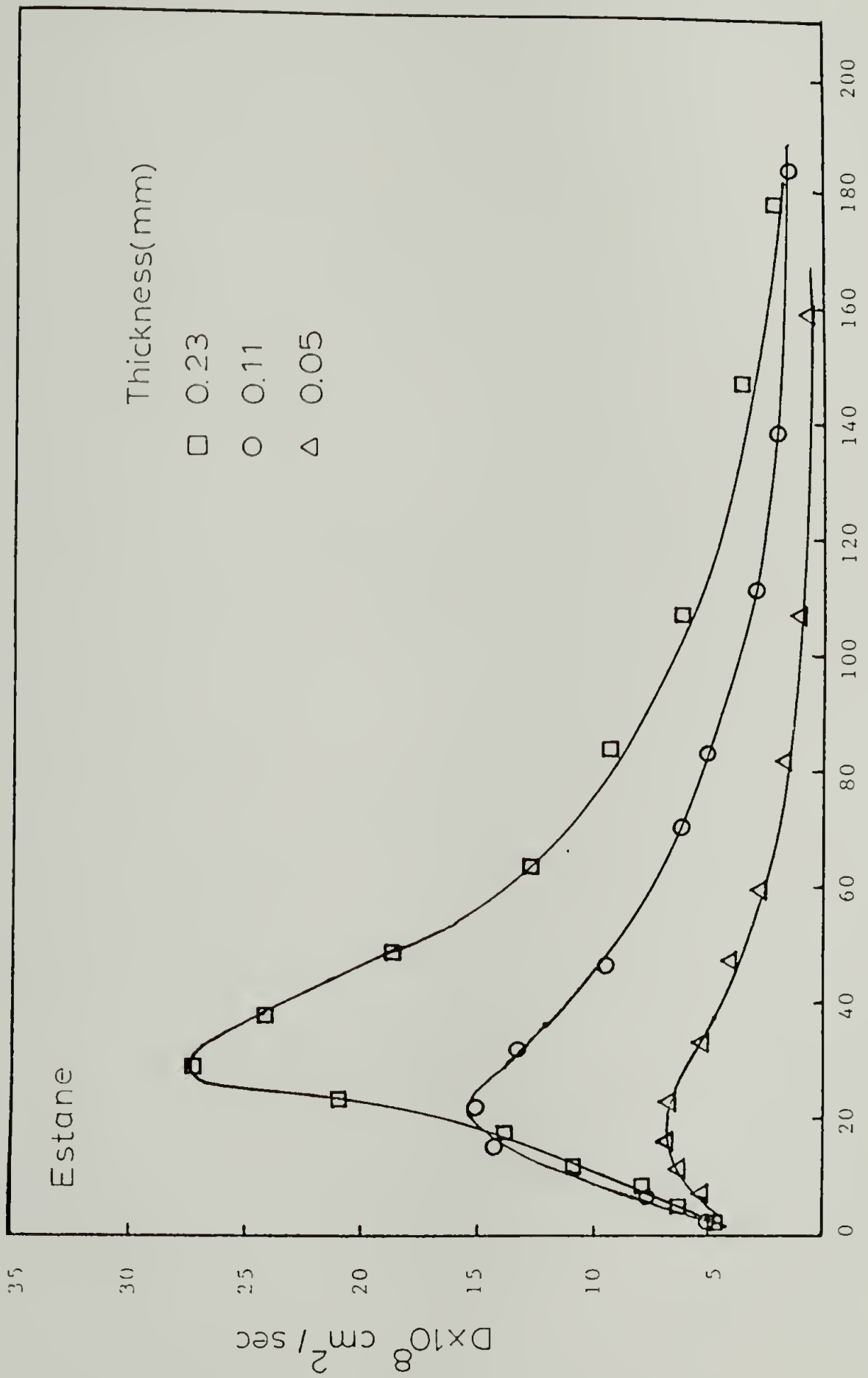

Figure 5.30 A comparison of D-C curves, determined from the sorption runs, for 1,2-dichloroethane in Estane with different film thicknesses.

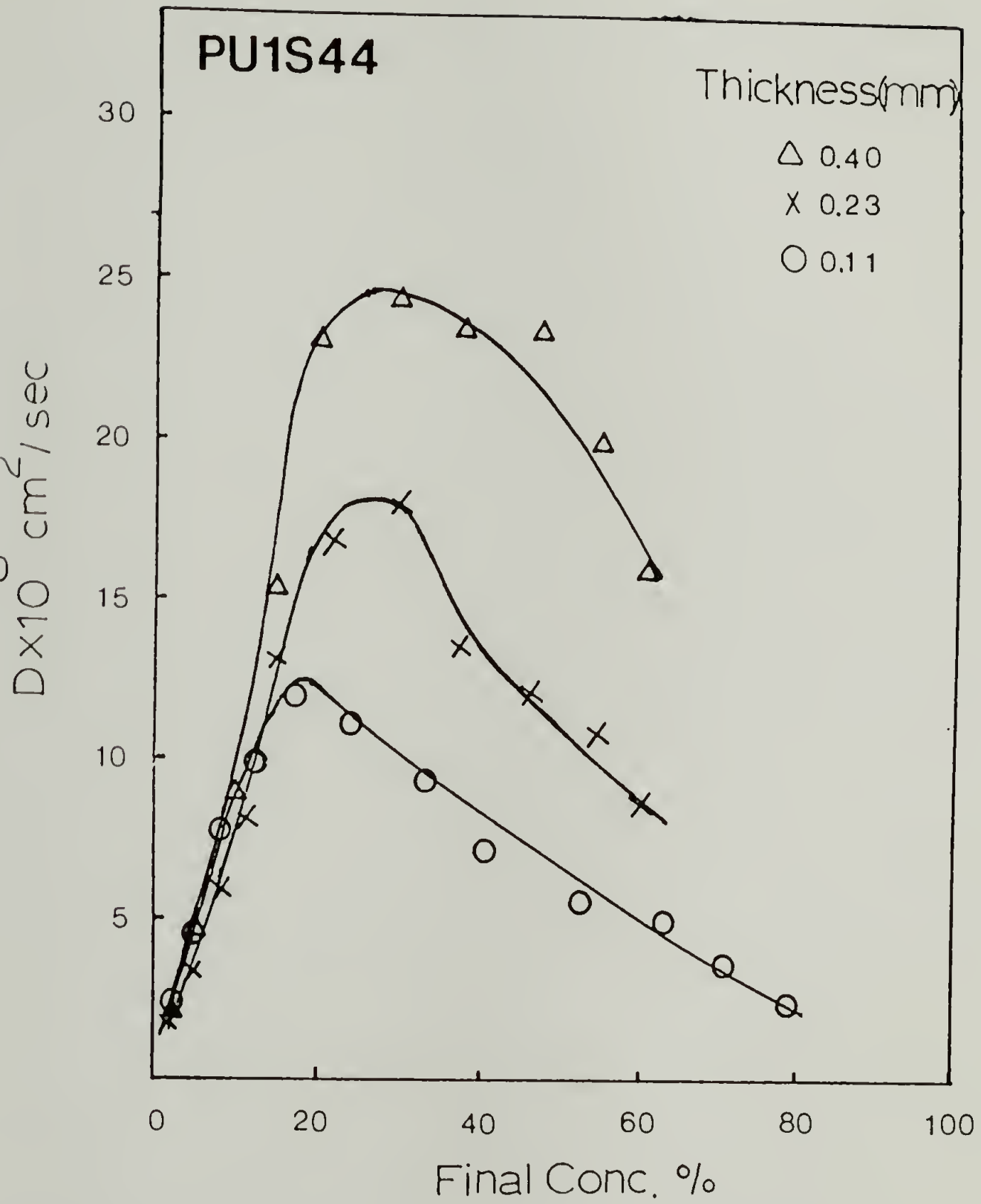

Figure 5.31 A comparison of D-C curves, determined from the desorption runs, for 1,2-dichloroethane in PU1S44 with different film thicknesses.

observe the relaxation behavior for a thin sample, and thus length-scaled sorption curves (weight gain vs.$t^{1/2}/l$) for polyurethanes will appear to be faster for a thick one than a thin one. In general, the diffusion coefficients of different film thickness are controlled by two factors, time and concentration. As film thickness increases, the controlling factor, time, appears to diminish, and the system becomes purely concentration dependent. Thus, the diffusion coefficient is higher for thicker samples.

It should be noted that the determination of D in desorption curve for PU1S44 in Figure 5.31 is by the initial slope method due to the appearance of these curves being Fickian in shape. As mentioned in the preceding section, the appearance of Fickian behavior in the desorption curves is due to the persistence of the relaxed structure which should produce a single diffusion curve of different film thicknesses with one diffusion coefficient at the same concentration range if this relaxation process is completed. However, as can be seen from Figure 5.31, the D-C curves are not superimposed to form a single curve, indicating that the relaxation is incompleted and there still exists some degree of relaxation process upon desorption.

5.4 Conclusions

The sorption and diffusion of 1,2-dichloroethane in segmented polyurethanes have been determined by performing incremental vapor

sorption and desorption experiments. The appearance of hysteresis behavior for samples with higher hard segment content in sorption isotherms indicates that there exists a relaxation process upon swelling in our penetrant-polymer system. In addition, the differences in the sorption isotherm curves for samples with different heat treatment suggest that the effect of the solvent on the glassy hard phase and/or interface is pronounced.

Anomalous sorption behavior, two stage and sigmoidal curves, were observed in our system at moderate and high vapor activities. Samples with higher hard segment content favor two-stage behavior, while sigmoidal curves were observed for lower hard segment content samples. In an attempt to examine the two-stage behavior, hysteresis, thickness, and annealing studies were performed. The results of these three types of experiments clearly indicate that the two-stage sorption behavior is a result of a relaxation process in the glassy hard phase and/or interface induced by the presence of the solvent.

The anomalous sorption behavior can be modeled very well by the Joshi-Astarita equation of Fickian diffusion coupled with a relaxation process, providing additional evidence that the non-Fickian behavior probably results from a relaxation process.

The D-C curves show pronounced maxima for all samples, especially for the higher soft segment content samples, indicating that the sorption of the solvent in the soft segment dominates the entire concentration ranges. The diffusion coefficient appears to

be higher at the higher concentration for higher hard segment content samples in D-C curves, suggesting the existence of the relaxation process at higher solvent concentration for samples with higher hard segment content.

In order to further examine the interaction between the solvent and the glassy hard phase and/or interface, DSC and NMR were used to determine this interaction and will be presented in the next chapter.

5.5 References

1. J. L. Duda and J. S. Vrentas, in "Encyclopedia of Polymer Science and Engineering", Vol. 5, 2Ed., John, Wiley, and Sons Inc., New York, 1986, P. 36.

2. H. B. Hopfenberg and V. Stannett, in "The Physics of Glassy Polymers", R. N. Haward, Ed., Wiley, New York, 1973, P. 504.

3. C. H. Jacque, H. B. Hopfenberg, and V. Stannett, in "Permeability of Plastic Films and Coatings", H. B. Hopfenberg, Ed., Plenum Press, New York, 1974, P. 73.

4. D. J. Enscore, H. B. Hopfenberg, and V. Stannett, Polymer, 18, 793 (1977).

5. P. Meares, J. A. C. S. 76, 3415 (1954).

6. P. Meares, Trans. Faraday Soc., 53, 101 (1957).

7. S. N. Zhurkov and G. Ya. Ryskin, J. Tech. Phys. (U.S.S.R.), 24, 797(1954).

8. A. Kishimoto, E. Mackawa, and H. Fujita, Bull. Chem. Soc. Japan, 33, 988 (1960).

9. A. R. Berens, Polymer, 18, 697 (1977).

10. H. L. Frisch, Polym. Eng. Sci, 20, 2 (1980).

11. H. Fujita, Fortschr, Hochpolym.-Forsch., 3, 1 (1961).

12. C. E. Rogers, in "Physics and Chemistry of the Organic Solid State", Vol. II, D. Fox, M. M. Labes, and A. Weissberger, Eds., Interscience, New York, 1965, Chap. 6.

13. H. Fujita, in "Diffusion in Polymers", J. Crank, and G. S. Park, Eds., Academic Press, New York, 1968, Chap. 3.

14. G. S. Park, in Ref. 13, Chap. 5.

15. J. Crank, "The Mathematics of Diffusion", 2nd ed,. Clarendon Press, Oxford, 1975.

16. H. Odani, K. Taira, N. Nemoto, and M. Kurata, Polym. Eng. Sci., 17, 527 (1977).

17. H. Odani, M. Uchikura, K. Taira, and M. Kurata, J. Macromol. Sci.-Phys., B17(2), 337 (1980).

18. K. T. Chiang and M. V. Sefton, J. Polym. Sci.: Polym. Phys. Ed., 15, 1927 (1977).

19. G. T. Caneba, D. S. Soong, and J. M. Prausnitz, J. Macromol. Sci.-Phys., B22(5&6), 693 (1983-4).

20. Y. S. Kang, J. H. Meldon and N. H. Sung, Polym. Eng. Sci., 26, 1045 (1986).

21. K. D. Ziegel, J. Macromol. Sci., B5, 11 (1971).

22. J. S. McBride, T. A. Massaro, and S. L. Cooper, J. Appl. Polym. Sci., 23, 201 (1979).

23. M. Serrano, Ph. D. Thesis, University of Massachusetts, 1986.

24. J. Sax, and J. M. Ottino, Polym. Eng. Sci., 23, 165 (1983).

25. R. Goydan, N. S. Schneider, and J. Meldon, Polym. Mater. Sci. Eng., 49, 249 (1983).

26. A. R. Berens, H. B. Hopfenberg, J. Polym. Sci., Polym. Phys. Ed., 17, 1757 (1979).

27. S. Joshi and G. Astarita, Polymer, 20, 455 (1979).

28. R. M. Felder and G. S. Hvard, "Methods of Experimental Physics", Vol. 16C, 1980, P. 315.

29. J. Flory, "Principles of Polymer Chemistry", 2nd ed., 1967.

30. A. R. Berens, J. Macromol. Sci.-Phys., B14(4), 483 (1977).

31. J. S. Vrentas, J. L. Duda, and Y. C. Ni., J. Polym. Sci., Polym. Phys. Ed., 15, 2039 (1977).

32. G. Rehage, O. Ernst, and J. Fuhrman, Discuss. Faraday Soc., 49, 208 (1970).

33. R. J. Bearman, J. Phys. Chem., 65, 1961 (1961).

CHAPTER VI

INVESTIGATION OF THE INTERACTION OF SOLVENT WITH PHASE SEGREGATED POLYURETHANES AND FUTURE WORK

6.1 Introduction

The transport properties of 1,2-dichloroethane in a variety of segmented polyurethanes have been studied and described in the previous chapter. The anomalous diffusion phenomena were observed and were attributed to the relaxation of hard block chains in the glassy hard phase and/or interface induced by the presence of the solvent. To verify the presence of the solvent in the glassy hard segment, further investigations on the interaction of solvent with the hard block chains in segmented polyurethane samples are clearly needed.

The swelling equilibria of ABA block copolymers have been treated both experimentally and theoretically by a number of authors (1-6). Most of them studied the swelling behavior of different solvents in styrene-isoprene-styrene (SIS) and styrene-butadiene-styrene (SBS) block copolymers in terms of interconnectivity and $\bar{M}c$, the average molecular weight of submolecular chains between effective crosslink points, due to their well-characterized morphology. The detailed descriptions on the swelling behavior of SBS and SIS are not described here. The purpose of this work is to

examine, qualitatively, the interaction between solvent and hard segment of polyurethanes in terms of molecular motions and to prove that the solvent is indeed present in the glassy hard phase and/or interface in polyurethanes.

DSC and NMR experiments were carried out to determine the mobility of the hard block chains. It is expected that the decrease in hard segment Tg and the increase in molecular motions of the hard block chains should be observed for swollen polyurethanes by performing DSC and NMR experiments if the solvent interacts with the hard segments.

6.2 Experimental

6.2.1 Materials

Polyurethane samples used in DSC and NMR studies are PU1S44 and PU2S34, respectively. The characteristics and the preparation of these samples are described in chapter IV. The swelling solvent used in both studies is 1,2-dichloroethane which is the same solvent used in studying the transport properties. Again, high purity solvent was purchased from the Aldrich Chemical Company and used as received.

6.2.2 Instrumentation

(A) Differential Scanning Calorimetry (DSC)

DSC experiments were carried out at a heating rate of 40°C/min using a Perkin-Elmer DSC-7 interfaced with a thermal analysis data station. The film sample and solvent were placed in a Perkin-Elmer stainless steel sample pan which contains an O-ring to prevent the weight loss of solvent from sample pan. The degree of swelling was determined by the weight of solvent divided by the dry sample weight.

(B) Nuclear Magnetic Resonance (NMR)

Carbon-13 NMR spectra were recorded at 50.3 MHz with a IBM 200 AF NMR using matched, spin-locked cross-polarization, and magic-angle sample spinning. Film samples were cut into 1.0-cm-wide strips, rolled to a diameter of 0.9 cm, and load into the sample rotor, along with a drop of 1,2-dichloroethane. Spinning the samples at a rate of 4200 Hz was sufficient to produce side band-free spectra. Rotating-frame relaxation times, $T_{1\rho}$, were determined from the slope of the initial decay (measured from 0.1 to 30 msec following removal of the proton rf field) with a rotating-frame Larmor frequency of 50 KHz.

6.3 Results and Discussion

6.3.1 DSC

The results of DSC studies for 1,2-dichloroethane in PU1S44 sample are shown in Figure 6.1. As can be seen from this figure, the Tg of the hard segment decreases from 104°C to 81°C as the degrees of swelling increase from 0% to 30%. This observation indicates that the mobility of the hard block chains increases due to the presence of the solvent in the glassy hard segment. However, even though the heating rate of DSC is 40°C/min, there still exists a temperature effect in this study. The penetration of the solvent into the glassy hard segment can occur at higher temperature rather than the room temperature, i.e. 24°C, which is the temperature that sorption experiments were carried out. In order to further examine this uncertainty, ^{13}C-NMR technique was used to investigate the the molecular motions of hard block chains due to swelling at room temperature. Figure 6.2 shows the DSC results for as-received dry PU1S44 and solvent-treated dry PU1S44. As can be seen from this figure, the Tm and heat of fusion for both samples are about the same, indicating that these is no detectable solvent induced crystallinity and that the crystalline hard phase is not penetrated by the solvent.

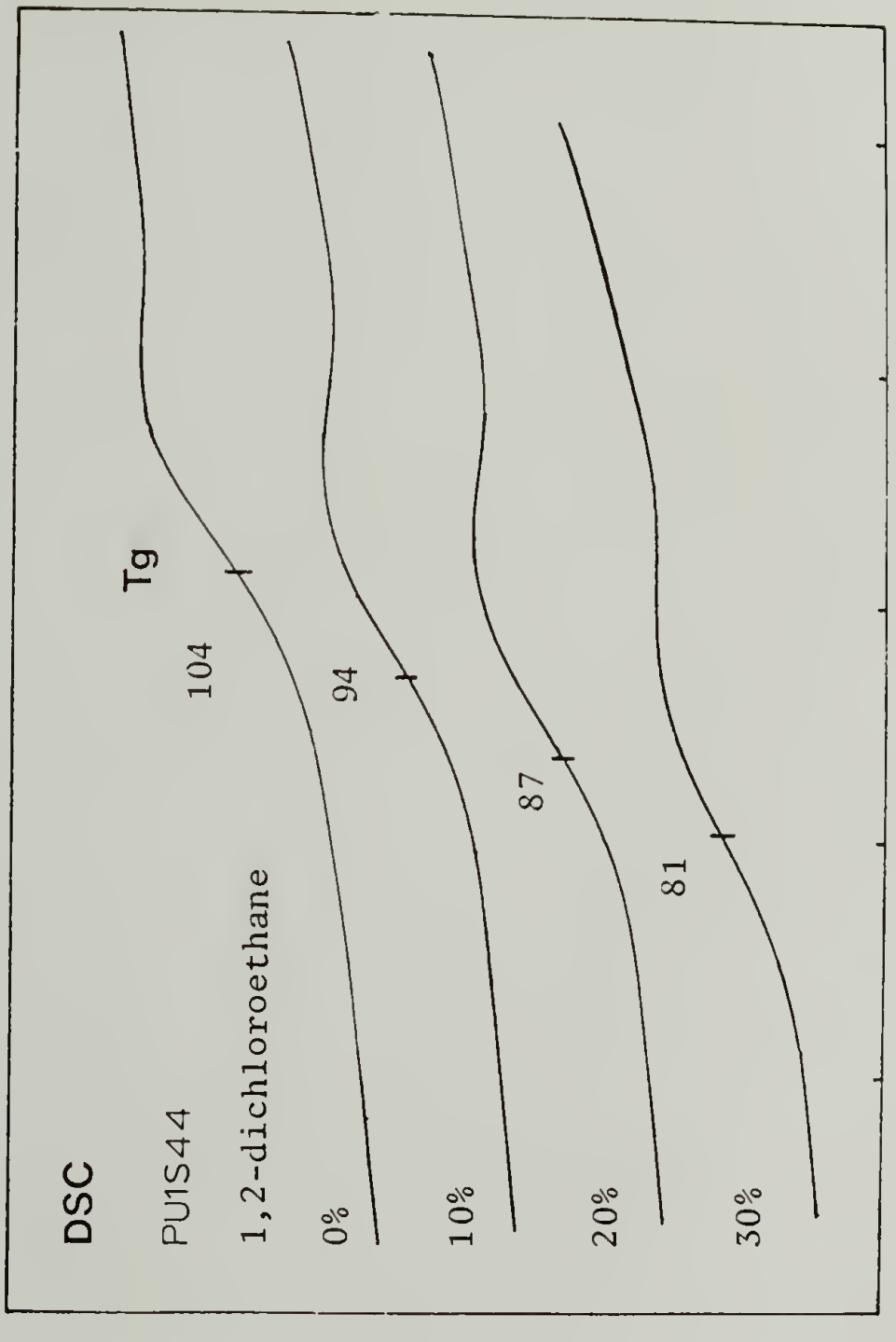

Figure 6.1 DSC traces of hard segment in PU1S44 at different degree of swelling of solvent, 1,2-dichloroethane

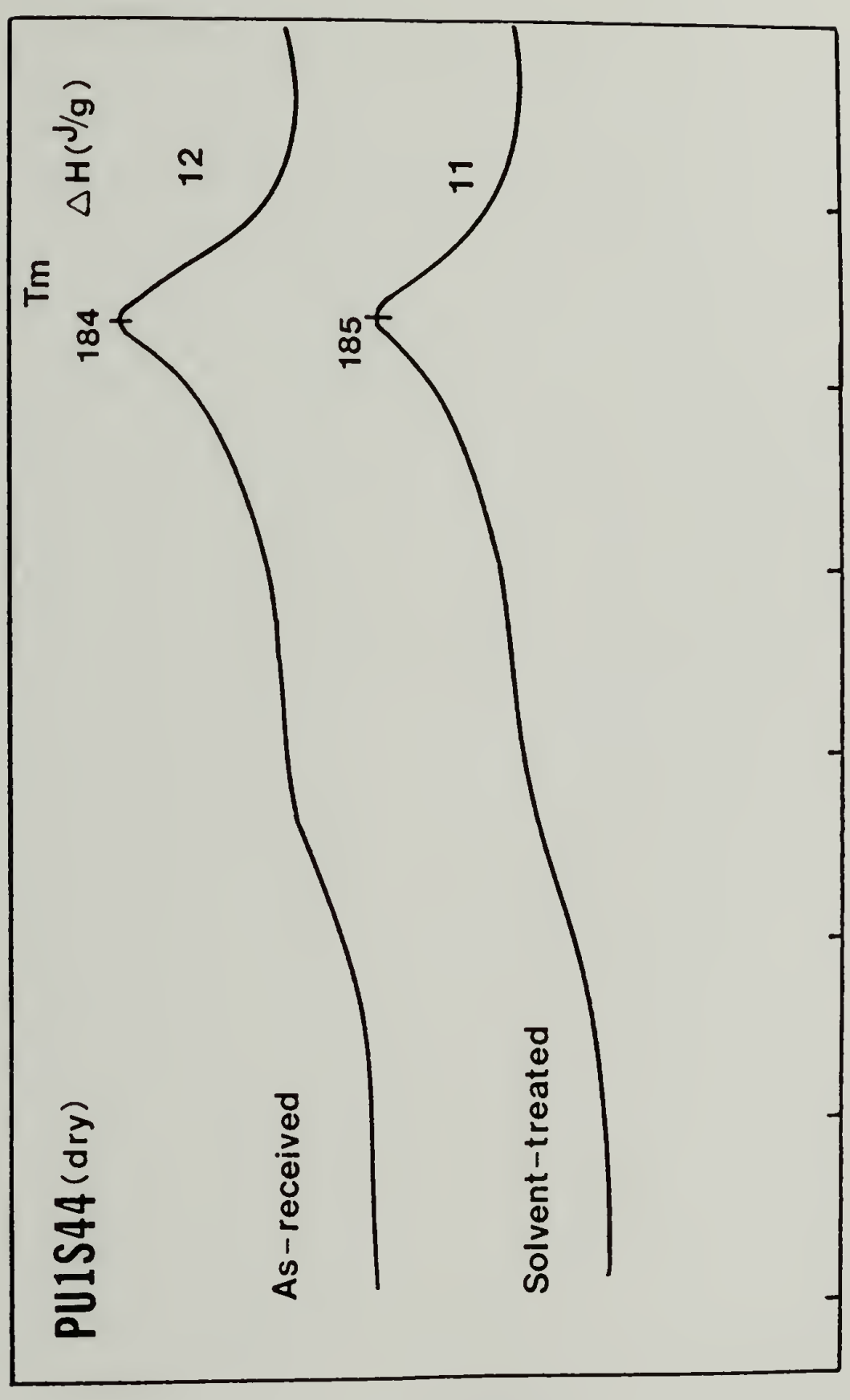

Figure 6.2 A comparison of DSC traces of hard segment for as-received dry PU1S44 and solvent-treated dry PU1S44.

6.3.2 C-13 NMR

The examination of molecular motions in solid polymers using Carbon-13 NMR have been reported by Schaefer and his coworkers (7-11). With cross-polarization and magic-angle sample spinning, C-13 NMR of solids is a high-resolution, high-sensitivity technique. C-13 rotating-frame relaxation, characterized by $T_{1\rho}$, arises from low to mid kilohertz modulation of the carbon-hydrogen dipole interaction. One of the interesting study by Schaefer et al. was the examination of the effect of gas treatment on the molecular motions in solid polymers. They found that the main-chain motions of PVC increase upon exposure to CO_2 followed by degassing, and these results can not be reconciled with dual-sorption-mobility model, which claims that gas molecules preferentially occupy preexisting sorption sites in a conditioned polymer with no perturbation of the polymer matrix.

In the present work, the hard segment molecular motions of PU2S34 sample in the swelling state were determined by C-13 NMR using cross-polarization technique. The results of this study is shown in Figure 6.3 and the values of rotating-frame relaxation time $T_{1\rho}$, calculated from the slope of the initial decay, are given in Table 6.1. Figure 6.3 plotted log I, the intensity of the peak for the spectra of the corresponding carbon, against τ (delay time in msec or 10^{-3} sec) for the dry and swollen PU2S34. Figure 6.3 were divided by four quarters which represented four different

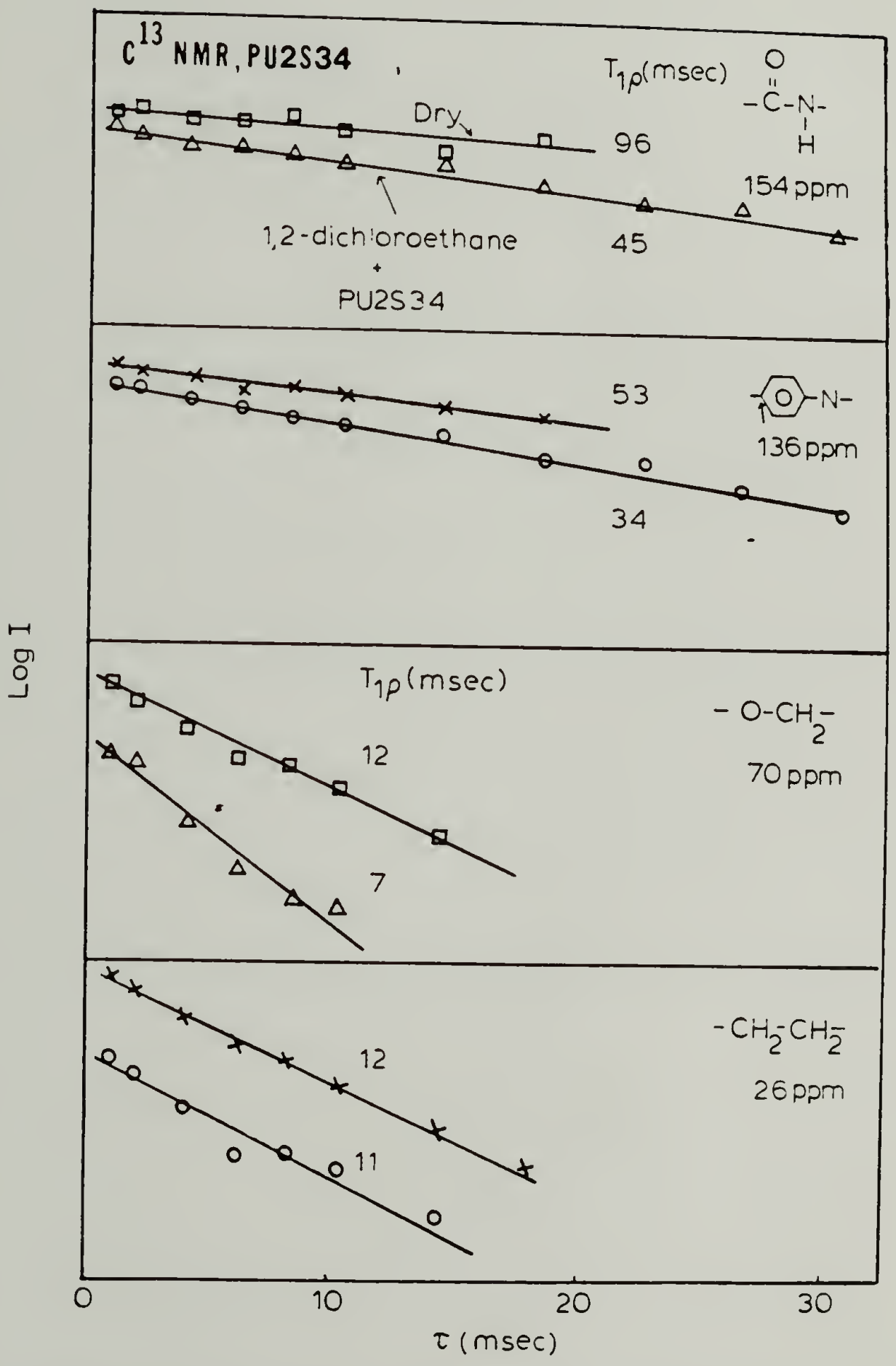

Figure 6.3 LogI vs. τ curves for four different functional groups in the dry and swollen PU2S34.

Table 6.1

C-13 NMR Rotating-Frame Relaxation Time, $T_{1\rho}$, for Dry and Swollen* Polyurethane, PU2S34

	$T_{1\rho}$ (msec)			
PU2S34	-CONH-	$-C_6H_4N-$	$-OCH_2-$	$-CH_2CH_2-$
Dry	96	53	12	12
Swollen	45	34	7	12

*1,2-dichloroethane

carbon groups with a given chemical shift. As can be seen from the top of the quarter in Figure 6.3, the intensity decreases as the time increases, and $T_{1\rho}$ of carbon in urethane functional group in the hard segment for the dry PU2S34 is about twice as high as that for the swollen PU2S34. This observation indicates that the motion of the hard segment chains are enhanced due to the presence of the 1,2-dichloroethane in the glassy hard phase or interface. Similar observations were found for carbon in the phenyl group and ether group. No detectable changes in $T_{1\rho}$ for carbon in the methylene group, which is present in the soft segment, was observed. This is probably because of the faster relaxation rate of the methylene group in the dry state. Both DSC and NMR results provide the strong evidence that an interaction between the solvent and the glassy hard phase or interface is present.

6.4 Suggestions for Future Work

The transport properties of 1,2-dichloroethane in phase segregated polyurethanes have been studied. The anomalous diffusion behavior, two-stage and sigmoidal curves, were observed by performing incremental vapor sorption and desorption experiments. Sorption isotherm curves, hysteresis studies, thickness studies, and annealing studies have shown that these anomalies are attributed to the relaxation process in the glassy hard phase and/or interfacial phase induced by the presence of the solvent. Both two-stage and

sigmoidal curves can be modeled very well by the Joshi-Astarita equation of a coupling of diffusion and relaxation processes. A pronounced maximum was observed in the plots of D vs. concentration for all polyurethane samples. This is primarily due to the thermodynamic effect. In addition, the results of C13-NMR experiments indicate that the interaction between the solvent and the hard segment is indeed present.

In order to completely understand the transport behavior of the phase segregated polyurethanes, samples with a well-defined structure are clearly needed. A monodisperse polyurethane is suggested to minimize the interfacial phase problems.

To understand the hysteresis behavior resulting from the relaxation process, a completely annealing study is recommended. The heat treatment probably results in different morphologies of polymers. Hence, the transport behavior can be compared for samples with different thermal history, and then, can be understood due to the morphological changes.

To obtain a purely concentration dependent diffusion curve, a complete thickness studies is required. It was generally observed that the sorption curves are appeared to be Fickian in shape for thicker films. Thus, a purely concentration dependent diffusion coefficient can be obtained by extrapolating the thickness to the infinite thickness.

A maximum was observed in D-C curves. To further understand this phenomenon, a single component polymer is needed, such as the

pure soft segment polyurethane. In addition, a mathematical model to describe the diffusion coefficient as a function of concentration needs to be developed although it is very difficult in two-component systems, especially in polyurethanes. Moreover, NMR technique is suggested to determine the self-diffusion coefficient and the mobility of the solvent.

On the basis of the NMR experiments, the results of rotating-frame relaxation time has shown that the interaction between the solvent and the glassy hard phase and/or interface is present. To further understand this interaction, the extensive studies for samples with different degree of swelling are required. The relationships between the degree of swelling and the relaxation time can then be defined.

6.5 References

1. D. J. Meier, J. Macromol. Sci.-Phys., B17(2), 181 (1980).

2. T. Uchida, T. Soen, T. Inoue, and H. Kawai, J. Polym. Sci., A2(10), 101 (1972).

3. W. J. Leonard, Jr., J. Polym. Sci., Polym. Symp. Ed., 54, 237 (1976).

4. D. J. Meier, Appl. Polym. Symp., 24, 67 (1974).

5. E. T. Bishop and S. Davison, J. Polym. Sci., C26, 59 (1969).

6. G. Holden, E. T. Bishop, and N. R. Legge, J. Polym. Sci., C26, 37 (1969).

7. J. Schaefer, E. O. Stejskal, and R. Buchdahl, Macromolecules, 10, 384 (1977).

8. T. R. Steger, J. Schaefer, E. O. Stejskal, and R. A. McKay, Macromolecules, 13, 1127 (1980).

9. J. Schaefer, E. O. Stejskal, T. R. Steger, M. D. Sefcik, and R. A. McKay, Macromolecules, 13, 1121 (1980).

10. M. D. Sefcik, J. Schaefer, E. O. Stejskal, and R. A. McKay, Macromolecules, 13, 1132 (1980).

11. M. D. Sefcik, J. Schaefer, and F. L. May, J. Polym. Sci., Polym. Phys. Ed., 21, 1041 (1983).

12. M. D. Sefcik and J. Schaefer, J. Polym. Sci., Polym. Phys. Ed., 21, 1055 (1983).

A P P E N D I X A

COMPUTER SUBROUTINE PROGRAM

The first derivative of the Joshi-Astarita equation, equation 5.5, with respect to three parameters, m, $\emptyset$, and Θ_D, was written to form a subroutine program which is called Astar. This subroutine program is connected to the main program (BMDP3R) in order to determine three parameters and to fit the experimental data. The file name of the main program is called PUA. The procedures for the connection of both subroutine and main programs is given below:

(a) create a data file with a given file name, say Data12, and then

(b) type Batch

```
Get, Astar
FTN5, I=Astar, L=0
Findlib, BMDP3R
Get, Data12
Get, PUA
BMDP3R, I=PUA, L=any name, B, W=2000
```

Subroutine program, Astar

```
      SUBROUTINE P3RFUN(FX,DERF,A,X,NI,I,NVAR,NPAR,IPASS,
     +XLOSS,IDEP)
      DIMENSION  A(3),DERF(3),X(200)
      T=X(1)**2
      PI=3.1415926E0
150    FORMAT(10X,3E15.3)
      BNS=0.0E0
      CNS=0.0E0
      DNS=0.0E0
      ENS=0.0E0
      FNS=0.0E0
      DO 100 N=1,300
      NN=N
      ANN=(FLOAT(NN)-0.5)*PI
      GN=-ANN*ANN*T/A(3)
      AN=0.0
      IF(GN.GT.-50.0) AN=EXP(GN)
      BN=-2.0*T*AN/A(3)/A(3)
      BNS=BNS+BN
      IF(ABS(BN).LE.1.0E-07)  GO TO 200
100   CONTINUE
200   CONTINUE
      DO 300 N=1,300
      NN=N
      ANN=(FLOAT(NN)-0.5)*PI
      GN=-ANN*ANN*T/A(3)
      AN=0.0
      IF(GN.GT.-50.0)  AN=EXP(GN)
      CN=-2.0*ANN*ANN*T*AN/(ANN*ANN-A(2)**2)/A(3)**2
      CNS=CNS+CN
      IF(ABS(CN).LE.1.0E-07) GO TO 400
300   CONTINUE
400     CONTINUE
      DO 500 N=1,300
      NN=N
      ANN=(FLOAT(NN)-0.5)*PI
      GN=-ANN*ANN*T/A(3)
      AN=0.0
      IF(GN.GT.-50.0) AN=EXP(GN)
      DN=4.0*A(2)*(1.0-AN)/(ANN**2-A(2)**2)**2
      DNS=DNS+DN
      IF(ABS(DN).LE.1.0E-07)  GO TO 600
```

```
500   CONTINUE
600   CONTINUE
      DO 700 N=1,300
      NN=N
      ANN=(FLOAT(NN)-0.5)*PI
      GN=-ANN*ANN*T/A(3)
      AN=0.0
      IF(GN.GT.-50.0)  AN=EXP(GN)
      EN=2.0*(1.0-AN)/ANN/ANN
      ENS=ENS+EN
      IF(ABS(EN).LE.1.0E-07)  GO TO 800

700   CONTINUE
800   CONTINUE
      DO 900 N=1,300
      NN=N
      ANN=(FLOAT(NN)-0.5)*PI
      GN=-ANN*ANN*T/A(3)
      AN=0.0
      IF(GN.GT.-50.0)  AN=EXP(GN)
      FN=2.0*(1.0-AN)/(ANN**2-A(2)**2)
      FNS=FNS+FN
      IF(ABS(FN).LE.1.0E-07)  GO TO 1000
900   CONTINUE
1000  CONTINUE
      EPHI=EXP(-A(2)*A(2)*T/A(3))
      FX=ENS-A(1)*(FNS-TAN(A(2))/A(2)*(1.0-EPHI))
      DERF(1)=-(FNS-TAN(A(2))/A(2)*(1.0-EPHI))
      DERF(2)=-A(1)*(DNS-(1.0-EPHI)*(A(2)/COS(A(2))**2
     +-TAN(A(2)))/A(2)/A(2)-2.0*TAN(A(2))*T*EPHI/A(3))
      DERF(3)=BNS-A(1)*(CNS+TAN(A(2))*A(2)*T/A(3)/A(3)*EPHI)
      RETURN
      END
```

BMDP3R main program, PUA

```
/PROBLEM TITLE IS 'SORPTION CURVE FITTED BY ASTARITA EQ.'.
/INPUT VARIABLES ARE 2.
       FORMAT IS '(2F10.4)'.
FILE=DATA12.
/VARIABLE NAMES ARE X, FO.
/REGRESS DEPENDENT IS FO.
         INDEPENDENT IS X.
         PARAMETERS ARE 3.
/PARAMETER INITIAL ARE .800, 6.00, 4000.000.
/ PLOT   VARIABLE IS X.
         RESIDUAL.
/END
```

A P P E N D I X B

DETERMINATION OF SELF-DIFFUSION COEFFICIENT

The mutual diffusion coefficient of a penetrant-polymer system is the product of the self-diffusion coefficient of the penetrant and the thermodynamic factor. This relationship is given below:

$$D = D_1 \underbrace{\phi_1 \phi_2 (\partial \ln a_1 / \partial \phi_1)}_{\text{thermodynamic factor}} \qquad \text{(B)}$$

(D_1: mobility factor or self-diffusion coefficient)

where D is the mutual diffusion coefficient; D_1 is the self-diffusion coefficient; a_1 is the activity of the solvent, and ϕ_1 and ϕ_2 are the volume fraction of the solvent and polymer, respectively. It is rather common for rubbery polymer that D_1 is an increasing function of the solvent concentration, wheares the thermodynamic factor usually decreases. Considering our system benig a solvent and a homo-polymer system (Acturally, it is not the case since polyurethane consists of soft and hard segment.), D can be measured from the experiments, and a_1, ϕ_1 and ϕ_2 can be calculated by assuming that the system is in an equilibrium state. The density of the solvent (1,2-dichloroethane) and the polyurethanes are assumed to be the same, 1.2 g/ml. Thus, D_1 can be determined from the above equation. It is to be noted that D_1 should be called effective

self-diffusion coefficient, since D in this system is effective mutual diffusion coefficient. The results of D_1 and D as a function of the solvent concentrations for the PU2S68 are shown in Figure B.1. As can be seen from this figure, the effective self-diffusion coefficient initially increases sharply, and then levels off as the concentration further increases. This observation indicates that the decrease in effective mutual diffusion coefficient D is probably attributed to the thermodynamic factor. However, up to date the bahavior of the effective self-diffusion coefficient as a function of concentration for glassy or multiphase polymer is not well defined. D_1 as a function of concentration determined from the equation B can only be described as a phenomenological behavior.

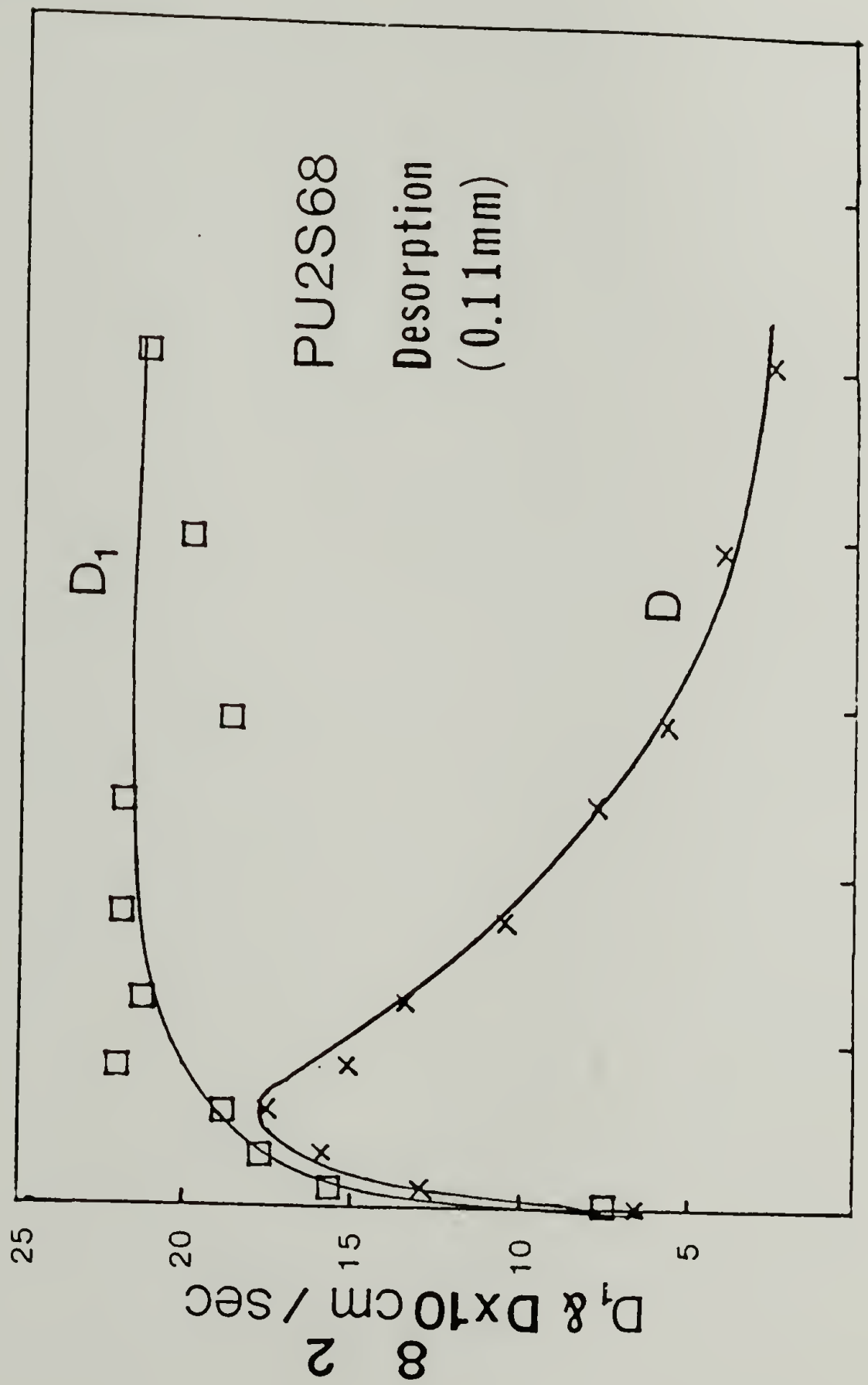

Figure B.1 Effective self-diffusion coefficient and mutual diffusion coefficient as a function of solvent concentration.

A P P E N D I X C

TABULATIONS

C.1 Tables for Sorption Isotherm

Table C.1.1 Estane[sorption], 0.11 mm

Final Conc.(%)	Activity
1.8	0.06
6.3	0.18
10.5	0.28
14.5	0.38
21.8	0.49
31.9	0.62
46.3	0.73
70.3	0.84
83.0	0.88
111.0	0.92
137.8	0.95
183.6	0.97
244.7	0.99

Table C.1.2 PU1S52[sorption(S) and desorption(D)], 0.11 mm

Final Conc.		Activity	
(S)	(D)	(S)	(D)
0.5	1.1	0.02	0.06
1.3	8.3	0.06	0.28
4.7	12.3	0.18	0.38
7.8	17.8	0.28	0.50
11.4	25.0	0.38	0.62
16.2	35.1	0.49	0.73
22.9	43.7	0.61	0.80
31.9	56.0	0.73	0.88
39.4	67.5	0.80	0.92
50.9	77.7	0.88	0.95
64.7	89.2	0.93	0.98
72.1		0.95	
82.7		0.97	
91.9		0.99	

Table C.1.3 PU1S44[sorption(S), desorption(D),and second sorption(R)], 0.11 mm

Final Conc.			Activity		
(S)	(D)	(R)	(S)	(D)	(R)
4.4	2.1	1.4	0.18	0.07	0.06
7.1	5.0	4.6	0.28	0.17	0.18
10.4	8.6	8.0	0.38	0.28	0.28
14.7	12.4	11.7	0.49	0.38	0.38
21.2	17.5	16.6	0.62	0.49	0.49
29.4	24.7	23.2	0.73	0.62	0.62
36.4	33.8	32.3	0.81	0.73	0.73
46.7	41.7	39.9	0.88	0.80	0.80
57.6	52.9	50.5	0.93	0.88	0.87
65.5	64.0	61.2	0.95	0.92	0.92
76.2	71.4	68.8	0.97	0.95	0.95
88.6	79.9	77.4	0.99	0.97	0.97

Table C.1.4 APU1S44[sorption(S) and desorption(D)], 0.11 mm

Final Conc.		Activity	
(S)	(D)	(S)	(D)
1.5	1.6	0.06	0.06
4.4	4.7	0.18	0.18
7.3	7.8	0.28	0.28
10.2	11.1	0.38	0.38
14.2	15.8	0.49	0.49
19.8	21.9	0.62	0.62
25.9	28.8	0.72	0.72
32.5	36.3	0.80	0.80
40.7	45.0	0.88	0.88
49.3	52.4	0.93	0.92
55.2	57.4	0.95	0.95
62.3		0.98	

Table C.1.5 PU2S68[sorption(S) and desorption(D)], 0.11 mm

Final Conc.		Activity	
(S)	(D)	(S)	(D)
2.2	0.1	0.07	0.01
6.6	2.3	0.18	0.07
11.0	6.8	0.29	0.18
15.9	11.6	0.39	0.28
22.4	16.9	0.49	0.39
31.7	24.0	0.62	0.49
44.6	34.2	0.73	0.62
55.6	47.6	0.80	0.73
73.2	58.1	0.87	0.79
95.4	78.0	0.93	0.87
130.0	100.1	0.97	0.93

Table C.1.6 PU2S44[sorption(S), desorption(D), and, second sorption(R)], 0.11 mm

Final Conc.			Activity		
(S)	(D)	(R)	(S)	(D)	(R)
1.9	4.0	1.9	0.07	0.08	0.07
5.3	6.7	5.0	0.18	0.17	0.18
8.3	10.2	8.0	0.28	0.28	0.28
11.5	14.0	10.9	0.38	0.38	0.38
15.6	19.0	16.4	0.49	0.49	0.49
21.7	25.8	23.2	0.62	0.62	0.62
29.9	36.7	32.3	0.73	0.73	0.73
37.2	44.4	40.0	0.80	0.80	0.80
50.3	57.0	49.7	0.88	0.88	0.87
61.0	68.7	59.9	0.92	0.92	0.92
80.2	76.7	66.9	0.97	0.95	0.95
94.8	86.2	75.4	0.99	0.97	0.97

Table C.1.7 PU2S34[sorption(S) and desorption(D)], 0.11 mm

Final Conc.		Activity	
(S)	(D)	(S)	(D)
1.4	2.0	0.06	0.06
3.7	5.2	0.18	0.18
6.5	8.6	0.30	0.30
8.9	11.0	0.38	0.39
12.4	15.7	0.49	0.49
17.4	21.1	0.62	0.62
23.6	27.3	0.73	0.73
34.6	39.3	0.86	0.87
44.8	47.2	0.93	0.93
55.1		0.98	

Table C.1.8 APU2S34[sorption(S) and desorption(D)], 0.11 mm

Final Conc.		Activity	
(S)	(D)	(S)	(D)
1.4	0.4	0.06	0.03
3.7	2.0	0.18	0.07
6.2	8.2	0.30	0.30
8.1	10.7	0.38	0.38
11.2	14.3	0.50	0.50
15.2	19.0	0.62	0.62
19.8	24.2	0.73	0.73
28.5	32.9	0.86	0.86
35.1		0.93	
42.4		0.98	

C.2 Tables for D-C Curves

Table C.2.1 Estane[sorption],0.05, 0.11 and 0.23 mm

Dx10⁸(cm²/sec)			C(%)		
0.05	0.11	0.23 mm	0.05	0.11	0.23 mm
5.3	5.0	4.6	7.3	1.8	2.2
6.5	7.5	6.3	11.7	6.3	5.0
6.8	10.3	7.8	16.5	10.5	8.2
6.7	14.4	10.8	23.2	14.5	12.2
5.2	15.1	13.7	33.6	21.8	17.1
3.9	13.5	21.0	47.1	31.9	23.4
2.6	9.4	27.2	60.0	46.3	28.9
1.6	5.8	24.1	81.8	70.3	38.1
1.3	4.9	18.6	107.0	83.0	49.0
0.5	2.9	12.8	159.0	111.0	63.4
0.2	1.4	9.0	242.3	183.6	83.7
	1.0	6.5		244.7	106.7
		2.8			147.1
		2.2			178.0
		0.7			306.0

Table C.2.2 Estane[desorption],0.11 and 0.23 mm

Dx10⁸(cm²/sec)		C(%)	
0.11	0.23 mm	0.11	0.23 mm
1.0	1.2	206.0	257.5
1.8	1.8	149.4	194.7
7.0	2.9	65.8	161.6
9.2	5.0	51.5	117.4
12.6	8.0	36.0	91.2
15.0	13.0	25.4	68.1
16.9	17.9	18.0	52.2
12.2	21.3	12.8	40.0
4.1	25.0	3.6	29.8
	20.5		23.8
	19.4		17.3
	15.0		12.0
	10.9		7.9
	7.6		4.4
	5.2		1.9

Table C.2.3 PU1S52[desorption], 0.11 mm

Dx10⁸(cm²/sec)	C(%)
2.7	1.0
7.5	8.3
11.7	12.3
13.9	17.8
11.7	25.0
9.9	35.1
7.3	43.7
7.1	56.0
5.6	67.5
4.7	77.7
4.3	89.2

Table C.2.4 PU1S44[sorption], 0.11 and 0.23 mm

Dx10⁸(cm²/sec)		C(%)	
0.11	0.23 mm	0.11	0.23 mm
2.2	2.3	4.4	4.1
4.2	2.9	7.1	7.0
6.9	4.4	10.4	10.1
9.6	7.7	14.9	14.3
10.6	12.4	21.2	20.0
10.0	12.8	29.4	27.6
8.6	13.9	36.4	34.2
6.5	12.8	46.7	42.9
4.6	10.2	57.6	51.8
3.8	9.3	65.5	58.0
2.8	7.2	76.2	65.7

Table C.2.5 PU1S44[desorption], 0.11, 0.23, 0.40 mm

Dx10⁸(cm²/sec)			C(%)		
0.11	0.23	0.40	0.11	0.23	0.40
2.3	1.8	2.2	2.1	1.6	2.0
4.3	3.3	4.7	5.1	4.9	5.4
7.6	6.0	8.9	8.6	8.0	9.8
9.8	7.9	15.4	12.4	11.4	14.9
11.9	13.2	23.2	17.5	14.7	21.0
10.8	16.8	24.4	24.7	22.3	30.8
9.2	17.8	23.5	33.8	30.5	38.6
7.0	13.5	23.6	41.7	37.5	47.7
5.5	12.2	20.2	52.9	46.7	55.8
4.8	10.9	16.1	64.0	54.8	61.3
3.4	8.8		71.4	59.8	
2.4			80.0		

Table C.2.6 PU1S44[second sorption], 0.11 mm

$Dx10^8$(cm²/sec)	C(%)
1.4	1.4
2.2	4.6
4.0	8.0
5.7	11.7
10.4	16.6
9.9	23.2
8.9	32.3
8.1	40.0
6.3	50.5
5.3	61.2
4.0	68.8
2.9	77.4

Table C.2.7 APU1S44[sorption and desorption], 0.11 mm

$Dx10^8$(cm²/sec)		C(%)	
sorption	desorption	sorption	desorption
2.5	2.5	4.4	1.6
3.6	5.9	7.3	4.7
5.2	6.6	10.2	7.8
9.4	10.9	14.2	11.1
10.6	15.3	19.8	15.8
9.7	15.8	25.9	21.9
8.8	11.6	32.5	28.8
6.9	10.5	40.7	36.3
5.0	9.5	49.3	45.0
4.3	7.3	55.2	52.4
4.0	6.4	62.6	57.4

Table C.2.8 PU2S68[sorption and desorption], 0.11 mm

$Dx10^8$(cm²/sec)		C(%)	
sorption	desorption	sorption	desorption
8.7	6.6	2.2	0.1
13.0	13.0	6.6	2.3
15.1	15.9	11.0	6.9
16.0	17.4	16.0	11.6
16.1	16.9	22.4	16.9
11.7	13.5	31.7	24.0
10.0	10.5	44.6	34.2
6.5	7.7	55.6	47.6
3.9	5.8	73.2	58.1
2.8	4.1	95.5	78.0
1.6	2.6	130.0	100.1

Table C.2.9 PU2S44[sorption snd desorption], 0.11 mm

$Dx10^8$(cm²/sec)		C(%)	
sorption	desorption	sorption	desorption
4.2	6.0	1.9	4.0
6.5	10.0	5.3	6.7
10.7	14.1	8.3	10.2
15.3	14.9	11.5	14.0
16.1	15.7	15.6	19.0
12.5	10.6	21.7	36.7
12.0	8.0	29.9	44.4
10.7	6.2	37.2	57.0
6.5	4.2	50.3	68.7
5.2	4.3	61.0	76.7
2.5	2.4	80.2	86.2
1.8		94.8	

Table C.2.10 PU2S34[sorption and desorption], 0.11 mm

$Dx10^8$(cm²/sec)		C(%)	
sorption	desorption	sorption	desorption
1.3	2.5	1.4	2.0
2.0	6.5	3.7	5.2
2.7	9.4	6.5	8.6
4.9	11.6	8.9	11.0
6.7	16.5	12.4	15.7
8.1	15.3	17.4	21.1
9.4	12.3	23.6	27.3
8.2	10.0	34.6	39.3
7.7	8.9	44.8	47.2
5.8		55.1	

Table C.2.11 APU2S34[sorption and desorption],0.11 mm

$Dx10^8$(cm²/sec)		C(%)	
sorption	desorption	sorption	desorption
2.2	2.1	1.4	0.4
3.1	4.3	3.7	2.0
4.9	11.4	6.2	8.2
7.8	14.5	8.1	10.7
9.2	18.4	11.2	14.3
11.7	17.9	15.2	19.0
12.7	16.3	19.8	24.2
11.2	15.4	28.5	32.9
10.8		35.1	
8.6		42.4	

BIBLIOGRAPHY

Abouzahr, S., Wilkes, G. L. and Ophir, Z., Polymer, 23, 1077 (1982).

Aggarwal, S. L. in "Block and Graft Copolymers", Eds., Burke, J. and Weiss, V., Syracuse University Press (1973), P. 157.

Alfrey, T., Gurnee E. F., and Lloyd, W. G., J. Polym. Sci., C12, 249 (1966).

Assink, R. A., J. Polym. Sci., Polym. Phys. Ed., 13, 1665 (1975).

Astarita, G., and Sarti, G. C., Polym. Eng. Sci., 18, 388 (1978).

Astarita, G., and Joshi, S., J. Membrane Sci., 4, 165 (1978).

Bagley, E., and Long, F. A., J. Am. Chem. Soc., 77, 2172 (1955).

Barrie, J. A., and Nunn, A., Div. Org. Coat. Plast. Chem. Pap., 34, 489 (1974).

Bearman, R. J., J. Phys. Chem., 65, 1961 (1961).

Berens, A. R., Angew. Makromol. Chem., 47, 97 (1975).

Berens, A. R., Polymer, 18, 697 (1977).

Berens, A. R., J. Macromol. Sci.-Phys., B14(4), 483 (1977).

Berens, A. R. and Hopfenberg, H. B., Polymer, 19, 489 (1978).

Berens, A. R. and Hopfenberg, H. B., J. Polym. Sci., Polym. Phys. Ed., 17, 1757 (1979).

Berens, A. R., Polym. Eng. and Sci. 20(1), 95 (1980).

Bishop, E. T. and Davison, S., J. Polym. Sci., C26, 59 (1969).

Bonart, R., J. Macromol. Sci.-Phys., B2, 115 (1968).

Bonart, R., Morbitzer, L., and Hentze, G. J., J. Macromol. Sci., Phys., B3(2), 337 (1969).

Boyarchuk, Y. M., Rappoport, L. Y., Mikitin, V. N., and Apukhtine, N. P., Polym. Sci. USSR, 7, 859 (1965).

Briber, R. M., and Thomas, E. L., J. Macromol. Sci.-Phys., B22(4), 509 (1983).

Briber, R. M., Ph. D. Thesis, University of Massachusetts, 1984.

Brunette, C. M., Ph. D. Thesis. University of Massachusetts, 1982.

Caneba, G. T., soong, D. S., and Prausnitz, J. M., J. Macromol. Sci.-Phys., B22(5&6), 693 (1983-4).

Chang, A. L., Briber, R. M., Thomas, E. L., Zhrahaln, R. J., and Critchfield, F. E., Polymer, 23, 1060 (1982).

Chern, R. T., Koros, W. J., Sanders, E. S., Chen, S. H., and Hopfenberg, H. B., in "Industrial Gas Separations, ACS Symposium Series 223", Whyte, T. E., Yon, C. M., and Wagener, E. H., Eds., American Chemical Society, Washington, D. C., 1983, P. 47.

Chiang, K. T., and Sefton, M. V., J. Polym. Sci., Polym. Phys. Ed., 15, 1927 (1977).

Clough, S. B., Schneider, N. S., and King, A., J. Macromol. Sci.-Phys., B2, 641 (1968).

Cooper, S. L., and Tobolsky, A. V., J. Appl. Polym. Sci., 10, 1837 (1966).

Crank, J., and Park, G. S., Eds., "Diffusion in Polymers" Academic Press, New York 1968.

Crank, J., "The Mathematics of Diffusion" 2nd Ed., Oxford University Press, London and New York, 1975.

Duda, J. L. and Vrentas, J. S., in "Encyclopedia of Polymer Science and Technology", Vol. 13, Wiley, New York, 1970, P. 326.

Duda, J. L. and Vrentas, J. S. in "Encyclopedia of Polymer Science and Engineering", Vol. 5, 2 Ed., John, Wiley, and Sons Inc., New York, 1986, P. 36.

Enscore, D. J., Hopfenberg, H. B., and Stannett, V., Polymer, 18, 793 (1977).

Estes, G. M., Cooper, S. L., and Tobolsky, A. V., J. Macromol. Sci., Rev. Macromol. Chem. C4(2), 313 (1970).

Felder, R. M. and Hvard, G. S., "Methods of Experimental Physics", Vol. 16C, 315 (1980).

Flory, J., "Principles of Polymer Chemistry", 2nd ed., 1967.

Fridman, I. D., Thomas. E. L., Lee, L. J., and Macosko, C. W., Polymer, 21, 393 (1980).

Frisch, H. L., Wang, T. T., and Kwei, T. K., J. Polym. Sci. 7 (A2), 879 (1969).

Frisch, H. L., Polym. Eng. Sci, 20(1), 2 (1980).

Fujita, H., Fortschr. Hochpolym.-Forsch., 3, 1 (1961).

Fujita, H., in "Diffusion in Polymers", Crank, J., and Park, G. S. Eds., Academic Press, New York, 1968, Chap. 3.

Goydan, R., Schneider, N. S., and Meldon, J., Polym. Mater. Sci. Eng., 49, 249 (1983).

Harrell, L. L., Jr., Macromolecules, 2, 607 (1969).

Hays, M. J. and Park, G. S., Trans. Farad. Soc., 51, 1134 (1955).

Hesketh, T. R., Van Bogart, J. W. C., Cooper, S. L., Polym. Eng. Sci., 20, 190 (1980).

Holden, G., Bishop, E. T., and Legge, N. R., J. Polym. Sci., C26, 37 (1969).

Hopfenberg, H. B. and Stannett, V., in "The Physics of Glassy Polymers", Haward, R. N., Ed., Wiley, New York, 1973, P. 504.

Hopfenberg, H. B., and Frisch, H. L., J. Polym. Sci., B7, 405 (1969).

Hopfenberg, H. B., Holley, R. H., and Stannett, V., Polym. Eng. Sci., 9, 242 (1969).

Hopfenberg, H. B., J. Membrane Sci., 3, 215 (1978).

Hu, C. B., Ward, R. S., Jr., and Schneider, N. S., J. Appl. Polym. Sci., 27, 2167 (1982).

Jacque, C. H., Hopfenberg, H. B., and Stannett, V, in "Permeability of Plastic Films and Coatings", Hopfenberg, H. B., Ed., Plenum Press, New York, 1974, P. 73.

Joshi, S. and Astarita, G., Polymer, 20, 455 (1979).

Kang, Y. S., Meldon, J. H., and Sung, N. H., Polym. Eng. Sci., 26, 1045 (1986).

Kishimoto, A., Fujita, H., Odani, H., Kurata, M., and Tamura, M., J. Phys. Chem., 64, 594 (1960).

Kishimoto, A., MacKawa, E., and Fujita, H., Bull. Chem. Soc. Japan, 33, 988 (1960).

Kishimoto, A., and Matsumoto, K., J. Polym. Sci., A2, 679 (1964).

Koros, W. J., Paul, D. R., and Rocha, A. A., J. Polym. Sci.-Polym. Phy. Ed., 14 687 (1976).

Kwei, T. K., and Wang, T. T., in "Permerbility of Plastic Films and Coatings", Hopfenberg, H. B., Ed., Plenum Press, New York, 1974, P. 63.

Leonard, W. J., Jr., J. Polym. Sci., Polym. Symp. Ed., 54, 237 (1976)

Long, F. A. and Richman, D., J. Am. Chem. Sci., 82, 513 (1960).

Lunardon, G., Sumida, Y., and Vogl, O., Angew Makromol. Chem., 87, 1 (1980).

McBride, J. S., Massaro, T. A., and Cooper, S. L., J. Appl. Polym. Sci., 23, 201 (1979).

MacKnight, w. J., and Yang, M., J. Polym. Sci., Polym. Symp. Ser., 42, 817 (1973).

Meares, P., J. A. C. S. 76, 3415 (1954).

Meares, P., Trans. Faraday Soc., 53, 101 (1957).

Meier, D. J., J. Macromol. Sci.-Phys., B17(2), 181 (1980).

Meier, D. J.. Appl. Polym. Symp., 24, 67 (1974).

Miller, J. A., Lin, S. B., Hwang, K. K. S., Wu, K. S., Gibson, P. E., and Cooper, S. L., Macromolecules, 18, 32 (1985).

Nakayama, K., Ino, T., and Matsubura, I., J. Macromol. Sci. Chem., A3(5), 1005 (1969).

Ng, N. H., Allegrezza, A. E., Jr., Seymour, R. W., and Cooper, S. L, Polymer, 14, 255 (1973).

Nielson, L. E., Rheol. Acta., 13, 86 (1974).

Odani, H., J. Polym. Sci., A-2, 5, 1189 (1967).

Odani, H., Kida, S., Kurata, M., and Tamura, M., Bull. Chem. Soc., Japan, 34, 571 (1961).

Odani, H., Hayashi, J., and Tamura, M., Bull. Chem. Soc., Japan, 34, 817 (1961).

Odani, H., Kida, S., and Tamura, M., Bull. Chem. Soc., Japan, 39, 2378 (1966).

Odani, H., Taira, K., Nemoto, N., and Kurata, M., Polym. Eng. Sci., 17, 527 (1977).

Odani, H., Uchikura, M., Taira, K., and Murata, M., J. Macromol. Sci., Phys., B17(2), 337 (1980).

Ophir, Z. and Wilkes, L., J. Polym. Sci.-Phys., 18, 1469 (1980).

Park, G. S., in "Diffusion in Polymers", Crank, J. and Park, G. S., Eds., Academic Press, New York, 1968, Chap. 5.

Peterlin, A., J. Polym. Sci., B3 1083 (1965).

Peterlin, A., Makromol. Chemie., 124, 136 (1969).

Peterlin, A., Polym. Eng. Sci., 20, 238 (1980).

Prager, S., Bagley, E., and Long, F. A., J. Am. Chem. Soc., 75, 1255 (1953).

Rahage, G., Ernst, O., and Fuhrman, J., Discuss. Faraday Soc., 49, 208 (1970).

Raucher, D. and Sefcik, M. D., in "Industrial Gas Separations, ACS Symposium Series 223", Whyte, T. E., Yon, C. M., and Wagener, E. H., Eds., American Chemical Society, Washington, D. C., 1983, P. 89 and P. 111.

Roche, E. J., and Thomas, E. L., Polymer, 22, 333 (1981).

Rogers, C. E., in "Physics and Chemistry of the Organic Solid State", Vol. II, Fox, D., Labes, M. M., and Weissberger, A., Eds., Interscience, New York, 1965, Chap. 6.

Sarti, G. C., Polymer, 20, 827 (1979).

Sax, J. and Ottino, J. M., Polym. Eng. Sci., 23, 165 (1983).

Schaefer, J., Stejskal, E. O., Steger, T. R., Sefcik, M. D., and McKay, R. A., Macromolecules, 13, 1121 (1980).

Schaefer, J., Stejskal, E. O., and Buchdahl, R., Macromolecules, 10, 384 (1977).

Schneider, N. S., Sung, C. S. P., Matton, R. W., and Illinger, S. L., Macromol., 8, 62 (1975).

Schneider, N. S., Dusablon, L. V., Snell, E. W., and Prosser, R. A., J. Macromol. Sci.-Phys., B3(4), 623 (1969).

Schneider, N. S., Sung, C. S. P., Polym. Eng. Sci., 17, 73 (1977).

Schneider, N. S., Desper, C. R., Illinger, J. L., King, A. O., and Barr, D., J. Macromol. Sci.-Phys., B11(4), 527 (1975).

Seefried, C. G., Jr., Koleske, J. V., and Critchfield, F. E., J. Appl. Polym. Sci., 19, 2493 and 2503 (1975).

Seefried, C. G., Koleske, J. V., Critchfield, F. E., and Dodd, J. L., Polym. Eng. Sci., 15, 646 (1975).

Sefcik, M. D., Schaefer, J., and May, F. L., J. Polym, Sci., Polym. Phys. Ed., 21, 1041 (1983).

Sefcik, M. D. and Schaefer, J., J. Polym. Sci., Polym. Phys. Ed., 21, 1055 (1983).

Sefcik, M. D., and Schaefer, J., Polym. Sci., Polym. Phys. Ed., 21, 1055 (1983).

Sefcik, M. D., Schaefer, J., Stejskal, E. O., and McKay, R. A., Macromolecules, 13, 1132 (1980).

Serrano, M., Ph.D. Thesis, University of Massachusetts (1986).

Seymour, R. W., and Cooper, S. L., Macromolecules, 6, 48 (1973).

Seymour, R. W., and Cooper, S. L., J. Polym. Sci., B9, 689 (1971).

Seymour, R. W., Estes, G. M., and Cooper, S. L., Macromolecules, 3, 579 (1970).

Seymour, R. W., Allegrezza, A. E., Jr., and Cooper, S. L., Macromolecules, 6, 896 (1973).

Seymour, R. W. and Cooper, S. L., J. Polym. Sci., 46(C), 69 (1974).

Seymour, R. W. and Cooper, S. L., Rubber Chem. Technol., 47, 19 (1974).

Smith, T. L., J. Polym. Sci.-Phys., 12, 1825 (1974).

Srichatrapimuk, V. W., and Cooper, S. L., J. Macromol. Sci.-Phys., B15(2), 267 (1978).

Steger, T. R., Schaefer, J., Stejskal, E. O., and McKay, R. A., Macromolecules, 13, 1127 (1980).

Stern, S. A. and Frisch, H. L., Ann. Rev. Mat. Sci., 11, 523 (1981).

Sung, C. S. P. and Schneider, N. S., Macromolecules., 8, 68 (1975).

Sung, C. S. P. and Schneider, N. S., Macromolecules, 10, 452 (1977).

Sung, C. S. P., and Schneider, N. S., J. Mat. Sci., 13, 1689 (1978).

Sung, C. S. P., Smith, T. W., and Sung, N. H., Macromolecules, 13, 117 (1980).

Tanaks, T., Yokoyama, T., and Yamaguchi, Y., J. Polym. Sci., Part A1, 6, 2153 (1968).

Thomas, N. L., and Windle, A. H., Polymer, 21, 613 (1980).

Thomas, N. L., and Windle, A. H., Polymer, 23, 529 (1982).

Uchida, T., Soen, T., Inoue, T., and Kawai, H., J. Polym. Sci., A2(10), 101 (1972).

Van Bogart, J. W. C., Lilaonitku, A., Lerner, L. E., and Cooper, S. L., J. Macromol. Sci.-Phys., 17, 267 (1980).

Van Bogart, J. W. C., Gibson, P. E., and Cooper, S. L., J. Polym. Sci.-Phys., 21, 65 (1983).

Vieth, W. R., Howell, J. M., and Hsieh, J. H., J. Membrane Sci., 1, 177 (1976).

Vrentas, J. S., Jarzebski, C. M., and Duda, J. L., AICHE J. 21, 894 (1975).

Vrentas, J. S., and Duda, J. L., J. Polym. Sci., Polym. Phys. Ed. 15, 403, 417, and 441 (1977).

Vrentas, J. S., Duda, J. L., and Ni, Y. C., J. Polym. Sci.-Phys. 15, 2039 (1977).

Vrentas, J. S., Duda, J. L., and Lau, M. K., J. Appl. Polym. Sci., 27, 3987 (1982).

Wang, C. B. and Cooper, S. L., Macromolecules, 16, 775 (1983).

Wang, T. T., Kwei, T. K., and Frisch, H. L., J. Polym. Sci. 7 (A2), 2019 (1969).

Zhurkov, S. N., and Ryskin, G. Y., J. Tech. Phys. (U.S.S.R.), 24, 797 (1954).

Ziegel, K. D., J. Macromol. Sci.-Phys. B5(1), 11 (1971).